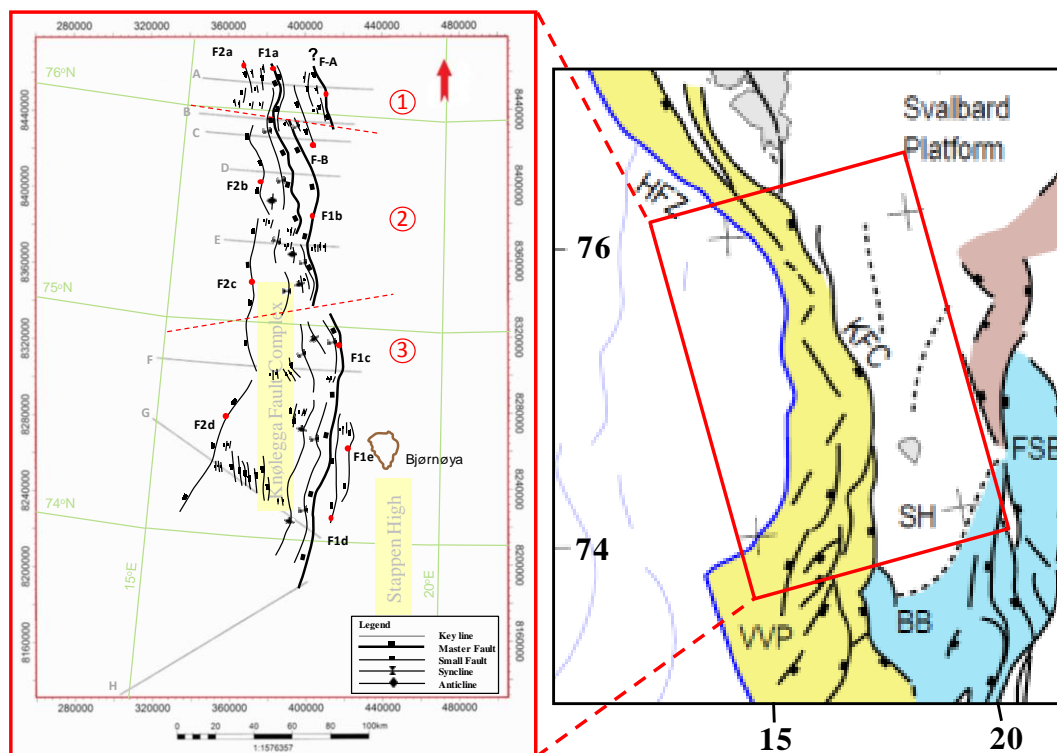


Structural Analysis of the Knølegga Fault Complex, NW Barents Sea

Attiq Ur Rehman



UNIVERSITY OF OSLO

FACULTY OF MATHEMATICS AND NATURAL SCIENCES

Structural Analysis of the Knølegga Fault Complex, NW Barents Sea

Attiq Ur Rehman



Master Thesis in Geosciences

Discipline: Petroleum Geology and Petroleum Geophysics

Department of Geosciences

Faculty of Mathematics and Natural Sciences

UNIVERSITY OF OSLO

June, 2012

© **Attiq Ur Rehman, 2012**

Tutor(s): **Roy H. Gabrielsen, Jan Inge Faleide and Michael Heeremans, UiO**

This work is published digitally through DUO – Digitale Utgivelser ved UiO

<http://www.duo.uio.no>

It is also catalogued in BIBSYS (<http://www.bibsys.no/english>)

All rights reserved. No part of this publication may be reproduced or transmitted, in any form or by any means, without permission.

Abstract

Structural analysis of the Knølegga Fault Complex has been done using 2D seismic reflection data set in order to understand the fault geometries, fault associated features, fault segmentation and temporal evolution of the study area. The boundary faults of the Knølegga Fault Complex comprises of the three softly-linked fault segments named as F-B, F1-b and F1c. The fault segments F-B and F1-b are ‘overlapping-synthetic’ fault segments while F1-b and F1-c are ‘approaching-synthetic’ fault segments. All three master faults have down-to-the west displacement. The displacement is transferred within the master faults; hence the master faults F-B, F1-b and F1-c represent the relay zones. The sole of the master faults is deeper than the Cenozoic sediments, which is in agreement with the observations made by previous authors. The master faults are placed in the category of ‘*First-Class*’ following Gabrielsen (1984). The maximum displacement is observed in the central master fault segment F1-b. The displacement decreases to the north and to the south of the key line E.

The structural analysis revealed that the Knølegga Fault Complex lies in a tectonic setting which has undergone both extension and contraction. The prominent structures identified are the rotated fault blocks, growth faults and staircase normal fault geometries. The contractional structures within the study area are synclines and anticline.

The major rifting event in the study area is related to break-up of the Norwegian-Greenland Sea in the early Eocene. The growth fault and minor faulting within the Oligocene sediments indicate the tectonic activity during the Oligocene. The contractional structures present in the study area seem to be the result of compression in the Oligocene?-Miocene in the direction of NW-SE to WNW-ESE. The compressional stresses have deformed both the hanging wall and the footwall. This contraction is older than the Pliocene-Pleistocene glacial sediments as no contractional structures are observed in the younger Pliocene-Pleistocene sediments in the study area.

Structural analysis of the Knølegga Fault Complex, NW Barents Sea

Acknowledgements

I would like to express special appreciation to my supervisor Professor Roy Helge Gabrielsen for his special attention throughout the work during this study. Discussions with him have been motivating and thought-provoking. Special gratitude to supervisor Jan Inge Faleide for guidance and discussions during the interpretation work and write-up. I would like to thank Dr. Michael Heeremans who has helped in the data management.

NPD and SINTEF are also acknowledged for making seismic data available.

I am thankful to my family for their love, support and encouragement during my entire studies. All my helpful and caring friends deserve special thanks those have been very supporting during studies at the University of Oslo.

Structural analysis of the Knølegga Fault Complex, NW Barents Sea

Contents

ABSTRACT	I
ACKNOWLEDGEMENTS	III
CHAPTER 1 INTRODUCTION.....	7
CHAPTER 2 GEOLOGICAL FRAMEWORK	9
2.1 GEOLOGICAL REGIONS AND STRUCTURAL ELEMENTS.....	9
2.2 REGIONAL TECTONOSTRATIGRAPHIC SETTINGS	10
2.3 THE KNØLEGGFA FAULT COMPLEX-A REVIEW	16
2.4 HORNSUND FAULT ZONE	18
2.5 STAPPEN HIGH	19
2.6 VESTBAKKEN VOLCANIC PROVINCE.....	20
CHAPTER 3 DESCRIPTION OF SEISMIC INTERPRETATION RESULTS	21
3.1 DATA	23
3.2 INTERPRETATION TOOL.....	23
3.3 SEISMIC INTERPRETATION PROCEDURE.....	25
3.4 DESCRIPTION OF STRUCTURAL ARCHITECTURE AND FAULT PLANE GEOMETRIES OF KEY SEISMIC LINES	27
3.4.1 Key Seismic Line A.....	35
3.4.2 Key Seismic Line B.....	38
3.4.3 Key Seismic Line C.....	40
3.4.4 Key Seismic Line D	43
3.4.5 Key Seismic Line E.....	45

Structural analysis of the Knølegga Fault Complex, NW Barents Sea

3.4.6 Key Seismic Line F.....	47
3.4.7 Key Seismic Line G.....	49
3.5 TIME-STRUCTURE (TWT) AND FAULT MAPS.....	51
3.5.1 Intra Eocene.....	51
3.5.2 Intra Oligocene.....	54
3.5.3 Intra Miocene.....	57
3.6 TIME-THICKNESS MAPS.....	61
3.6.1 Intra Eocene-Near Base Eocene.....	61
3.6.2 Intra Oligocene-Intra Eocene.....	61
3.6.3 Intra Miocene-Intra Oligocene.....	62
CHAPTER 4 DISCUSSION.....	67
4.1 FAULT CLASSIFICATION.....	67
4.2 FAULT GEOMETRY.....	72
4.2.1 Displacement along the master fault.....	74
4.3 FAULT DATING.....	75
4.4 STRUCTURAL ARCHITECTURE OF THE STUDY AREA (HANGINGWALL BLOCK AND FOOTWALL).....	78
4.5 TEMPORAL EVOLUTION OF THE STUDY AREA.....	82
CHAPTER 5 SUMMARY OF THE STUDY.....	91
5.1 CONCLUSIONS.....	91
5.2 RECOMMENDATIONS FOR THE FUTURE WORK.....	92
REFERENCES.....	93

Chapter 1 Introduction

The study area lies in the northwestern part of the SW Barents Sea. An area of approximately 1.3 million km² is covered by the Barents Sea continental shelf (Worsley, 2008). The Barents Sea incorporates a large epicontinental sea which in the north and west contains young passive continental margins. Geographically, Svalbard archipelago and Franz Josef Land is located in the north, Novaya Zemlya to the east, Norwegian-Greenland Sea to the west and northern Norwegian coast and Kola Peninsula lies to the south as shown in Fig.1 (Faleide et al., 1984; Faleide et al., 1993a).

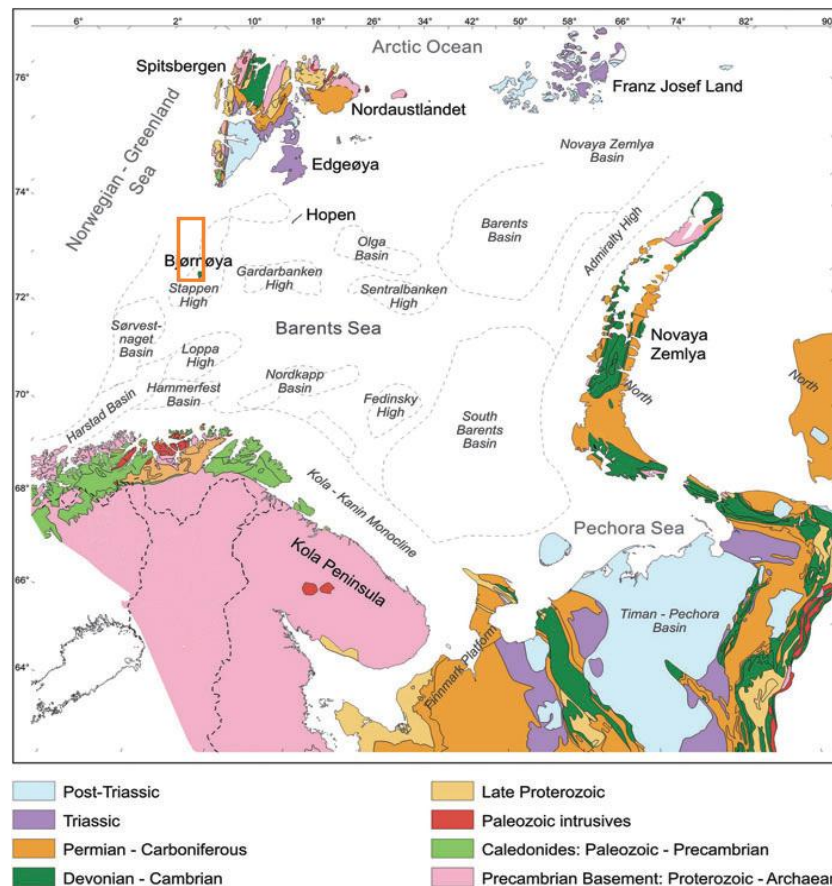


Figure 1: The Barents Sea and geographically surrounding areas, orange box shows location of the study area. (Modified from Worsley, 2008. Original source Mork, 1999).

The evolution of the North Atlantic Ocean is comprised of two main stages. During the first stage continental break-up occurred in the early Eocene while a change in the spreading direction from NNW-SSE to NW-SE occurred took place in the beginning of the second stage of North Atlantic evolution in the early Oligocene (Talwani and Eldholm, 1977; Czuba et al., 2011). The evolution of the Barents Sea is influenced by the opening of the Norwegian-Greenland Sea. The Barents Sea contains thick sediments from the late Paleozoic to the Cenozoic. Structurally, the Barents Sea represents a complicated network of fault complexes, basins, platforms and highs with various geometrical and genetic characteristics. (Gabrielsen, 1984; Faleide et al., 1993a). The study area is the Knølegga Fault Complex which is part of Hornsund Fault Zone in the NW Barents Sea (*Fig.1*) separating the Svalbard Platform from narrow basins along the western Barents Sea margin (Myhre et al. 1982, Gabrielsen et al. 1984, Gabrielsen et al. 1990). This Fault Complex trends NNE-SSW to NS from 73°30'N to 75°50'N at approximately 18°E. The Knølegga Fault Complex delineates the western part of Stappen High. (Faleide et al., 1984; Faleide et al., 1988; Myhre and Eldholm, 1988; Gabrielsen et al., 1990).

The main objectives of thesis work are to investigate the 'structural styles and evolution of the Knølegga Fault Complex'. To do so, fault classification, fault geometry, fault dating, structural architecture within the hangingwall block and the footwall, and temporal evolution of the study area have been prime focus of the present study.

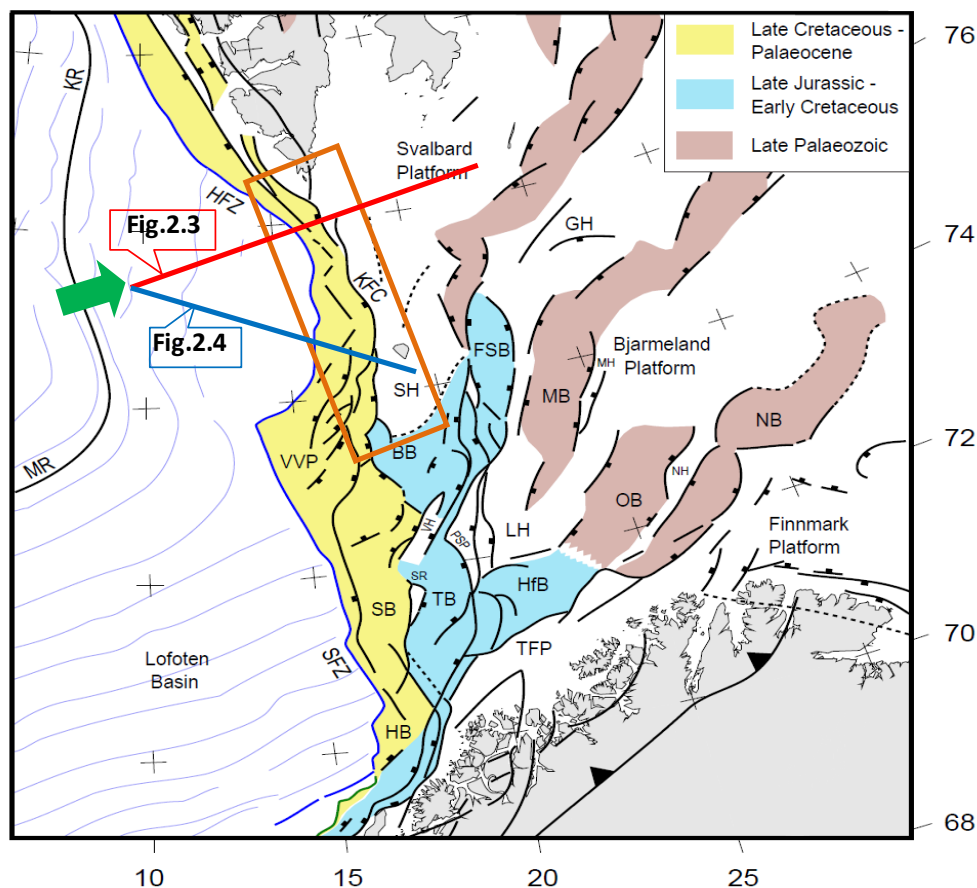
Chapter 2 Geological Framework

2.1 Geological Regions and Structural Elements

The western Barents Sea can be divided into three geological regions of Paleozoic to Cenozoic time on the basis of its structural elements (*Fig.2*). These are: (1) the Svalbard Platform; (2) a basinal province between Svalbard Platform and the Norwegian coast; and (3) the western continental margin (Faleide et al., 1984; Faleide et al., 1993; Faleide et al., 2010).

The Svalbard Platform is in northwestern part of the Barents Sea and covering northern part of the regional basin province. The Hornsund Fault Zone, Knølegga Fault Complex and Stappen High constitute the western boundary of the Svalbard Platform (Faleide et al., 1984; Faleide et al., 2010). Sub-basins and highs with a pronounced increasing structural relief to the west distinguish the basinal province between the Svalbard Platform and the Norwegian coast (Faleide et al., 1993). Faleide (1993) further divided the western continental margin into three main segments; (a) a southern sheared margin along the Senja Fracture Zone; (b) a central rifted complex south-west of Bjørnøya which is associated with volcanism; and (c) a northern margin which was initially sheared and later rifted along the Hornsund Fault Zone.

The arrangement of structural elements in the western Barents Sea is considered to be complex because of reactivation of long lived fault zones during the tectonic events (Gabrielsen, 1984). The dominant trend of Barents Continental Shelf is ENE-WSW to NE-SW and NNE-SSW to NNW-SSE whereas WNW-ESE striking elements impart local influence on the region. There are two major fault zones to the north and south. To the north, the Hammerfest and Nordkapp Basins are surrounded by a fault zone with major fault complexes and a dominant ENE-WSW trend. Loppa High is separated from the Bjornoya Basin by a major zone consisting of the Veslemøy High and the fault complexes and this zone has a trend subparallel to the major fault zone in north. To the west and northwest, Barents continental shelf is dominated by N-S trends including the Tromso Basin, Knølegga Fault Complex and Hornsund Fault Zone (Gabrielsen et al., 1990).



BB = Bjørnøya Basin *KFC=Knølegga Fault Complex* *KR = Knipovich Ridge*
LH = Loppa High *FSB = Fingerdjupet Sub-basin* *MB = Maud Basin*
MH = Mercurius High *MR = Mohns Ridge* *GH= Gardarbanken High*
NB = Nordkapp Basin *NH = Nordsel High* *OB = Ottar Basin* *HB = Harstad Basin*
PSP = Polheim Sub-platform *SB = Sørvestsnaget Basin* *SFZ = Senja Fracture Zone*
HfB = Hammerfest Basin *SH = Stappen High* *SR = Senja Ridge* *TB = Tromsø Basin*
HFZ = Hornsund Fault Zone *TFP = Troms-Finnmark Platform*
VH = Veslemøy High *VVP = Vestbakken Volcanic Province*

Figure 2.1: Main Structural elements in the western Barents Sea and adjacent areas, rectangle shows location of study area i.e., Knølegga Fault Complex on the western part of Stappen High and as a part of the Hornsund Fault Zone in NW Barents Sea. Structural setting reveals that basins become younger from east to west. Green arrow on left middle indicates the crustal transect (red line) of KFC in EW direction. Location of profiles in Figures 4&5 is shown by red and blue color transects respectively (Modified from Faleide et al., 2010).

2.2 Regional Tectonostratigraphic Settings

The Barents Sea has an intracratonic setting and has witnessed various phases of tectonic activity after the termination of Caledonian orogeny (Gabrielsen et al., 1990). A thick succession of Paleozoic to Cenozoic strata underlies the Barents Sea. The lateral as well as vertical variations

in thickness and facies are shown by this succession. The succession is marked by Upper Paleozoic mixed carbonates, evaporites and clastics whereas Mesozoic-Cenozoic clastic sedimentary rocks overlie Paleozoic strata (Faleide et al., 2010). The stratigraphy of the western Barents Sea along with the megasequences and major tectonic events are demonstrated in Figure 3. The Basement that underlies most of the western part of the Barents shelf was metamorphosed during the Caledonian Orogenic events as indicated from indirect evidence (Faleide et al., 1984; Faleide et al., 2010).

The metamorphic basement of the western Barents Shelf is formed of the Caledonides. These Caledonides were consolidated during the Late Silurian to Early Devonian Caledonian orogeny. The suturing of the North America–Greenland and the Fennoscandian-Russian plates is caused by this Caledonian orogeny. Old Red molasse sediments are deposited as a result of strong uplifts followed by erosion after orogeny (Faleide et al., 1984).

The Late Paleozoic history of the western Barents Sea is considered to have some events involved; these are: (1) during Caledonian orogeny the basement was consolidated, (2) a tectonic regime during the Devonian time including both extensional and compressional events, (3) widespread rifting during the Carboniferous and Permian times, and (4) in Permian time a non-fault-related regional subsidence was developed gradually (Gudlaugsson et al., 1998). The graben structures having north-south trend consist of Devonian strata which is then discordantly overlain by Carboniferous strata (Faleide et al., 2010).

Sediments deposited during lower to lower Upper Carboniferous time were mostly clastics and deposited in extensional basins (Faleide et al., 2010). The extensional features recognized as the oldest are large rollovers or tilted fault blocks. These blocks are associated with listric normal faults turning into low-angle sole faults. The Barents Sea is documented as affected by the crustal extension between Norway and Greenland which then led to the initial development of the northeast Atlantic rift at the close of Devonian times but the Barents Sea rift in a north-eastern direction, is interpreted to have been formed during the Middle Carboniferous. This

Barents Sea rift is structurally fan shaped and the structural style is one of interconnected and segmented basins which is characterized by half-graben geometries (Gudlaugsson et al., 1998). The formation of various interconnected extensional basins which are filled with syn-rift deposits and separated by fault-bounded highs is a result of the rift phase of the Carboniferous time. In most of the southwestern Barents Sea the structural trends strike northeast to north are dominated. The Tromsø, Bjørnøya, Nordkapp, Fingerdjupet, Maud and Ottar basins are interpreted as rift basins formed at the Carboniferous time. To the end of the Carboniferous time fault movements were ceased in the eastern part. The structural relief was filled by a platform succession of Late-Carboniferous-Permian times. From the lower to upper this succession contains cyclic dolomite and evaporites to massive limestones. A regionally mapped widespread layer of evaporites lies in the southwest Barents Sea which is of latest Carboniferous-earliest Permian times (Faleide et al., 2010).

The thickness of salt layer which is concluded to reach 4-5 km locally in the Nordkapp Basin shows that a depression which is generated by fault was either in place or developed during early Late Carboniferous age (Faleide et al., 2010). Carbonates were deposited on a broad shelf during Bashkirian to Artinskian-Early Kugurian age. The carbonates build up at basinal margins and these were followed by the deposition of basinal evaporites during Gzelian-Asselian and Sakmarian times. Upto late Early Permian time carbonate sediments were deposited followed by clastic deposition during Early Permian times (Faleide et al., 2010).

In Permian-Early Triassic times renewed faulting, uplift and erosion affected the western part of the rift system. The rift phase of Permian-Early Triassic that affects the N-S structural trend is indicated by the normal faulting along the western margin of the Loppa High and also the uplift, tilting and erosional truncation. The erosional surface of this rift phase is extended from the Loppa High to the Stappen High. In the southern part of Spitsbergen a tectonic activity occurred in Permian time on Bjørnøya and the Sorkapp High (Faleide et al., 2010).

During Triassic clastic Sediments were deposited as the Barents Sea was covered by a regional deepwater basin. Source of sediments was mainly Uralian highland. Salt diapirism in the Nordkapp Basin and possibly in other salt basins in SW Barents Sea was activated because of

differential loading. Late Permian and Early Triassic period was dominated by marine conditions. At the end of this period shallowing up and partial exposure of some areas started. In Middle Triassic time continental regime dominated in large areas. During the Middle Triassic marine conditions existed in the central and northern basins (Faleide et al., 2010).

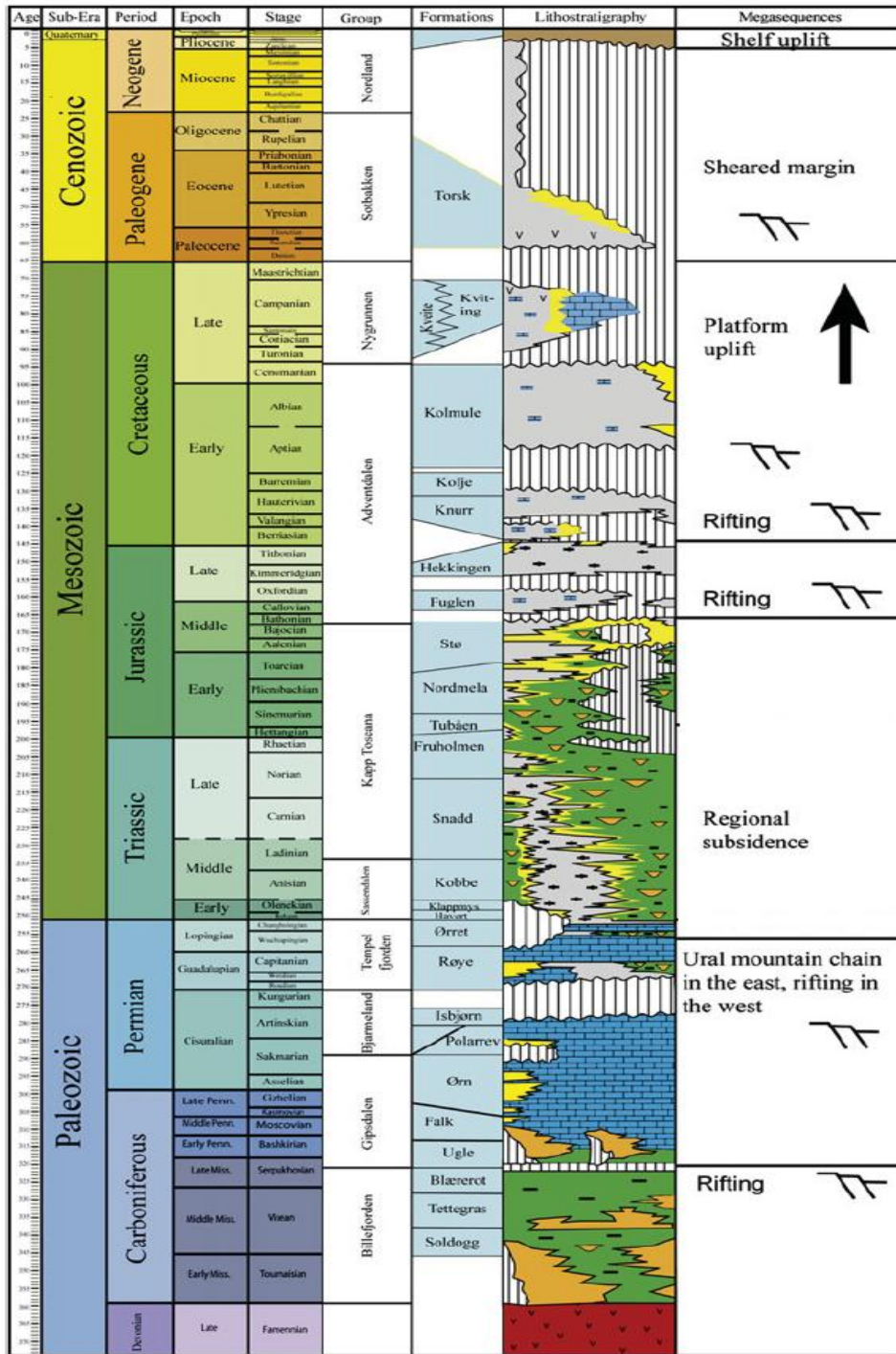


Figure 2.2: Stratigraphy of the western Barents Sea, megasequences and major tectonic events are also demonstrated (Modified from Glorstad-Clark et al., 2010).

The Barents Sea is prevailed by sandstones during the Lower-Middle Jurassic. The early stage of rifting in the southwestern Barents Sea was marked by the late Middle Jurassic sequence boundary. The unconformities in the Upper Jurassic sequence are demonstrated by the continued rifting and sea-level changes. The sequence is very thin so resolution of this sequence and unconformities on the seismic scale is very low (Faleide et al., 2010).

During the Late Jurassic-earliest Cretaceous the regional extensional structuring along with strike-slip adjustments with old structural lineaments occur in the SW Barents Sea which developed the prominent rift basins i.e., Bjørnøya, Tromsø and Harstad basins. The tectonic events in the North Atlantic-Arctic region are related to the evolution of these basins. This rifting continued in Early Cretaceous time whereas in the SW Barents Sea an important event of Aptian faulting is observed. The very deep basins in the SW Barents Sea are the result of various phases of Late Mesozoic and Early Cenozoic rifting (Faleide et al., 2010).

The Lower Cretaceous times is dominated by three sedimentary units i.e., shales and claystones, thin interbeds of silt, limestone and dolomite, from Valanginian to Cenomanian ages, which are making the main basin fill in the deep SW Barents Sea (Faleide et al., 2010). In Early Cretaceous time a widespread magmatism without any signs of faulting prevailed the northern Barents Sea. In the northern Barents Sea a regional Large Igneous Province (LIP) in the Arctic is observed at both onshore including Svalbard and Franz Josef Land, and offshore. In response to faulting in the Sørvestsnaget and thermal subsidence in Tromsø, the SW Barents Sea continued to subside and there is little or no sedimentation in the Barents Sea in Upper Cretaceous time in contrast with the SW Barents Sea (Faleide et al., 1984; Faleide et al., 2010).

During Cenozoic times, the structures developed are result of the opening of mainly rifted Norwegian-Greenland Sea and formation of sheared western Barents Sea continental margin. The western Barents Sea margin was developed as a sheared margin along the De Geer Zone. The lithospheric break up was preceded by a rift phase during the Campanian age distinguished by low angle normal faulting on the outer margin (Sundvor and Eldholm 1976; Myhre et al., 1982; Gabrielsen et al., 1984; Faleide et al., 1988; Myhre and Eldholm., 1988; Gabrielsen et al., 1990; Faleide et al., 1991; Faleide et al., 2008; Faleide et al., 2010). Opening of the Norwegian-

Greenland Sea, formation of the Vestbakken Volcanic Province and extensional faulting and uplift along the Senja Fracture Zone are recognized as the major events during Early Eocene time. Structural rejuvenation along parts of the continental margin occurred in Oligocene age (Faleide et al., 1993b).

The sediments have been eroded away after the uplift of the Barents continental shelf during the Late Cenozoic time. The western Barents Sea has gone through extensive erosion. This erosion is particularly more extensive in the NW region including Svalbard where erosion of more than 3,000 m sedimentary strata is observed. Differential uplift and erosional pattern in the NW Barents Sea are determined on the basis of seismic data. The Palaeogene and Mesozoic rocks are unconformably overlain by the Neogene and Quaternary rocks which become thicker at the margin. Late Pliocene to Pleistocene-Holocene age rocks are composed of the glacial sediments (Faleide et al., 2010). These glacial sediments are present at the western part of the study area.

2.3 The Knølegga Fault Complex-A Review

The Knølegga Fault Complex lies on the western part of the Stappen High and is part of the Hornsund Fault Zone in NW Barents Sea (Figure 2). The Knølegga Fault Complex trends NNE-SSW to NS from 73°30'N to 75°50'N at approximately 18°E. The Hornsund Fault Zone marks the continent-ocean boundary and is associated with the Cenozoic opening of the Norwegian-Greenland Sea. This fault separates the Svalbard Platform from the narrow basins along the western Barents Sea margin. The strata along Hornsund Fault Zone fault complex are of Late Cretaceous-Palaeogene age. Knølegga Fault Complex was referred to as the Bjørnøya-Sorkapp fault zone. The structure of Knølegga Fault Zone is named after the break in slope towards deep waters west of Bjørnøya. (Sundvor and Eldholm 1976; Myhre et al., 1982; Gabrielsen et al., 1984; Faleide et al., 1988; Myhre and Eldholm., 1988; Gabrielsen et al., 1990; Faleide et al., 1991; Faleide et al., 2008; Faleide et al., 2010).

On the upthrown side, Jurassic and Triassic crop out on the sea floor and the throw of the fault complex is very large. On downthrown side the depth of Jurassic is unknown; it may be below 3-

4 km below the sea floor or probably more. The detachment of fault lies at a depth of more than 6 km and fault may have listric geometry. Knølegga Fault Complex terminates in a structurally complex area along southwest of the Stappen High. A change in orientation and a style of deformation is observed as it terminates to the north (Gabrielsen et al., 1990).

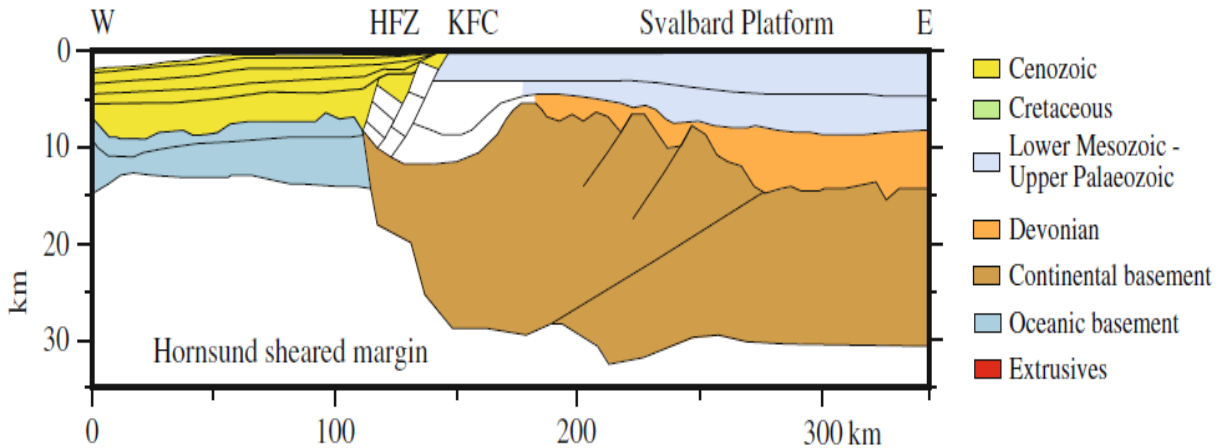


Figure 2.3: Regional transect of NW Barents Sea showing profile view of Hornsund sheared margin. The Knølegga Fault Complex is along the eastern margin of Hornsund Fault Zone; see Fig. 2.2 for location of transect by red color line. Color on right side demonstrates different ages (Faleide et al., 2010). KFC: Knølegga Fault Complex, HFZ: Hornsund Fault Zone.

According to Gabrielsen et al., (1990) seismic data suggests that the main phase of movement occurred in Tertiary time but it is also considered that this event may represent reactivation of an older fault. An east-west regional transect along NW Barents Sea demonstrates the profile view of Hornsund sheared margin (*Fig. 2.3*) along western part of Svalbard Platform (Faleide et al., 2010).

Based on the available data Gabrielsen et al., (1990) interpreted that the Knølegga Fault Complex has listric geometry also that location of its sole is at Jurassic or a deeper level. The presence of a large hanging-wall anticline supports this interpretation. The Knølegga fault Complex is considered to be basically an extensional fault but the Tertiary movement may have a dextral lateral component (Gabrielsen et al., 1990).

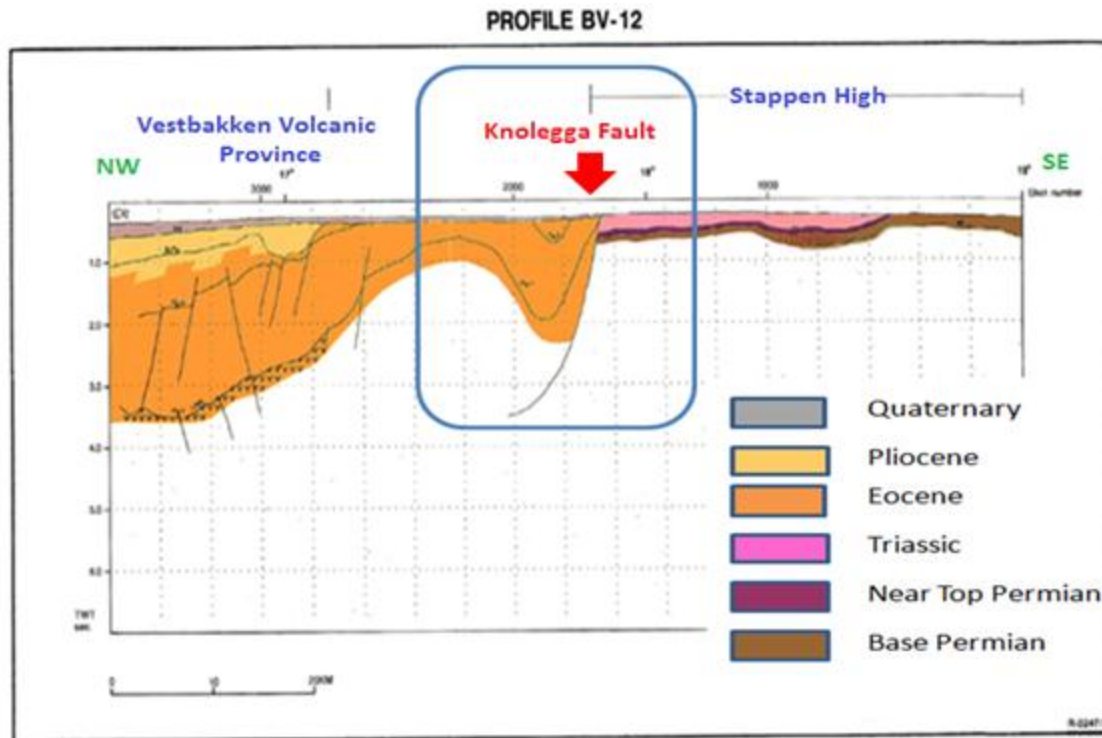


Figure 2.4: NW-SE profile view showing the Knølegga Fault on the western part of the Stappen High, for location of profile see blue line transect on left middle in Figure 2 (modified from Gabrielsen et al., 1990).

2.4 Hornsund Fault Zone

The two major fault zones bordering the continental shelf of the western Barents Sea are the Senja Fracture Zone and Hornsund Fault Zone to the W (Fig. 2.3), and the Troms-Finnmark Fault Complex to the S. The Senja Fracture Zone and the Hornsund Fault Zone are believed to be the most fundamental as these zones are coincident with the transition zone between the oceanic and continental crust (Gabrielsen, 1984). The central and the NNE segments of the Hornsund Fault Zone SW of Bjørnøya are rifted passive margins while the other parts of the boundary could be either sheared or sheared rifted type (Myhre et al., 1982; Gabrielsen, 1984). The Hornsund Fault Zone is termed '*First-Class*' by Gabrielsen, 1984. According to Gabrielsen, 1984, the characteristics of '*First-Class*' are: these faults involve basement, have regional significance, reactivated and separate the areas of different tectonic outline (Gabrielsen, 1984).

2.5 Stappen High

The Stappen High is situated in the western part of the Svalbard platform areas at the boundary with the Barents Sea Margin (*Fig. 2.4*). It is an elongate, north-south trending structure which has witnessed a complex tectonic history involving several phases of tectonic uplift and tilting. The composition of the High varies as it is made up of basement blocks of varying composition, as indicated by gravity and magnetic modeling, bounded by NNW- trending Knølegga Fault to the west of the Stappen High (Gabrielsen et al., 1990; Grogan et al., 1999). The Stappen high is one of the seven structural elements of the Svalbard Platform identified by Grogan (1999) and lies in the south of Svalbard. The Stappen High trends N-S from $73^{\circ}30'N$ to $75^{\circ}30'N$ at approximately $18-19^{\circ}E$. The Highest point of the Stappen high is Bjørnøya. From Bjørnøya, the high trend continues towards Sørkapp on Spitsbergen. The Knølegga Fault limits the western boundary of the Stappen High (*Figs. 2.1 and 2.5*). The Bjørnøya Basin and the Sørkapp Basin delimits the southern and eastern parts of the High respectively (*Fig. 2.1*). The NNE-SSW trending faults influenced the southern boundary. The Pre-Triassic levels of the High give the impression of gently elongated domes (Gabrielsen et al., 1990). The thickness of the Cretaceous sediments deposited in the Bjørnøya basin slightly reduces to the Stappen High and then disappears because of the erosion. In late Paleozoic, the Stappen high was a positive element followed by subsidence in the Early Cretaceous and uplift in the Tertiary. During the Late Paleozoic to Jurassic time period, the Stappen High was situated in a marginal position in the Barents Sea. The subsidence in the Early Cretaceous and uplift in the Tertiary were closely linked with activity along the Knølegga Fault Complex and the Hornsund Fault Zone. This activity then is associated with the opening of the Norwegian –Greenland Sea (Gabrielsen et al., 1990).

2.6 Vestbakken Volcanic Province

The Vestbakken volcanic province is in the south of the Knølegga Fault Complex between 73°30' N to 74°30' N, to the south and west of Bjørnøya and also between the oceanic crust and approximately 17°E (Figs. 2.1 and 2.5). The boundary of oceanic crust is poorly defined (Gabrielsen et al., 1990). The province has intrusions which could be linked to the volcanic activity. The intrusions are younger than the lavas according to the seismic interpretation as the age of the lavas was reported as Early Tertiary. The Vestbakken volcanic province now represents a structurally homogeneous area as it was structured after the formation of the lavas (Faleide et al., 1988; Gabrielsen et al., 1990).

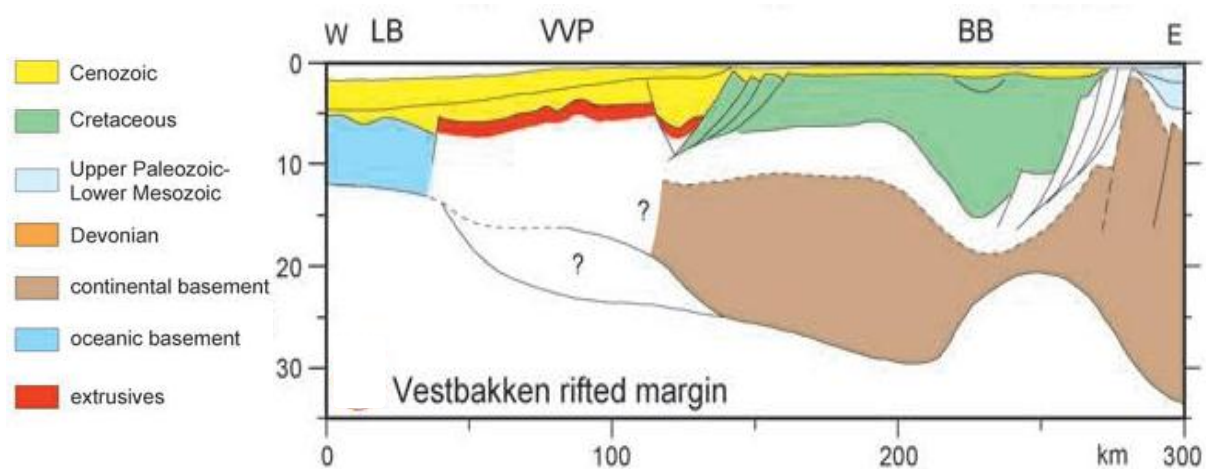


Figure 2.5: A crustal transect crossing Western Barents Sea-Svalbard margin in the southern part of the study area (modified from Faleide et al., 2008). BB: Bjørnøya Basin, LB: Lofoten Basin, VVP: Vestbakken volcanic province.

Chapter 3 Description of Seismic Interpretation Results

This chapter deals with the seismic interpretation results and their description in order to accomplish structural analysis of the area under investigation. During the structural interpretation and description of the seismic interpretation results, the scheme followed is summarized in Table 3.1.

<i>Phase 1</i>	Structural Interpretation Of Seismic Lines (2D)	Selection of Appropriate Horizons (Reflections)	Stratigraphic Calibration, Seismic to Well tie
<i>Phase 2</i>	Selection and Detailed Interpretation of Key Seismic Lines	TWT Structure Maps and Fault Maps	TWT Time-Thickness Maps
<i>Phase 3</i>	Fault Analysis (Fault Classification, Fault Geometry, Fault Dating)	Structures in Hanging Wall and Footwall	Temporal Evolution Of the Study Area

Table 3.1: An outline of the workflow followed during the study, *phase 1* and *2* are focused in this chapter, while *phase 3* is addressed in chapter 4 (Discussion).

The present work can be generally divided into three phases. The motivation of all these phases is to analyze the structural configuration and evolution of the Knølegga Fault Complex. The work of previous authors is also studied to relate and compare the present interpretation work, and to build an understanding of the geological history of the study area.

During the description of seismic interpretation results, terms key seismic section, key seismic line or the key line refers to selected 2D seismic lines offered to represent geometry and structural architecture of the study area. The seven key seismic lines are selected from 2D seismic data set of the area under observation, named as A, B, C, D, E, F and G. The eighth line H is the reference seismic line crossing the exploration borehole 7316/5-1, used for the stratigraphic calibration (*Fig. 3.1 and Fig. 3.7*). The key lines A, B, C, D, E and F are oriented E-

W while, the key line G is oriented NW-SE. The orientation of key line H crossing reference borehole is NE-SW (*Fig. 3.1*).

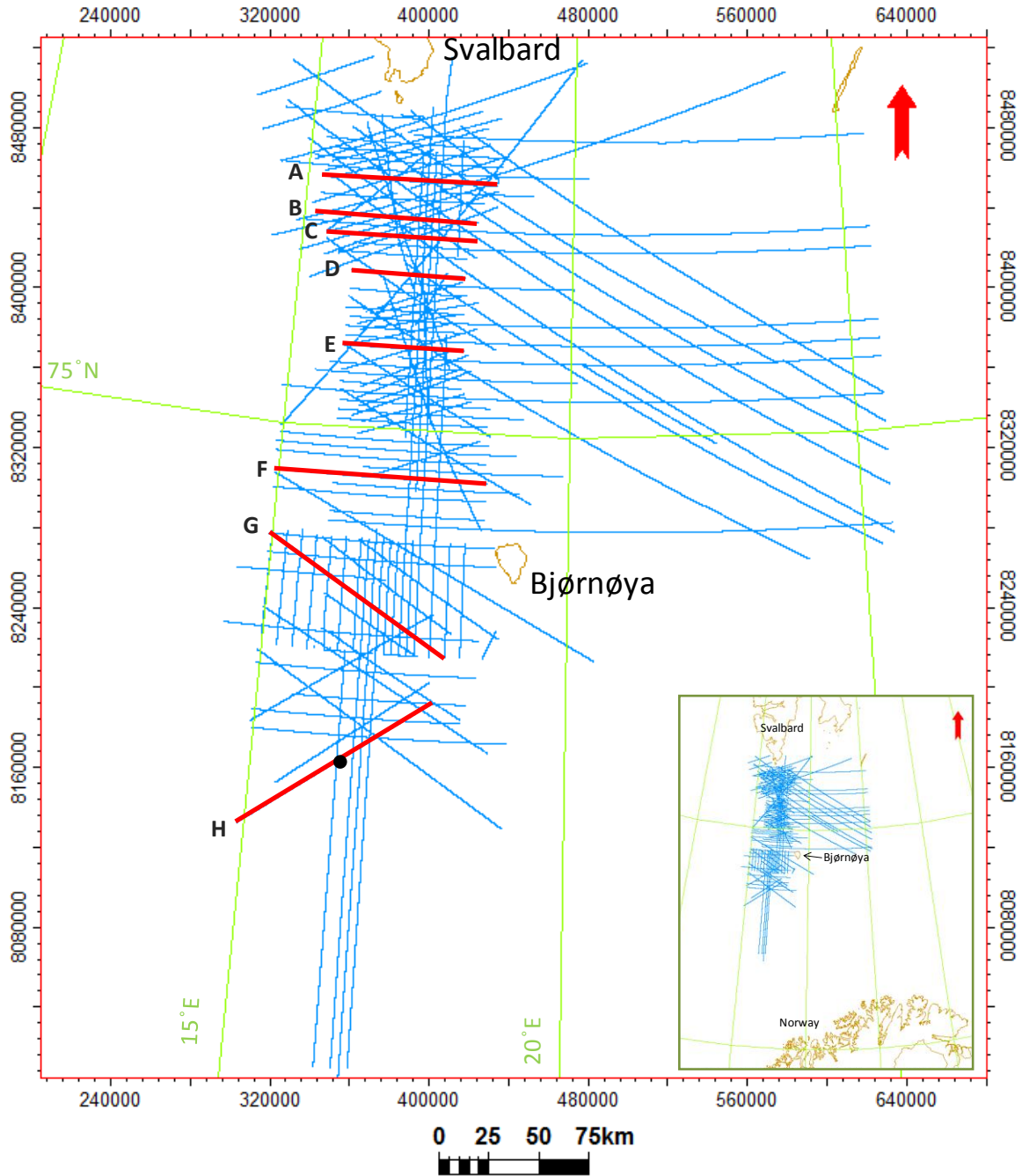


Figure 3.1: Base map of the study area showing 2D seismic data set and location of the well 7316/5-1 used indicated by black dot at seismic line H. The red lines show the seismic key lines from A to H.

3.1 Data

The data set for current study included a grid of 2D seismic lines and borehole data of the well 7316/5-1 (*Fig. 3.1*). The base map observations revealed that the data provided was dense and consisted of dip, diagonal and strike lines. The 2D data set belongs to different vintages that provided the good areal coverage, however, several mistie issues directly originates from such a data set. The 2D seismic data set includes the dip, the diagonal and the strike lines. The dip lines are mostly E-W oriented; diagonal lines are both NW-SE and NNE-SSW to ENE-WSW. The strike lines are N-S, NE-SW and NW-SE oriented (*Fig. 3.1*). The seismic data set covers an area of about 73°-76°N and 13° -26°E with the line spacing of approximately 8 x 9 km. The only well available for seismic to well tie in the study area is 7316/5-1. The seismic line H crossing the wellbore is interpreted to calibrate the seismic data. This well, drilled in the Vestbakken Volcanic Province, is located at 73°31' N, 16°26' E about 150 km south southwest of the Bjørnøya (Eidvin et al., 1998b). The first well drilled in the study area is 7316/5-1 with underlying objective of testing the hydrocarbon potential of the Tertiary basins in western Barents Shelf (Eidvin et al., 1998b). The well tops data from the borehole is recorded with reference to the Kelly Bushing (RKB) and this data is used as such during present study. Three well formation tops used for seismic to well tie includes the Nordland Group encountered at 473 m, the Torsk Formation at 945 m and the Kveite Formation at 3752 m (*Table 3.2*). The total depth (MD) was 4027 m and the oldest penetrated formation (Kveite formation) is of the Late Cretaceous period (www.npd.no).

3.2 Interpretation tool

The interpretation of 2D seismic data is performed using Petrel 2011 software. The software is designed by Schlumberger , which can perform various tasks including 2D/3D seismic interpretation, mapping, basic well logs analysis, volumetric estimation, well placements, subsurface modeling, reservoir modeling etc. Structural integrity, stratigraphic features, fluid contacts and property distributions are some of the parameters which are possible to assess using

Petrel 2011 (www.slb.com). During this study structural interpretation and the consequent time-structure and the time-thickness maps became possible by utilizing Petrel 2011.

Well name	7316/5-1
NS UTM (m)	8159255.68
EW UTM (m)	545381.15
UTM Zone	33
Drilling operator	Norsk Hydro Produksjon AS
Area	BARENTS SEA
Discovery	7316/5-1
Field	NOT YET DEVELOPED
Drilling facility	POLAR PIONEER
Drilling days	77
Entry date	21.07.1992
Completion date	05.10.1992
Type	WILDCAT
Status	Plug and Abandoned
Contents	GAS
Kelly bushing elevation (KB) [m]	23
Water depth [m]	450
Total Depth (MD) [m RKB]	4027
Oldest penetrated age	LATE CRETACEOUS
Oldest penetrated formation	KVEITE FM

Table 3.2 General information of the well 7316/5-1 used during this study work (modified from www.npd.no).

3.3 Seismic Interpretation Procedure

All seismic lines were first generally observed to see the quality and resolution of the lines and also to acquire a fundamental understanding of the structural features. Besides providing the general structural information the QC of seismic data allowed to differentiate between the areas of good and poor seismic resolution. Fault interpretation followed the first phase of seismic data QC. Once regional and local faults were interpreted, an approach of the structural architecture of the study area was built. This approach provided the key to interpret the continuity of the stratigraphy.

The next step was to load the well and the well tops into the software. The seismic-to-well tie was made for the calibration of seismic data with the borehole data (*Fig. 3.4*). The oldest penetrated formation is the Kveite Formation of the Late Cretaceous period. The Kveite Formation has no prominent reflection at available seismic line crossing the borehole. Therefore it was preferred to interpret a prominent reflection above the Kveite Formation. The reflection interpreted above the Kveite Formation is named as the near base-Eocene which is also the oldest interpreted reflection of the study area. All the seismic reflections are assigned a different color code (*Fig. 3.2*).

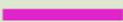




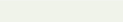


Reflection	Color Code
Upper-Neogene	
Intra-Pliocene	
Intra-Miocene	
Intra-Oligocene	
Intra-Eocene	
Near base-Eocene	
Intra-Triassic	
Top-Permian	

Figure 3.2: Color codes used for the interpreted reflections of the study area.

The top Permian and the intra Triassic are interpreted on the basis of work done by Glørstad-Clark et al. (2010). The seismic reflections selected and interpreted include the intra-Triassic, the top Permian, the near base-Eocene, the intra-Eocene, the intra-Oligocene, the intra-Miocene, the intra-Pliocene and the upper Neogene (*Fig. 3.3*). The structure maps (time-structure and fault maps) and isopach (time-thickness) maps have also been generated at different selected levels which enhanced the understanding by providing basis for the structural analysis of the area under investigation (*Figs. 3.16-3.22*).

The key seismic lines, of comparatively better resolution, have been selected in order to provide maximum information about all the important architectures within the structural sub-areas. These selected seismic profiles are then used to analyze the structural style, fault geometry and the associated stratigraphic patterns.

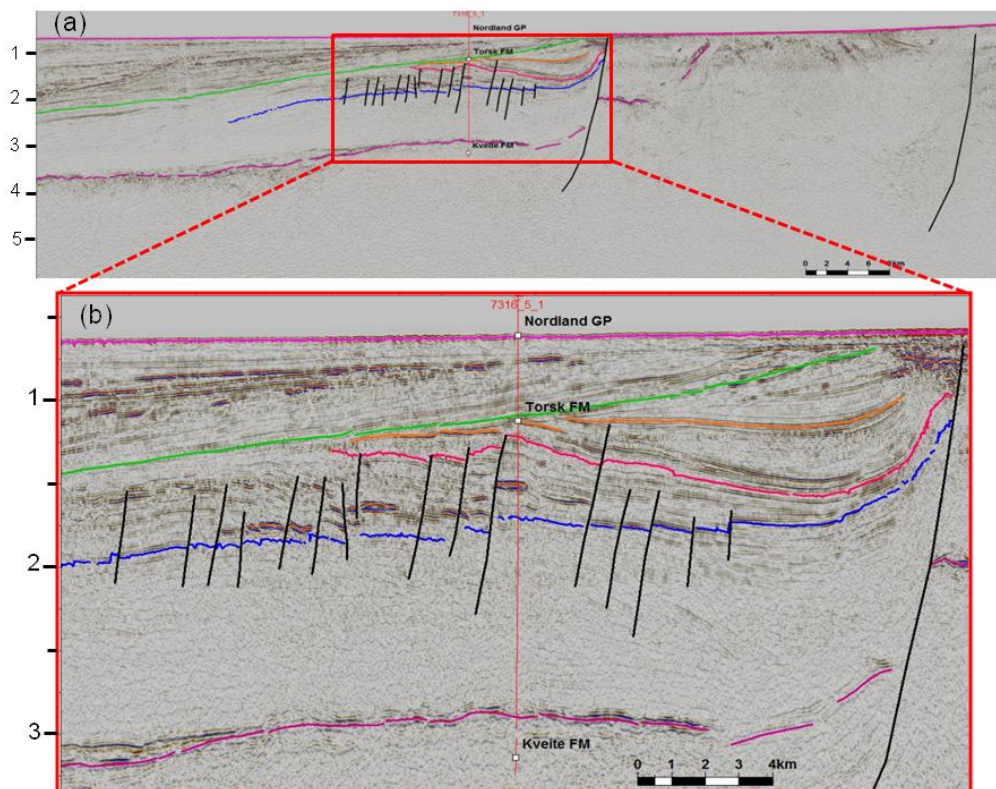


Figure 3.3: The seismic line crossing the borehole 7316/5-1 in the Vestbakken Volcanic Province. The seismic reflections from the near base Eocene to the upper-Neogene are interpreted. In the figure **a**) represents the entire seismic line H while **b**) shows the more focused view of the red outlined box in figure a. For color codes refer to the Fig. 3.2 and for the well tops information refer to the Fig. 3.4.

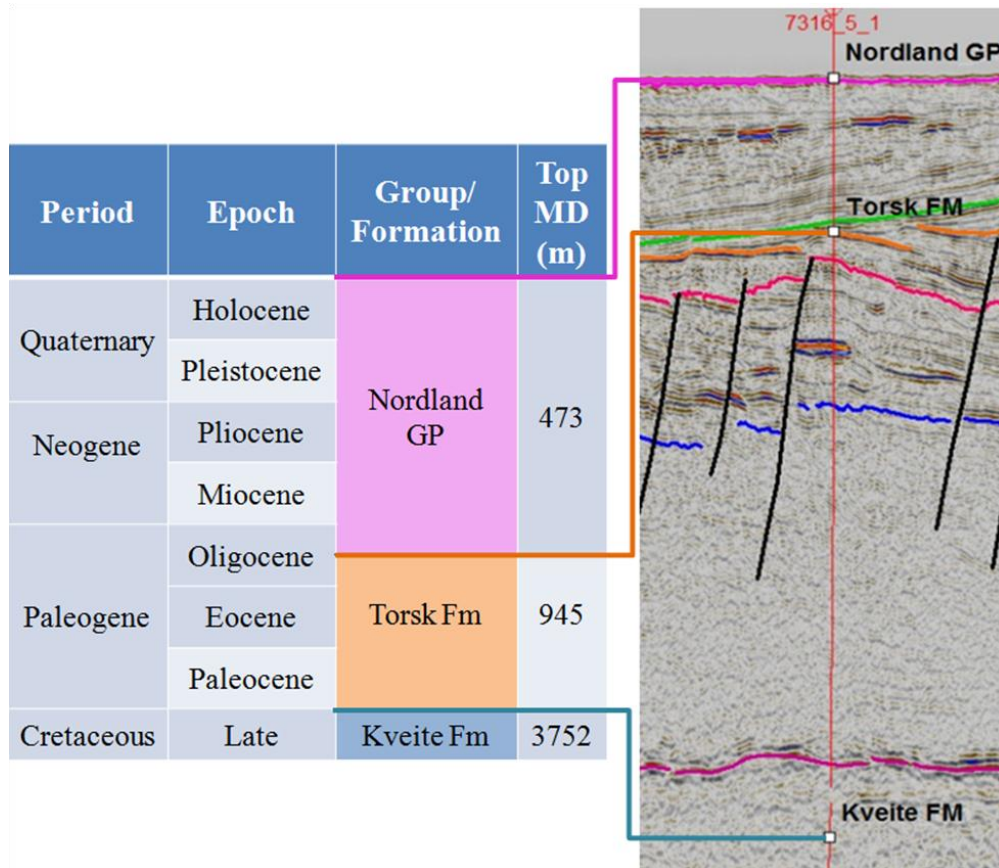


Figure 3.4: Seismic tie to well 7316/5-1. This well is located at the Vestbakken Volcanic Province which is on the southern most part of the study area. For the location of the well refer to the Fig. 3.1.

3.4 Description of Structural Architecture and Fault Plane Geometries of Key Seismic Lines

This section is presented to illustrate the major structural elements and their features within the study area. The area under observation is divided into the fault segments (*Fig. 3.5*) and structural sub-areas (*Fig. 3.8 a, b*). Seven key seismic lines have been selected to describe all the structural elements and sub-features which will be described in detail later in this section.

The study area is divided into three main fault segments as seen in the map view (*Figs. 3.5 and 3.6*). These segments extend from north to south in the area and are termed “*segments 1, 2 and 3*”. The reasons to divide the area into three segments are:

- The master faults are divided into various segments on the basis of changes in their orientation and continuity along the strike.
- **The segment 1** is particularly defined on the basis of master faults F-A and F-B (*Fig 3.5*). These faults are either related to the Knølegga Fault Complex area or represent overstepping to the Svalbard structural elements.
- The subdivision of the Knølegga Fault Complex into **segments 2 and 3** is based on contrast in the trend of the master faults. Thus, the trend of master faults F1-a, F1-b and F2-b is NNW-SSE in **segment 2**. F2-c and the southern part of F1-c trends N-S in **segment 2**, as seen along strike (*Fig. 3.5*).
- The trend of **segment 3** changes from N-S to NNE-SSW (*Fig. 3.5*).
- **The segment 3** has only two structural sub-areas (*Fig. 3.7*).

The normal faults F1-, F2-, F-A and F-B represent the master faults of the study area separating structural subareas, and having a general westward dip of the fault planes. F-A and F-B are only present in **segment 1**. The nomenclature F1-, F2-, F-A and F-B is only dedicated to master faults, important is to consider that no small fault has such names. Master fault F1 has three more segments F1-a, F1-b, F1-c, and two splays F1-d and F2-e. For example, master fault F1 separates the Knølegga Fault Complex (hanging wall) in the west, from the Stappen high (footwall) in the east as is illustrated by *Fig. 3.8 a, b*. Master fault F-2 is the western most master fault of study area (*Fig. 3.5*). Similarly, F2 has four segments F2a, F2b, F2c and F2d. F2 is the most westerly master fault (*Fig. 3.5*). F1 and F2 encompass the Knølegga Fault Complex area. The master fault F-B, F1-b and F1-c are boundary faults as these separate the hanging wall from the footwall, and are termed the Knølegga Fault. Generally, depth of the Knølegga Fault (F-B, F1-b, F1-c) increases from the north to the south of the area under investigation (*Figs. 3.9-3.15*). In twt, the Knølegga Fault cuts the reflections up to approximately 2, 2.5, 3.2, 3.3, 3.5, 3.2, 2.5 sec (TWT) in all key seismic lines from A to G, respectively (*Figs. 3.9-3.15*). Therefore, the displacement along the boundary faults is maximum at location of key seismic line E (*Fig. 3.13*).

The nomenclature used to define the small faults within the Knølegga Fault Complex is that the small faults are represented by the alphabet ‘f’ with numeric ‘1, 2, 3...n’ representing their

numbers ascending from the east to the west of the each seismic line. The same nomenclature will be used during description of all key seismic lines of the study area.

The frequency of faulting in *segment 1* is dense as compared to *segment 2* and *segment 3* (*Fig. 3.5*). To make a confident linkage of the master faults in *segment 1* with the Svalbard structural elements, sufficient seismic data is required further to the north of the study area. *Segment 2* in the middle and segment 3 at the south of the fault map are believed to represent the Knølegga Fault Complex area (*Fig. 3.5*). Two key seismic lines A, B from *segment 1*, three key seismic lines C, D and E from segment 2 and two key seismic lines F, G have been selected to describe *segment 3* in detail (*Fig. 3.5*).

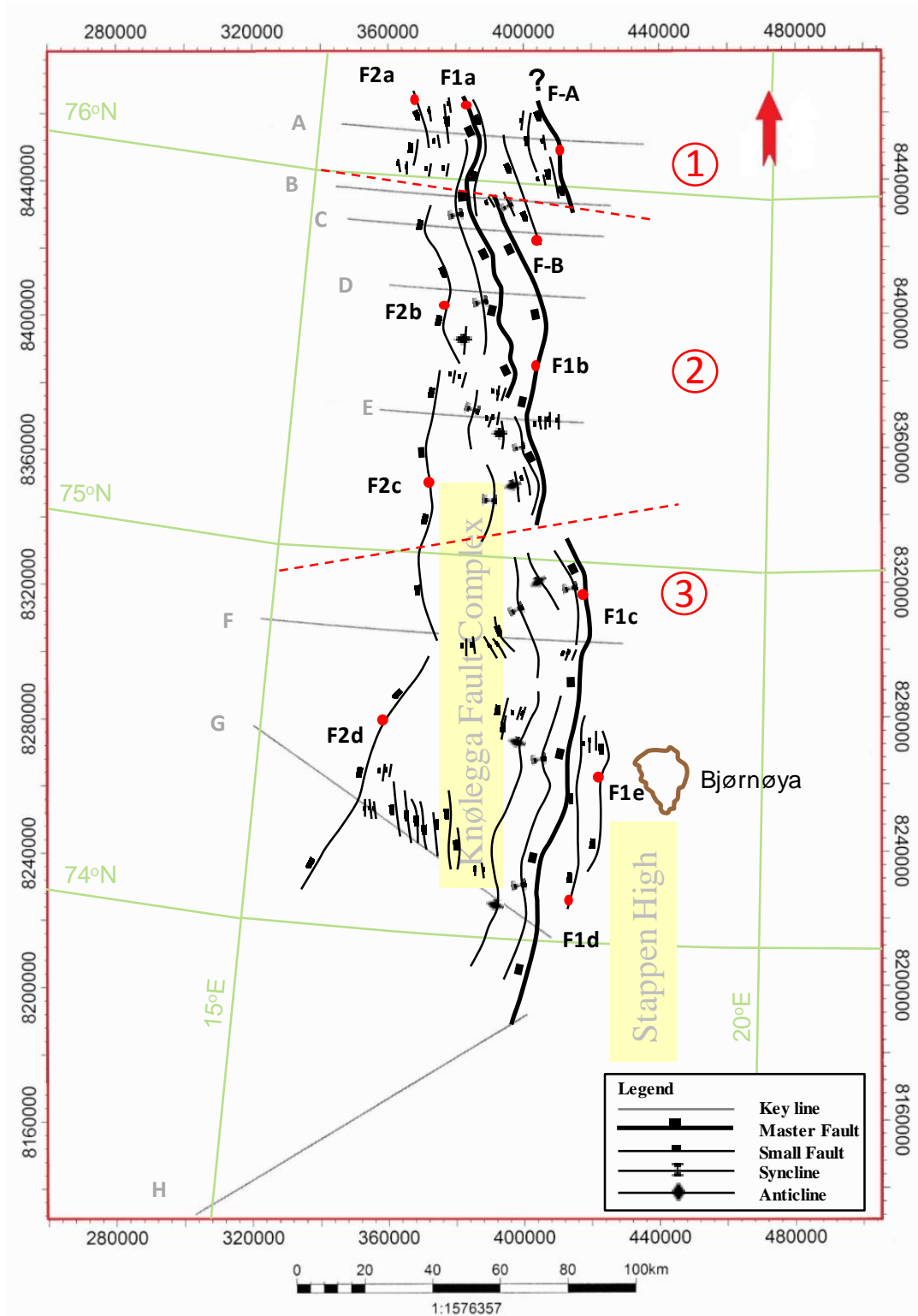


Figure 3.5: Fault map at the near base Eocene level showing the different faults, synclines, anticline and three master fault segments of the study area.

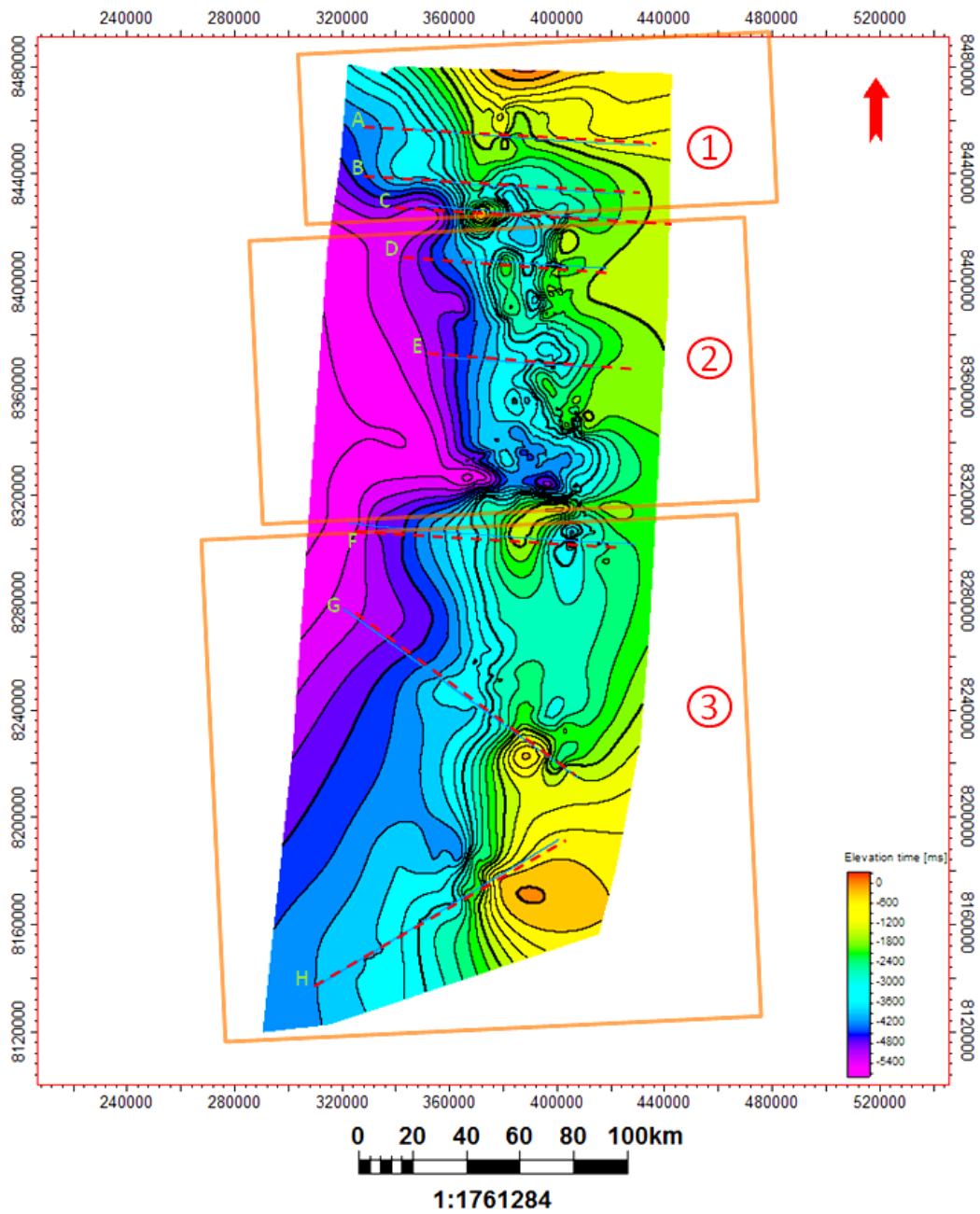


Figure 3.6: Time structure map at the near base Eocene, the rectangles show structural segments of the main study area. Location of the key seismic lines is also indicated by red dotted lines. The black contour lines, particularly within the *segment 2*, are created by Petrel software because of dense contouring.

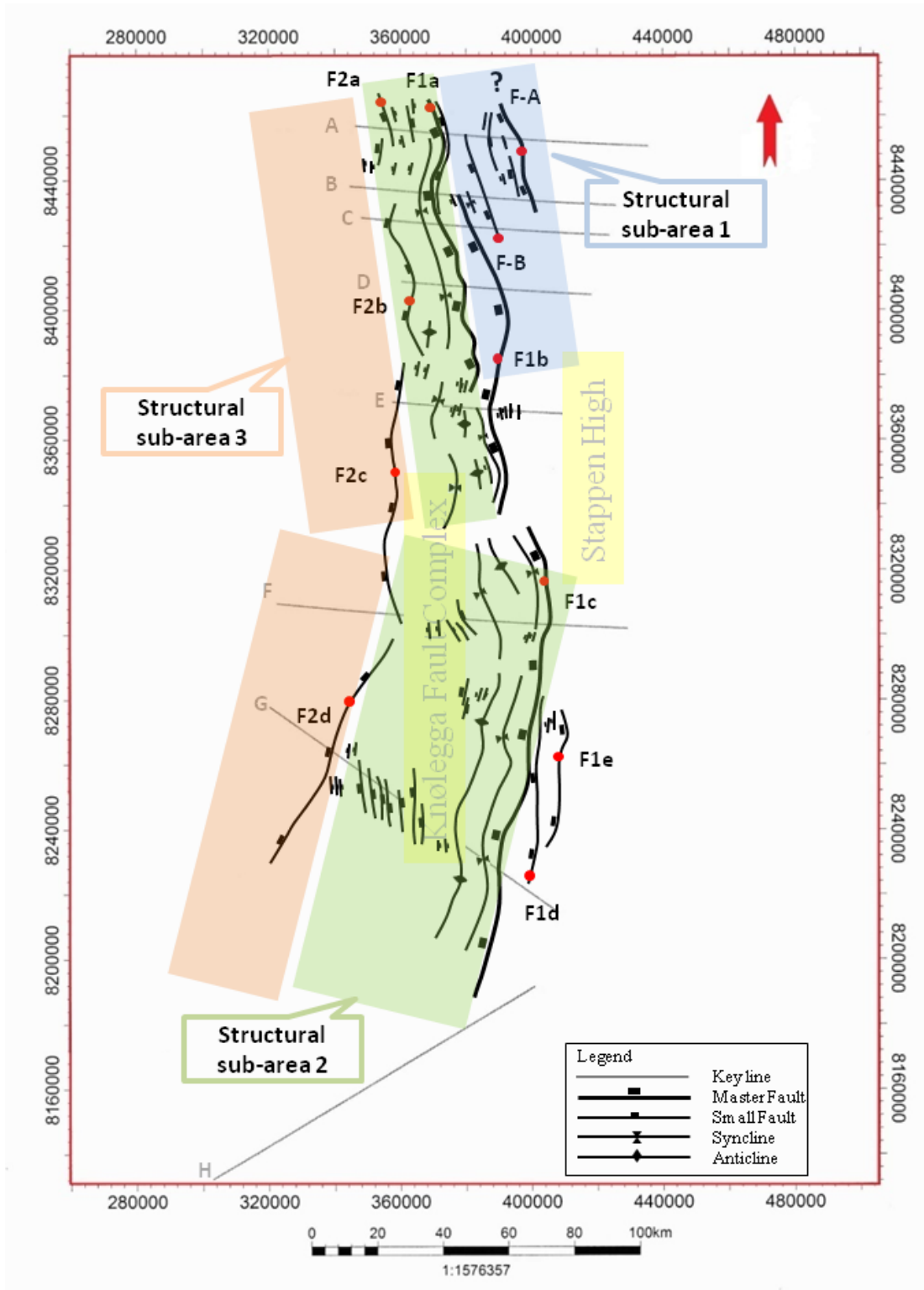


Figure 3.7: The structural sub-areas are indicated by different rectangles. This figure also shows that the structural *sub-area 1* is only in the northern part of the study area. In the southern part only two *sub-areas* (2 and 3) represents the study area. The structural *sub-area 2* is wider in the south of area under description.

The key seismic lines are described according to **structural sub-areas 1, 2 and 3**, from the east to the west of each key line (*Figs. 3.7 and 3.8 a, b*). The structural **sub-area 1** is defined by F1-a in the east and F-A, F-B or F1-b in the west (*Figs. 3.7 and 3.8 a, b*). The **sub-area 2** is limited by the master faults F1-a, southern part of F1-b and F1-c in the east and master fault F2 in the west (*Figs. 3.7 and 3.8 a, b*). The structural domain on the west of the hanging wall is the structural **sub-area 3** (*Figs. 3.7 and 3.8 a, b*). The **sub-area 1** is present on the east of the F1-a (*Fig. 3.5 a*), therefore, this sub-area is constrained by the termination of F1-a, between the key lines D and E (*Fig. 3.7*). Only two structural sub-areas can be defined in the area covered by the key line E to the key line G, which are **sub-area 2** and **sub-area 3** (*Fig. 3.7*). The width of **sub-area 1** decreases from the key line A to key line D as its eastern boundary shifts from F-A to F-B and then F1-b, while the width of **structural sub-area 2** increases southwards of key line E (*Fig. 3.7*).

A general demonstration of the structural sub-areas, master faults, syncline and anticline is seen from the key lines C and F (*Fig. 3.8 a, b*). Another important feature within the area under observation is presence of synclines and an anticline. The syncline in the west of master fault F1 is termed Syn-A (*Fig. 3.8 a, b*). The axis of Syn-A runs parallel to F1-a, F1-b and F1-c from north to south in all the three segments (*Fig. 3.5*). On the west of Syn-A an anticline is observed (*Fig. 3.8 b*), which is not continuous in **segment 2** but seems to be continuous in **segment 3**. The anticline is nearly parallel to Syn-A in **segment 3** (*Fig. 3.5*). Between Syn-A and F2-b another syncline, termed as Syn-B is interpreted (*Fig. 3.5*). The anticline and Syn-B is not observed in **segment 1**.

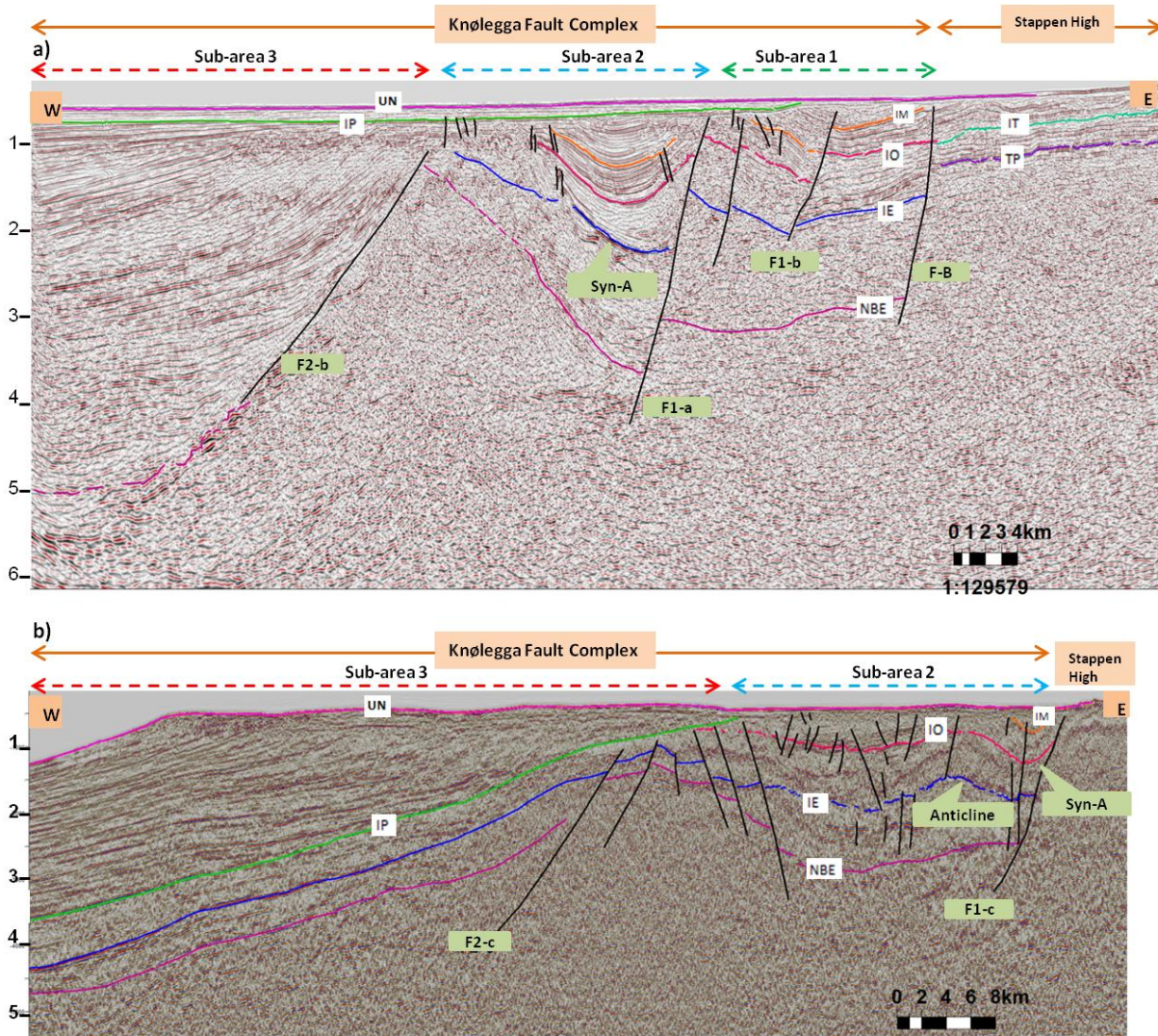


Figure 3.8: The key seismic line C (a) and key seismic line F (b) demonstrating the structural sub-areas and master faults. Also the variation in structures within sub-areas from the north to the south is illustrated in line C and F, respectively.

The general outline follows the specific description of seven key lines, starting from the key seismic lines of *segment 1* to *segment 3*. It is important to note that when dips and fault plane geometries are given during the description, these are based on the seismic data which is not depth-converted.

3.4.1 Key Seismic Line A

The key E-W oriented seismic line A is the northern most key line and belongs to *segment 1* (Fig. 3.5). This most deformed key line images the NW-SE trending master faults F-B, F1-a and F2-a with NE-SW dip (Figs. 3.5, 3.9). These master faults are steep to planar normal faults (Fig.3.9). This key line could be the transition from the Knølegga Fault Complex to the structural elements of Svalbard in the north of the study area. The master fault controlling the main structural features is F-B (Fig.3.9). F-B separates the platform in the west from the tectonically deformed Knølegga Fault Complex in the east of this key line (Fig.3.9). The sediments to the west of F-B are of the Cenozoic sub-era (Fig.3.9). The set of small normal faults f3 to f22 shows synthetic to antithetic behavior (Fig.3.9). F-B, F1-a, F2-a f9, f11 and f15 cut the sediments at levels deeper than the near base Eocene (Fig.3.9). The platform is deformed by F-A, f3, f4 and f5 (Fig.3.9). F-A (70°) shows minor offset within the platform, f3 is antithetic to F-A while f4 and f5 are synthetic (Fig.3.9). The intra Miocene is eroded at this location (Fig.3.9).

The *structural sub-area 1* is delimited by F-B steep (70-80°) to the east and F1-a to the west (Fig.3.9). A syncline is observed in sub-area 1 (Fig.3.9). This syncline in *sub-area 1* is only observed at this location and has no extent to the south of key line A (Fig.3.9). f6 shows antithetic behavior while f7 to f12 demonstrates synthetic to vertical in *sub-area 1* (Fig.3.9). The reflection intra Oligocene terminates along the upper Neogene reflection (Fig.3.9).

The *sub-area 2* is structural domain defined by F1-a (80°) to the east and F2-a to the west (Fig.3.9). The prominent feature of *sub-area 2* is the syncline Syn-A which is interpreted within the entire Knølegga Fault Complex and is the key feature of *sub-area 2* (Fig.3.9). The axis of Syn-A is parallel to the fault plane of F1-a. The seismic reflections near base Eocene, intra Eocene and intra Oligocene terminate with F1-a in the eastern flank of Syn-A (Fig.3.9). In *sub-area 2* the deeper deformed reflections terminate to the undeformed upper Neogene reflection at the top (Fig.3.9). The sediments acquired maximum thickness along the axis of Syn-A (Fig.3.9). Syn-A terminates with f15 on its western flank (Fig.3.9). The area between f15 and F2-a is deformed by antithetic f16 and synthetic f17, f18 small faults (Fig.3.9).

The sub-area is delimited to the west by F2-a (50-70°) planar to listric normal fault (*Fig.3.9*). f19 to f22 are synthetic to vertical faults with minor offset (*Fig.3.9*). The intra Pliocene reflection is shallower at this location and defines an unconformable contact (*Fig.3.9*).

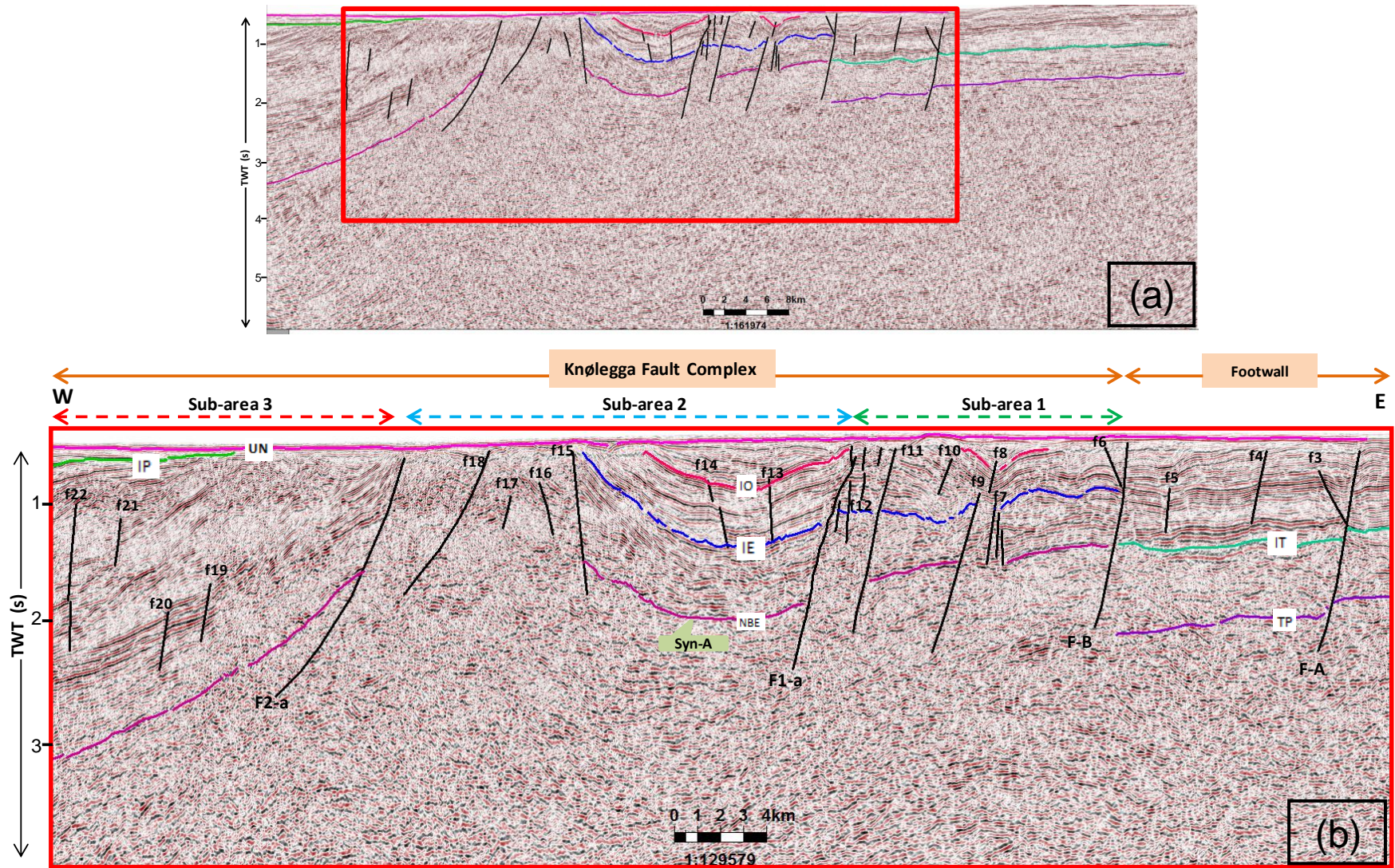


Figure 3.9: The key seismic line A. This line represents the *structural sub-areas 1, 2 and 3*, master and small faults, interpreted seismic reflections. The age of each reflection is also shown by small boxes at each reflection of the hangingwall and footwall. For the location of this line refer to the Fig. 3.1. The abbreviations in white boxes at each reflection are: UN-upper Neogene, IP-intra Pliocene, IM-intra Miocene, IO-intra Oligocene, IE-intra Eocene, NBE-near base Eocene, IT-intra Triassic, TP-top Permian.

3.4.2 Key Seismic Line B

The key E-W oriented seismic line B is located in the south of *segment 1* and northern part of the area under observation (*Fig. 3.5*). This key line provides a transition from *segment 1* to *segment 2*. The key line images the master faults F-A, F-B, F1-b, F1-a and F2-b from the east to west of the line (*Fig. 3.10*). All these master faults are planar normal faults and are dipping NNE-SSW to NW-SE (*Fig. 3.10*). F-A (65-70°), F1-b (55°) and F2-b (60°) are steep planar normal fault, cutting the sediments at levels deeper than the near base Eocene. 'f3' to 'f19' represents small normal faults (45-70°) defining moderate extension of the hanging wall (*Fig. 3.10*). The footwall is also deformed at location of key line B. F-A, f3 and f5 deformed the footwall (*Fig. 3.10*). f6, f9, f11 and f16 are antithetic while all other small faults from f3 to f19 are synthetic to the master faults in behavior (*Fig. 3.10*). The most deformed reflection in the key line B is the intra Eocene. The intra Oligocene also experienced tectonic deformation. The intra Miocene at this seismic section is least deformed (*Fig. 3.10*).

The *sub-area 1* in this key line is defined by the structural domain limited by F-A in the east and F1-b in the west (*Fig. 3.10*). Two important observations in this sub-area are the existence of a roll-over anticline along F-B and rotated fault block along F1-b (*Fig. 3.10*). F1-b represents a planar rotational normal fault as the block over it is rotated along the fault plane. To the eastern flank of Syn-A, the area between F1-b and F1-a is deformed by the small faults f8 to f11 (*Fig. 3.10*). f8 and f9 are antithetic to F1-b while f10 is synthetic to both F1-b and F1-a. The area bounded by F1-b and F1-a seems to be an anticline deformed along its axis (*Fig. 3.10*).

The *sub-area 2* is the structural area delimited by F1-a in the east and F2-b in the west (*Fig. 3.10*). The prominent feature in this sub-area is the presence of a folded structure i.e., the syncline Syn-A in the west of F1-a. The western flank is more deformed by small faults f12 to f16 (*Fig. 3.10*). This syncline is imaged from the north to the south in all the key seismic sections. The thickness of sediments increases along axis of Syn-A (*Figs. 3.9-3.15*). The reflections intra Oligocene and intra Miocene terminates along the intra Pliocene, which overlies unconformably (*Fig. 3.10*). The intra Pliocene shows an unconformity in the study area (*Figs. 3.9-3.15*).

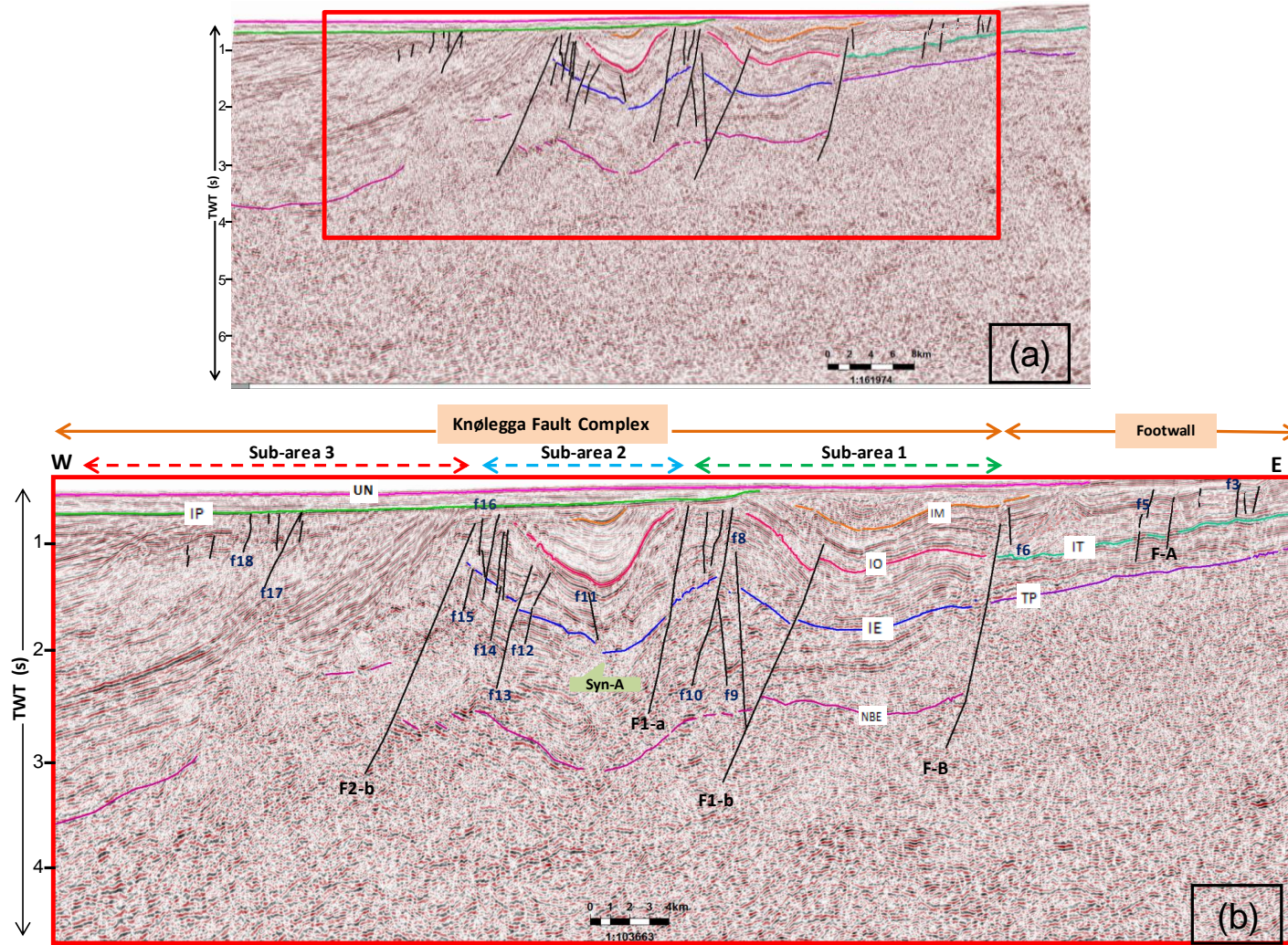


Figure 3.10: The key seismic line B. This line represents the structural *sub-areas 1, 2 and 3*, master and small faults, interpreted seismic reflections. The age of each reflection is also shown by small boxes at each reflection of the hangingwall and footwall. For the location of this line refer to the Fig. 3.1. The abbreviations in white boxes at each reflection are: UN- upper Neogene, IP- intra Pliocene, IM- intra Miocene, IO- intra Oligocene, IE- intra Eocene, NBE- near base Eocene, IT- intra Triassic, TP- top Permian.

The *sub-area 3* images the wedge shaped reflections in the west of F2-b (*Fig. 3.10*). The western area reflected by this section shows thick sedimentary wedge (*Fig. 3.10*). *Sub-area 3* is less deformed than *sub-area 1* and *2*.

3.4.3 Key Seismic Line C

The key E-W oriented seismic line C is located in the northern part of *segment 2* (*Fig. 3.5*). The key line is described according to the structural sub-areas. The important features imaged by this key line are the tilted fault block between F1-a and F1-b in *sub-area 1*, and the syncline Syn-A in *sub-area 2* on the west of F1-a (*Fig. 3.11*). The line displays faulted, folded and westward dipping reflections in *sub-areas 1, 2* and *3* respectively (*Fig. 3.11*). This key line illustrates that the frequency of faulting varies from the east to the west in this location (*Fig. 3.11*). This line displays the master faults F-B, F1-b, F1-a and F2-b, from the east to the west of the line (*Fig. 3.11*). The dip of fault planes of F-B, F3 and F1-a is NNE-SSW while the dip of F2-b is NE-SW. Hence most of the fault planes are westward dipping (*Fig. 3.11*). The master faults F-B, F1-a and F2-b cut the sediments at levels deeper than the near base Eocene. Therefore the throw along these three faults is greater in sum than that of the other faults seen in this line. The key line is described according to the structural sub-areas. The important features imaged by this key line are the tilted fault block between F1-a and F1-b in *sub-area 1*, and the syncline Syn-A in *sub-area 2* on the west of F1-a (*Fig. 3.11*). The line displays faulted, folded and westward dipping reflections in *sub-areas 1, 2* and *3* respectively (*Fig. 3.11*). This key line illustrates that the frequency of faulting varies from the east to the west in this location (*Fig. 3.11*).

The series of small normal faults represent a moderate extension within *sub-area 1 and 2*. These small faults are from f1 to f11. In this line two faults with the same dip are given only one fault name which includes f5, f6, f7, f8 and f10. Small faults in *sub-areas 1 and 2* have mostly disturbed the sedimentary package between the intra Oligocene and the intra Miocene in *sub-area 1*. Fault f3 is synthetic to F1-a. The other small faults f2, f5 and f6 in *sub-area 2* have also interrupted the continuity of the reflections between the intra Eocene to the intra Miocene. Faults f1, f4, f7, f8, f9 and f11 shows westward dip and hence are termed synthetic to the master faults

(F-B, F1-b, F1-a and F2-b). Faults with an eastward dip represent antithetic behavior and these are f2, f5, f6 and f10 which are mostly concentrated in **sub-areas 1 and 2** (Fig. 3.11).

The structural sub-area 1 at this location is defined by F-B in the east and F1-a in the west (Fig. 3.11). In this sub-area, fault frequency is more than **sub-areas 2 and 3**. The master fault F-B is a normal planar fault and is synthetic to the master fault F1-a. F-B cuts the stratigraphic succession from the intra Miocene to the near base Eocene. The hanging wall is more deformed as compared to the footwall as displayed by key line C (Fig. 3.11). The Stappen high has almost sub parallel reflections as the top Permian and the intra-Triassic reflections (Fig. 3.11). The master fault F-B also defines the eastern boundary of the study area. The reflections intra-Eocene, intra-Oligocene and intra-Miocene between F-B and F1-b, are dipping westward. F1-b shows listric normal geometry. The fault plane geometry of F1-b is less steep as compared to F-B and F1-a. F1-b cuts the stratigraphic succession from the intra Miocene to the intra Eocene. The seismic reflection near base Eocene is deformed by the three faults F-B, F1-a and F2-b as these faults extend to greater depth as compared to F1-b and F3.

The sub-area 2 is defined by an area in the west of F1-a and has prominent feature of the syncline Syn-A (Fig. 3.11). The sedimentary package becomes thicker along axis of the syncline, while it thins at crestal flank of the syncline. The seismic reflections near base Eocene, intra Eocene, intra Oligocene and intra Miocene terminates along the fault F1-a on the eastern crestal level of the syncline. The seismic reflections including the intra-Eocene, the intra-Oligocene and the intra-Miocene in **sub-area 2** pinch out towards western limb of the syncline. In **sub-area 2**, F1-a interrupted the succession from the intra Miocene to the near base Eocene. An almost complete syncline in **sub-area 2** at this key line is represented by seismic reflections of the intra Oligocene and the intra Miocene (Fig. 3.11).

The sub-area 3 is structural domain in the west of this dip line separated by the master fault F2-b (Fig. 3.11). The **sub-area 3** has least frequency of faults. F2-b is less steep as compared with the other master faults. On the west of F2-b the reflections are dipping westward and the area is tectonically less deformed. These seismic reflections represent the thick sedimentary wedge of Pliocene-Pleistocene epoch (Faleide et al., 1996; Hjelstuen et al., 1996; Bergh and Grogan., 2003).

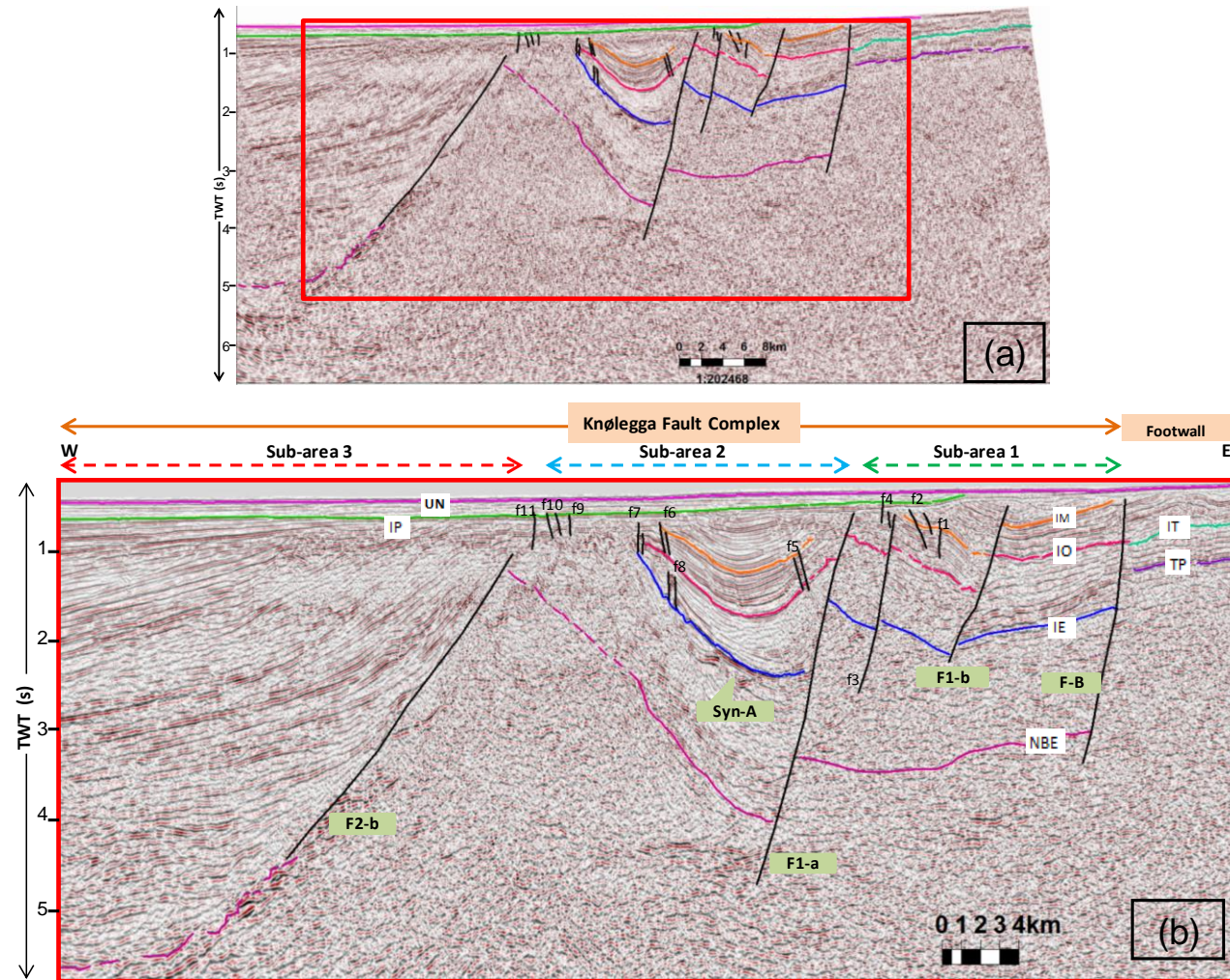


Figure 3.11: The key seismic line C. This line represents the structural *sub-areas 1, 2 and 3*, master and small faults, interpreted seismic reflections. The age of each reflection is also shown by small boxes at each reflection of the hanging and footwall. For the location of this line refer to the Fig. 3.1. The abbreviations in white boxes at each reflection are: UN-upper Neogene, IP-intra Pliocene, IM-intra Miocene, IO-intra Oligocene, IE-intra Eocene, NBE-near base Eocene, IT-intra Triassic, TP-top Permian.

3.4.4 Key Seismic Line D

The key E-W oriented seismic line D is located in the northern part of both segment 2 and the study area (*Fig. 3.5*). This seismic section illustrates that less deformation is experienced by the Knølegga Fault Complex area at this location. The structure of syncline Syn-A is prominently imaged at this location (*Fig. 3.12*). The master faults F-A and F-B terminates to the north of the key line D (*Fig. 3.5*), hence these master faults have not effected the location imaged by the key line (*Fig. 3.12*). Therefore, F1-b in the east separates the Knølegga Fault Complex from the Stappen High (*Fig. 3.12*). The other master faults in the key line are F1-a and F2-b (*Fig. 3.12*). f3 to f9 are the small faults representing moderate extension, interpreted in the *sub-area 1* except f9 (*Fig. 3.12*). The moderate synclines and anticlines in the footwall also show the effect of folding within the top Permian and intra Triassic reflections (*Fig. 3.12*). The interpreted reflections demonstrate less deformation at this location (*Fig. 3.12*).

The *sub-area 1* is structural domain defined by F1-b in the east and F1-a in the west (*Fig. 3.12*). F1-b is listric normal fault as its dip decreases with depth from 70° to 55° (*Fig. 3.12*). f3, f4 and f7 are antithetic while f5, f6 and f8 are synthetic to F1-b. f8 cut the sediments at levels deeper than intra Eocene (*Fig. 3.12*). The *sub-area 2* illustrates the structural domain bounded by F1-a in the east and F2-b in the west (*Fig. 3.12*). The axis of Syn-A seems parallel to F1-a (*Fig. 3.12*). F1-a is steep ($50-80^{\circ}$) planar to listric normal fault. The reflections intra Oligocene and intra Miocene terminates along the intra Pliocene (*Fig. 3.12*). The structural *sub-area 3* is sedimentary wedge bounded in the east by F2-b, the steep (60°) planar normal fault (*Fig. 3.12*). *Sub-area 3* is tectonically less deformed (*Fig. 3.12*).

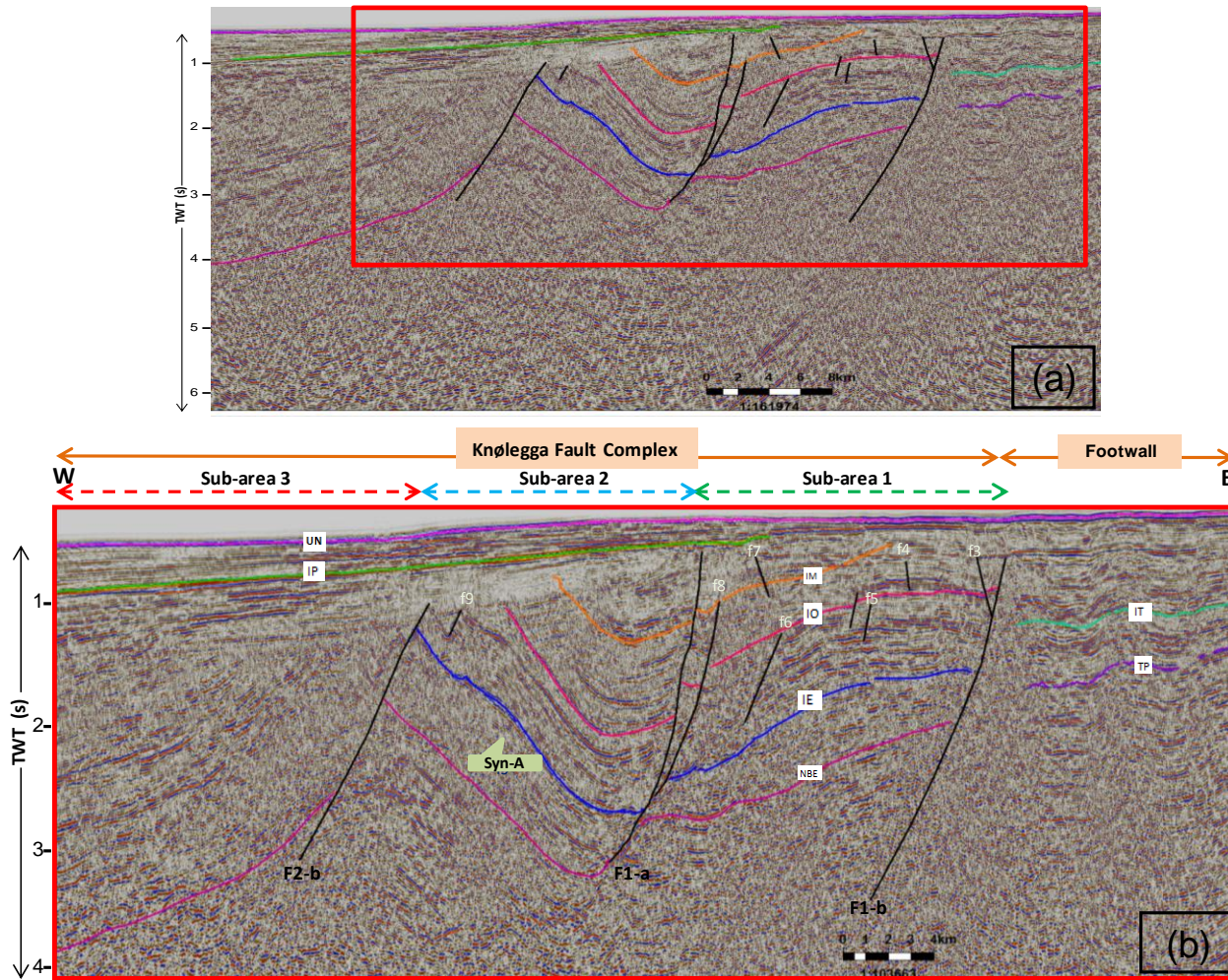


Figure 3.12: The key seismic line D. This line represents the structural *sub-areas 1, 2* and *3*, master and small faults, interpreted seismic reflections. The age of each reflection is also shown by small boxes at each reflection of the hangingwall and footwall. For the location of this line refer to the Fig. 3.1. The abbreviations in white boxes at each reflection are: UN-upper Neogene, IP-intra Pliocene, IM-intra Miocene, IO-intra Oligocene, IE-intra Eocene, NBE-near base Eocene, IT-intra Triassic, TP-top Permian.

3.4.5 Key Seismic Line E

The key E-W oriented seismic line E belongs to *segment 2* in the central part of the study area (*Fig. 3.5*). This line images the NW-SE dipping master faults F1-b and F2-c which bounds two structural sub-areas (*Fig. 3.13*). The displacement along the boundary fault F1-b is maximum i.e. c. 3.5 sec, at location of key seismic line E which decreases towards the north and south of this key line (*Fig. 3.13*). Two synclines and an anticline are interpreted at this location (*Fig. 3.13*). F1-b in the east is the main boundary fault separating the deformed hanging wall from the less deformed footwall in the west (*Fig. 3.13*). The sub-parallel seismic reflections interpreted within the footwall are the top Permian and the intra Triassic (*Fig. 3.13*). The fault zone along the boundary of hanging wall and footwall is deformed by steep (80°) to vertical faults at this location (*Fig. 3.13*). The series of small faults f3 to f18 represents moderate extension and antithetic to synthetic behavior (*Fig. 3.13*).

The *structural sub-area 2* is defined by the F1-b ($50-80^\circ$) normal planar to listric fault in the east and F2-c steep (80°) planar normal fault in the west. This sub-area demonstrates folded structures including two synclines Syn-A in the east, Syn-B in the west and an anticline in the middle of both synclines (*Fig. 3.13*). All the seismic reflections interpreted at levels deeper than intra Pliocene terminate along F1-b (*Fig. 3.13*). The sediments thickness is maximum along the axis of Syn-A. The axis of Syn-A is nearly parallel to the fault plane of F1-c (*Fig. 3.13*). Syn-B is wider and deeper than Syn-A but is not interpreted within the entire Knølegga Fault Complex (*Figs. 3.5 and 3.13*). The reflections along the axis of anticline become at shallower level (*Fig. 3.13*). f13 and f14 are antithetic faults, while all other f7 to f16 are synthetic to slightly vertical small faults mostly concentrated along the axis of anticline (*Fig. 3.13*).

The *sub-area 3* is least deformed structural domain to the west of F2-c (*Fig. 3.13*). f17 is an antithetic and f18 is nearly vertical small fault.

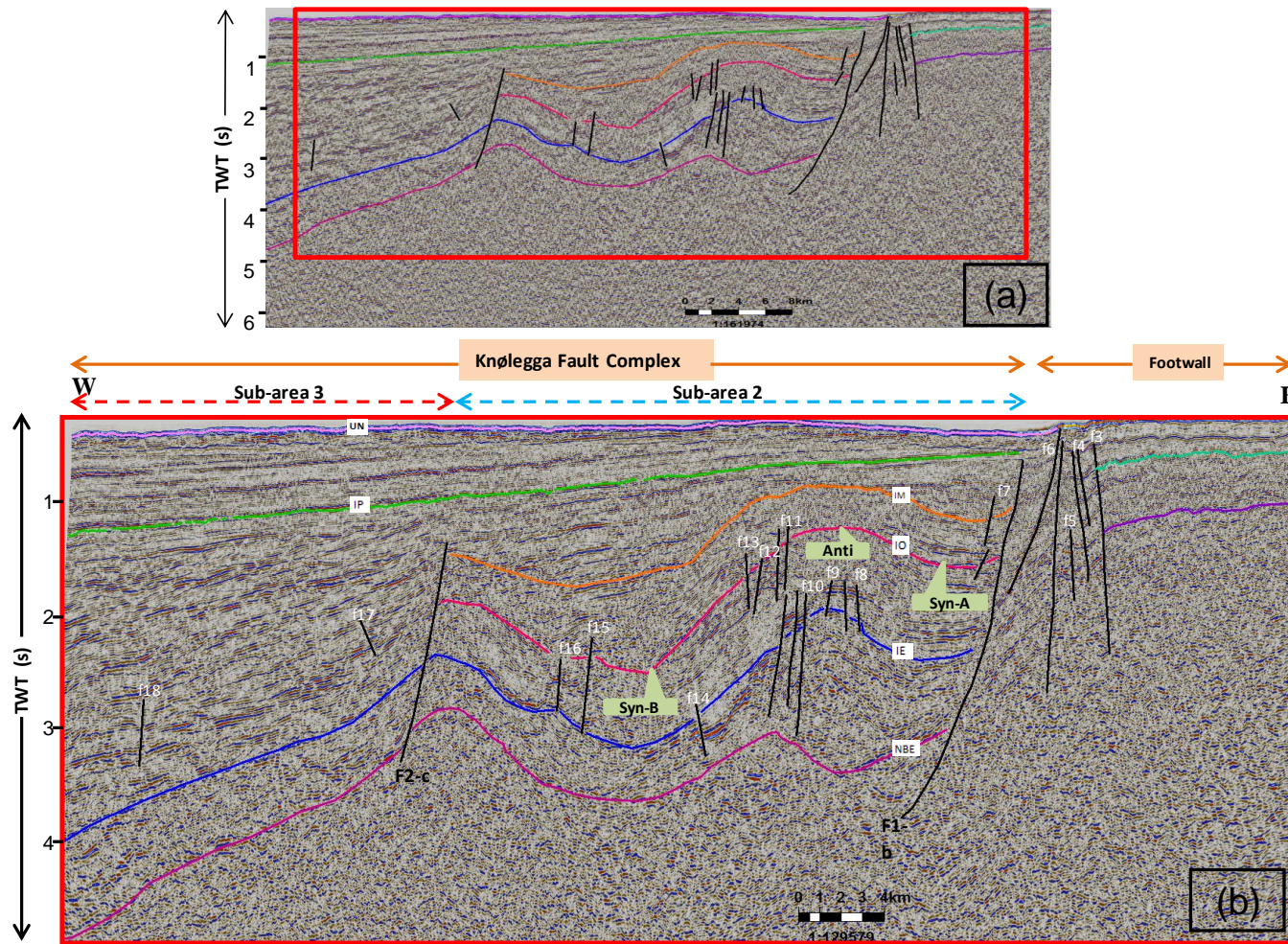


Figure 3.13: The key seismic line E. This line represents the structural *sub-areas 2* and *3*, master and small faults, interpreted seismic reflections. The age of each reflection is also shown by small boxes at each reflection of the hangingwall and footwall. For the location of this line refer to the Fig. 3.1. The abbreviations in white boxes at each reflection are: UN-upper Neogene, IP-intra Pliocene, IM-intra Miocene, IO-intra Oligocene, IE-intra Eocene, NBE-near base Eocene, IT-intra Triassic, TP-top Permian.

3.4.6 Key Seismic Line F

The key E-W oriented seismic line F is located in the north of *segment 3* and southern part of the study area (*Fig. 3.5*). The Knølegga Fault Complex at this location is divided into two segments i.e., *segment 2* and *3*. As key seismic section E, prominent features displayed by the key line F are also the synclines Syn-A and Syn-B, and an anticline between these two synclines (*Figs. 3.13 and 3.14*). The dip of faults shown by this key seismic section is 45-80° (*Fig. 3.14*). The master faults imaged by the key line are F1-c and F2-c with dip in the west (*Fig. 3.14*). f3 to f21 are synthetic to antithetic faults which are described in *sub-area 2* in detail. Nearly all seismic reflections below the intra Pliocene are deformed at this location (*Fig. 3.14*).

The *structural sub-area 2* is defined by the master fault F1-c in the east and F2-c in the west (*Fig. 3.14*). F1-c (45-60°) is steep planar to listric normal fault which separates the more deformed Knølegga Fault Complex in the west from the less deformed footwall in the east (*Fig. 3.14*). f3 is steep (80°) planar normal fault dipping in the west and cut the sediments along the axis of Syn-A (*Fig. 3.14*). f4 and f5 are synthetic to f3. F6 is characterized by a planar normal fault parallel to the axis of anticline (*Fig. 3.14*). Syn-B is the wider and deeper syncline defined by f6 in the east to the f14 in the west. Syn-B is intensely deformed by synthetic and antithetic small faults (*Fig. 3.14*). Most of the small faults are planar normal synthetic faults except some antithetic faults f9, f10, and f13. Staircase geometry is observed along f14, f15 and f16 (*Fig. 3.14*).

The *sub-area 3* is structural domain to the west of the steep (45-50°) normal planar master fault F2-c (*Fig. 3.14*). The westward dipping reflection of intra Pliocene is deeper at this location than the key seismic lines to the north of key line F (*Figs. 3.9-3.11, 3.14*).

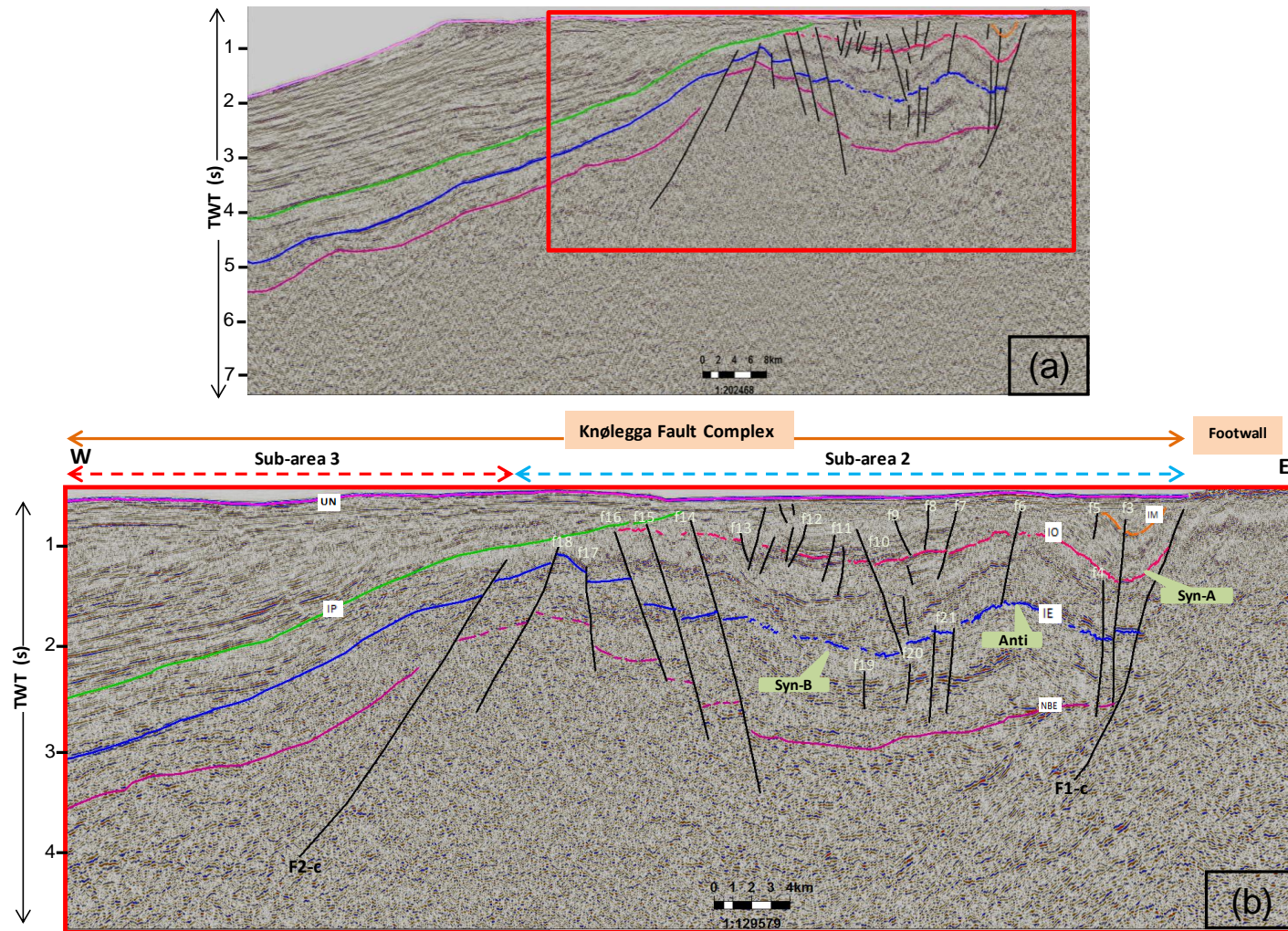


Figure 3.14: The key seismic line F. This line represents the structural *sub-areas 2* and *3*, master and small faults, interpreted seismic reflections. The age of each reflection is also shown by small boxes at each reflection of the hangingwall and footwall. For the location of this line refer to the Fig. 3.1. The abbreviations in white boxes at each reflection are: UN-upper Neogene, IP-intra Pliocene, IM-intra Miocene, IO-intra Oligocene, IE-intra Eocene, NBE-near base Eocene, IT-intra Triassic, TP-top Permian.

3.4.7 Key Seismic Line G

The key NW-SE oriented seismic line G is the southernmost oblique seismic section offered to represent structural architecture of the study area (*Fig. 3.5*). The resolution of this key line is low which prevented to interpret the seismic reflections well laterally and also to tie it with other seismic lines. The NE-SW trending master faults F1-c and F2-d with general dip to the west are displayed by this key line (*Figs. 3.5, 3.15*). f3 to f16 are small faults from the east to the west of the line (*Fig. 3.15*). The study area at this location is deformed by the faulting and folding particularly in **sub-area 2** (*Fig. 3.15*). Syn-A and anticline are observed to the west of F1-c. The area under description experienced greater throw at this location than in the north (*Figs. 3.9-3.15*). F1-c and F2-d cut the sediments deeper than 4-6 sec twt (*Fig. 3.15*).

The **sub-area 2** is structural domain defined by F1-c in the east to F2-d in the west (*Fig. 3.15*). The sub-area at this location is wider than illustrated at locations of key lines A to F (*Figs. 3.9-3.15*). F1-c (55-80°) is steep planar to listric normal fault defining the eastern boundary of the Knølegga Fault Complex by separating it from the Stappen High (*Fig. 3.15*). The footwall is less deformed and shows sub-parallel the top Permian and the intra Triassic reflections. Small faults f3, f8 are vertical, f7, f10, f14, f15, f16 are antithetic while all other small faults are synthetic (*Fig. 3.15*). The series of small faults f3 to f16 represent a moderate extension within sub-area 2 (*Fig. 3.15*). Small faults deformed at levels deeper than the intra Miocene (*Fig. 3.15*). The intra Miocene reflection seems to be eroded within the core of Syn-A (*Fig. 3.15*). The reflections intra Oligocene, intra Miocene and intra Pliocene are also eroded over the anticline (*Fig. 3.15*). The near base Eocene observed along the axis of anticline is at the shallowest level in this key line as compared to the other key lines in the north of the study area (*Figs. 3.9-3.15*).

The **sub-area 3** is structural domain separated in the west of F2-d (*Fig. 3.15*). F2-d is steep (70°) normal planar fault (*Fig. 3.15*). This sub-area is least deformed and has seismic reflections dipping to the west (*Fig. 3.15*).

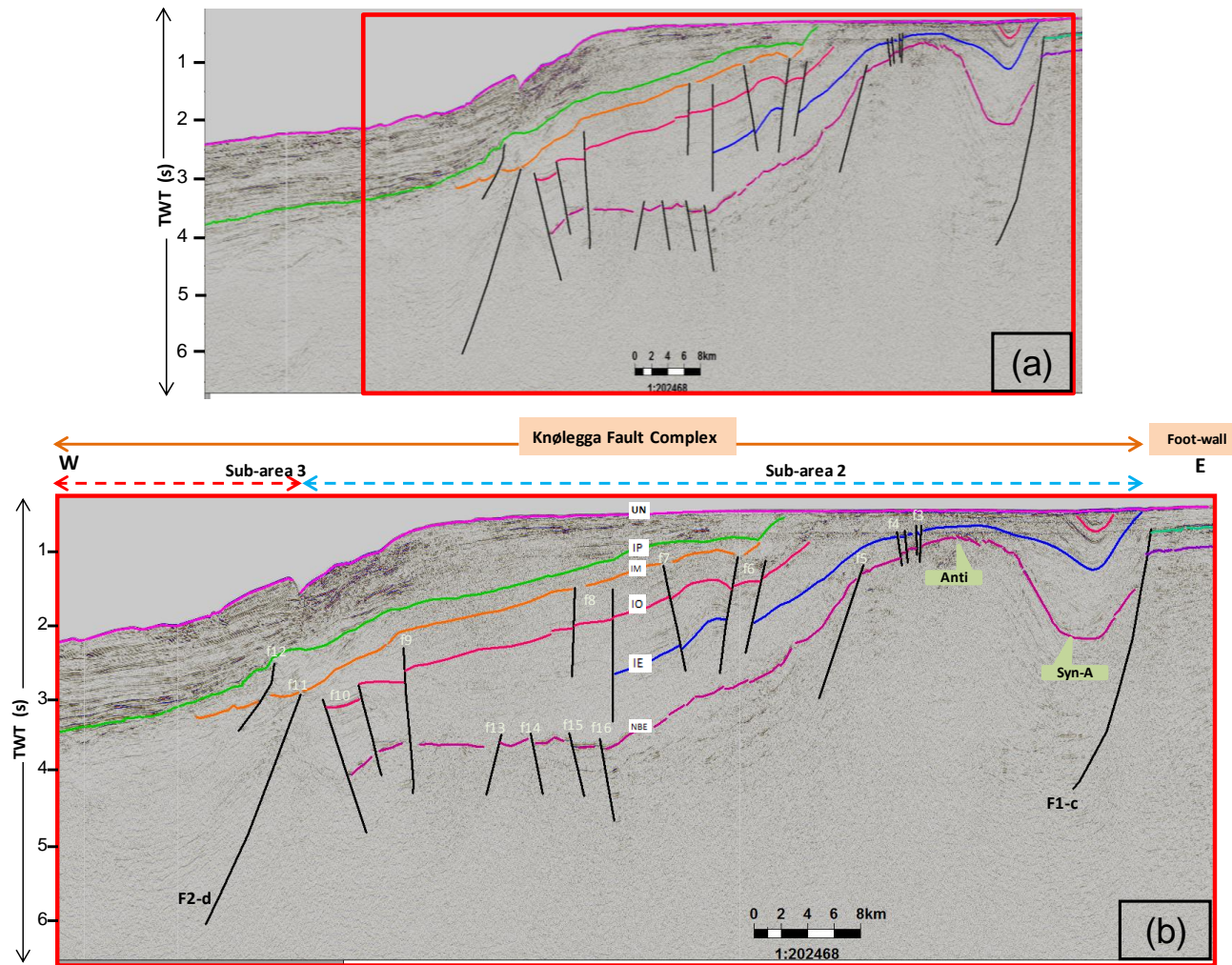


Figure 3.15: The key seismic line G. This line represents the structural *sub-areas 2 and 3*, master and small faults, interpreted seismic reflections. The age of each reflection is also shown by small boxes at each reflection of the hangingwall and footwall. For the location of this line refer to the Fig. 3.1. The abbreviations in white boxes at each reflection are: UN-upper Neogene, IP-intra Pliocene, IM-intra Miocene, IO-intra Oligocene, IE-intra Eocene, NBE-near base Eocene, IT-intra Triassic, TP-top Permian.

3.5 Time-Structure (twt) and Fault Maps

This section mainly deals with the description of the time structure maps and the fault maps. These structural maps have been used to illustrate the fault segmentation, related structures (synclines, anticline) and the lateral orientation of structural elements. The reflections near base Eocene, intra Oligocene and intra Miocene terminate along the master faults F-A, F-B and F1- in the east. Therefore, these reflections are not present over the Stappen High. However, the time-structure maps of these levels show them on the footwall area. It is important to explain that these reflections are not assumed to be zero by the contouring algorithm of “Petrel 2011”, instead the software spread certain values in the footwall area. Therefore, this software glitch should be taken into account when considering the time-structure maps.

The time-structure and fault maps of the near base Eocene level have already been described (refer to *section 3.4* for details) in order to illustrate the structural segmentation and sub-areas of the study area (Figs. 3.5 and 3.6). Therefore, in this section the time-structure and fault maps generated at the levels of intra Eocene, intra Oligocene and intra Miocene are described in going up-section approach.

3.5.1 Intra Eocene

The intra Eocene reflection interpreted shows the tectonic activity within the Knølegga fault Complex at this level (Figs. 3.16 and 3.17). The time structure map of the intra Eocene generally represents westward deepening of the reflection, which is shown by the color variation from shallow to deep (Fig. 3.16). The map shows variation in the trend of master faults (Fig. 3.16). To the east of the master faults time-structure map indicates high structural area (the Stappen High). Alternating time values in the west of the master faults represent synclines and anticlines such as observed along key lines B, C, D, E and F (Fig. 3.16). Displacement along the master faults F-A, F-B and F1- in the east is clear from this reflection (Fig. 3.16). This reflection also displays that the study area become wider from the north to the south (Fig. 3.16). Hence put on view of wider structural *sub-area 2* in the south. The westward variant time values mark the deepening of the

reflection in **sub-area 3** (*Fig. 3.16*). The folded structures i.e., synclines Syn-A, Syn-B and anticline interpreted, are clearly defined by both the time structure and fault maps at the intra Eocene (*Figs. 3.16, 3.17*). The time structure and fault map reveals that the northern part of the study area is more deformed than the southern part at the intra Eocene reflection (*Fig. 3.16*).

The fault map at the intra Eocene level give an idea about the fault interpretation at this level (*Fig. 3.17*). The master faults are dipping in the west while small normal faults show dip both in the west and in the east (*Fig. 3.17*). For that reason, small faults are termed as the synthetic and antithetic respectively (*Fig. 3.17*). The intense faulting is observed in **segment 1**. An important feature observed at this reflection is clear change in the trend of strike showing segmentation of the area under observation (*Fig. 3.17*). The trend of F1- and F2- changes from NW-SE to N-S in **segment 2**, pointing the transition of the trend between **segment 2** and **segment 3** (*Fig. 3.17*). In **segment 3** F1-c and F2-d strikes NE-SW (*Fig. 3.17*). The area seems to be tectonically active in the intra Eocene epoch as all the master faults with number of small faults interpreted, reveals that the area underwent tectonic activity during this time period (*Fig. 3.17*). The frequency of faulting is denser near master fault F1-. The axis of the interpreted synclines and anticline runs parallel to F1-. The axis of anticline is not as continuous and parallel as Syn-A along F1- (*Fig. 3.17*). Syn-A is in the proximity of F1-. Syn-A and anticline are well interpreted in **segment 3** (*Fig. 3.17*).

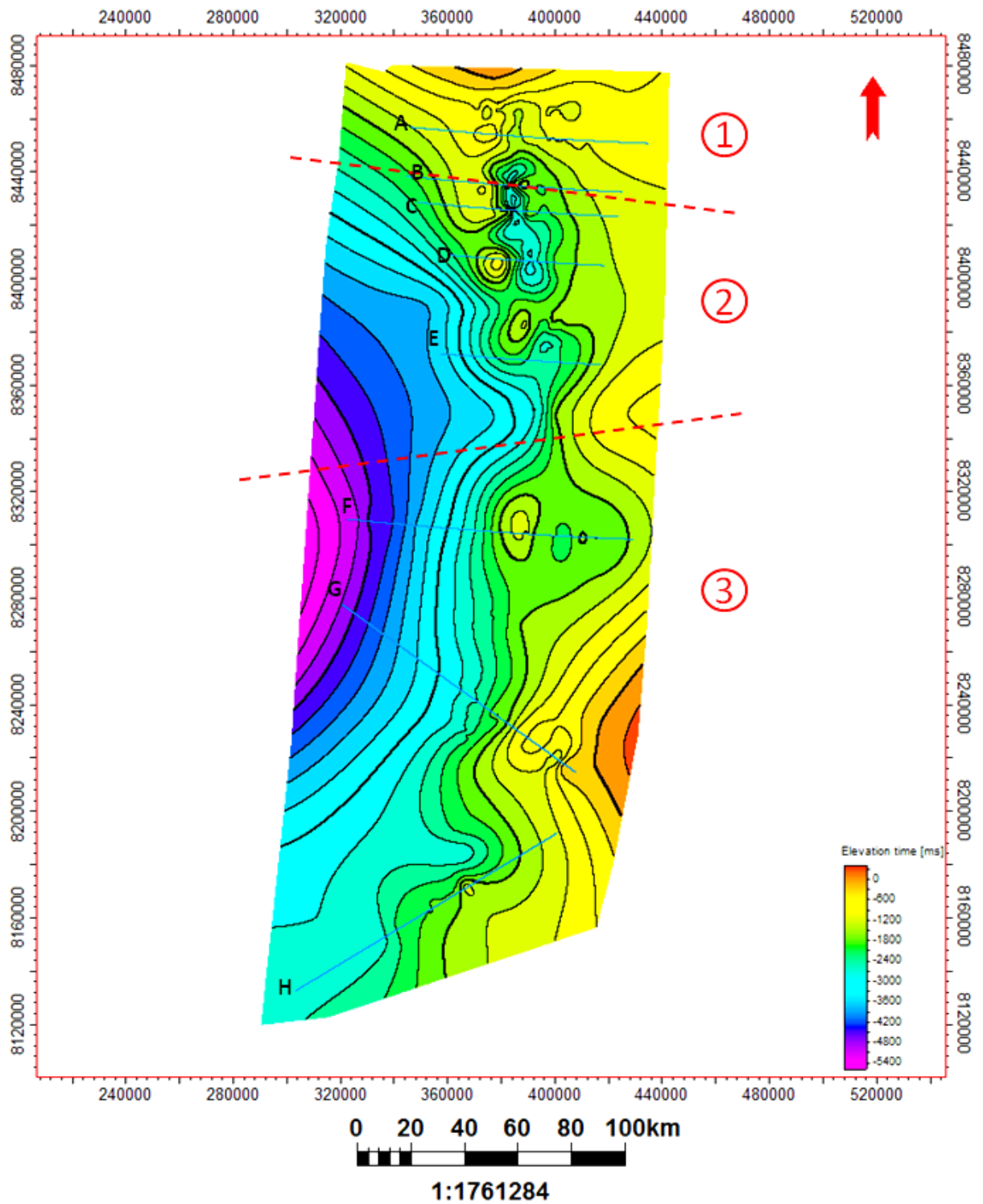


Figure 3.16: Time-structure map at the intra Eocene level with different segments shown. Location of the key seismic lines is also indicated.

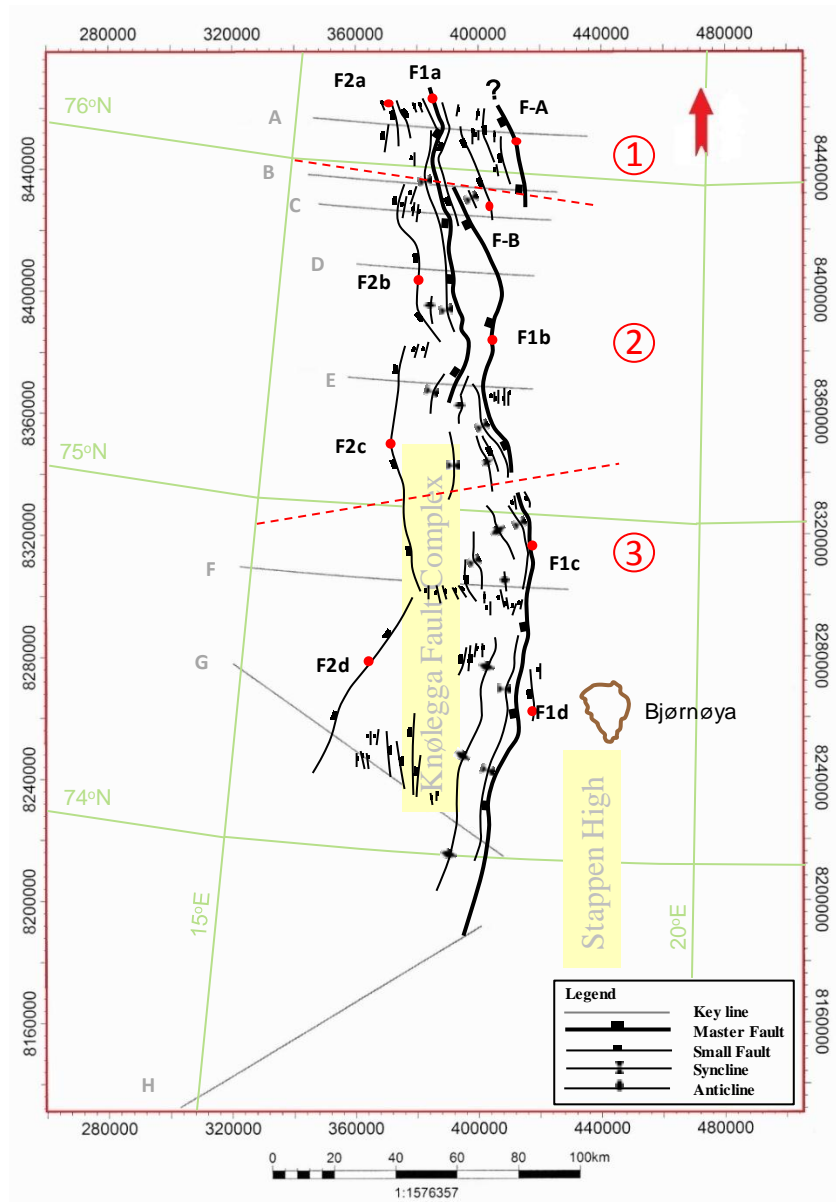


Figure 3.17: Fault map at the intra Eocene level with different segments of the master faults. Location of the key seismic lines is also indicated.

3.5.2 Intra Oligocene

The intra Oligocene time-structure map represents less color variation as compared to the maps of near base Eocene and intra Eocene levels (Figs. 3.6, 3.16, 3.18). The color variation is less than at the intra Eocene level (Fig. 3.16, 3.18). The reflection is shallower at the northern and the eastern part but deepens in the west (Fig. 3.18). The area between the master faults F1- and F2-

becomes narrow than at the intra Eocene (*Figs. 3.17-3.19*). The time-structure map indicates that the deformation in this reflection is less than the deeper reflections (*Fig. 3.16 and 3.18*).

The fault map of the intra Oligocene level defines the trend of master faults. The trend of F1-a, F1-b, F2-a, F2-b and F2-c is NNW-SSE in *segment 1, 2* and NNE-SSW in *segment 3* (*Figs. 3.18, 3.19*). This reflection comparatively experienced less faulting as compared to the two deeper levels i.e., near base Eocene and intra Eocene (*Figs. 3.5, 3.17, 3.19*). F-A and F-B did not disturb this reflection in *segment 1* except at key line A (*Fig. 3.19*). The F1-a terminates north of the key seismic line E (*Fig. 3.19*). F2-b also less deformed this reflection in *segment 2*.

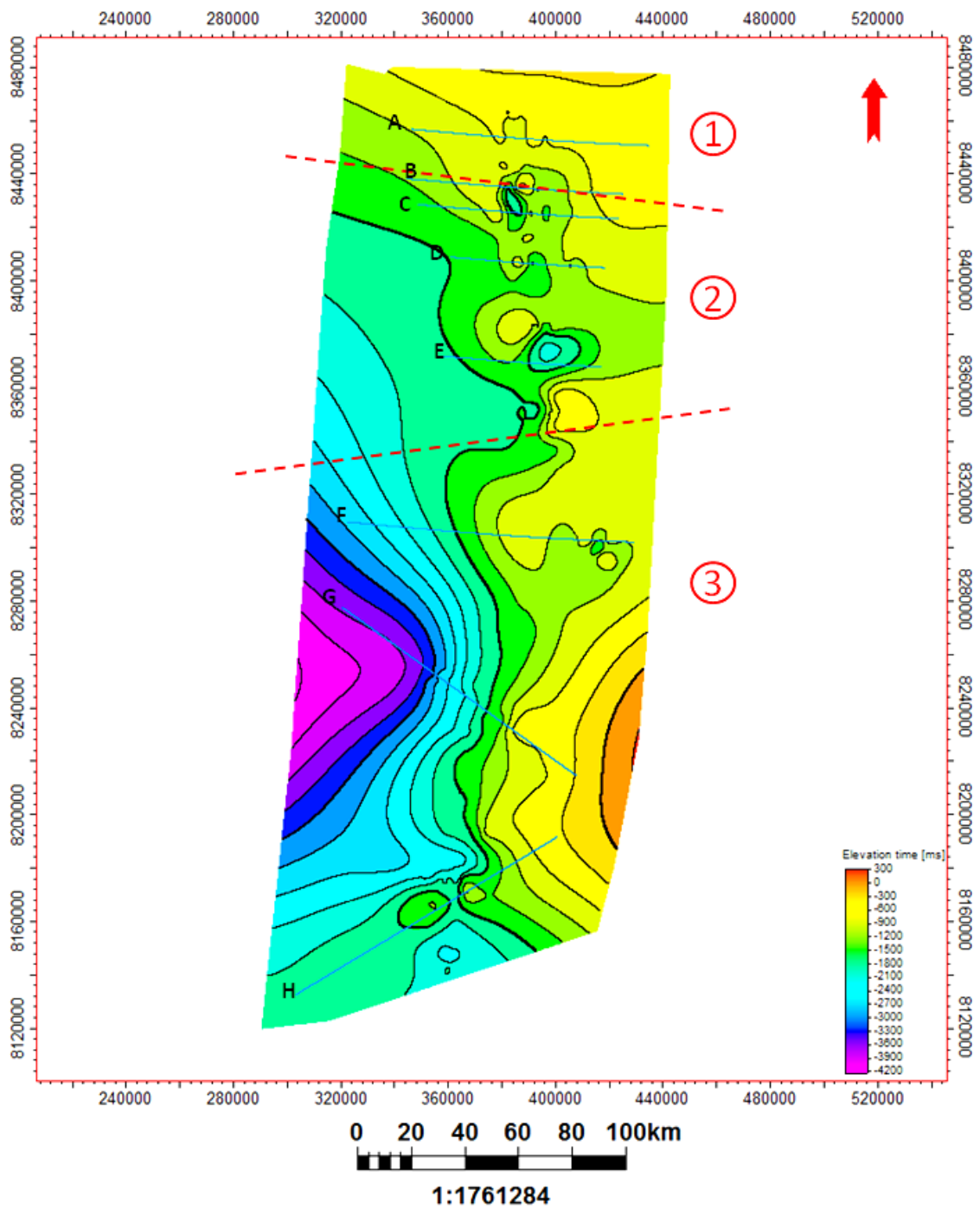


Figure 3.18: Time-structure map at the intra Oligocene level with different segments shown. Location of the key seismic lines is also indicated.

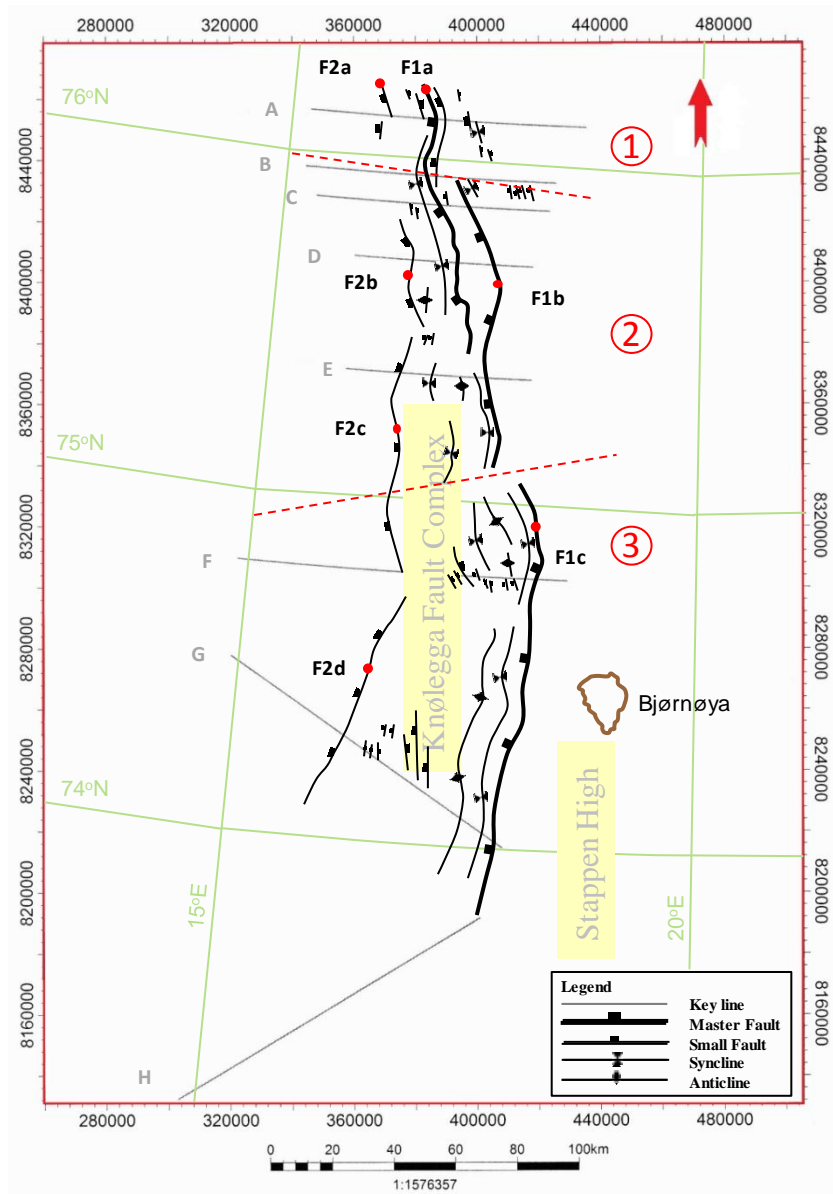


Figure 3.19: Fault map at the intra Oligocene level with different segments of the master faults. Location of the key seismic lines is also indicated.

3.5.3 Intra Miocene

The structure maps of the intra Miocene reveals the absence of any pronounced faulting experienced by this reflection (Figs. 3.20, 3.21). This reflection is mostly interpreted in the core of the syncline (Figs. 3.8, 3.9). The time structure map shows the reflection in the northern part and over the Stappen High, but as already mentioned it is software extrapolation of values. The

time structure map reflects the master faults striking NNW-SSE in *segment 2* and NNE-SSW in *segment 3* (Figs. 3.20). The area encompassed by the master faults F1- and F2- becomes narrow at this level (Figs. 3.20). Key seismic sections described in section 3.4, illustrate that intra Miocene is less faulted (Figs. 3.9-3.15). The westward deepening of the intra Miocene reflection is observed in *segment 3*, which also shows location of the deepest area of this reflection (Fig. 3.20).

The fault map of this reflection shows the least deformation than the other deeper reflections interpreted (Figs. 3.5, 3.17, 3.19, 3.21). The master faults, synclines and anticline are also interpreted at the fault map of this level (Fig. 3.21). The fault map demonstrates that the intra Miocene experienced more folding than faulting (Fig. 3.21). The trend of F1- and F2- is along NE-SW in *segment 1* and *2* (Figs. 3.20, 3.21). The intra Miocene is absent in the north of *segment 1*. Therefore F-A, F-B, F2-a and northern part of F1-a are absent in the fault map of the intra Miocene (Fig. 3.21). *Segment 2* and *segment 3* mainly represents master faults along with synclines and anticline.

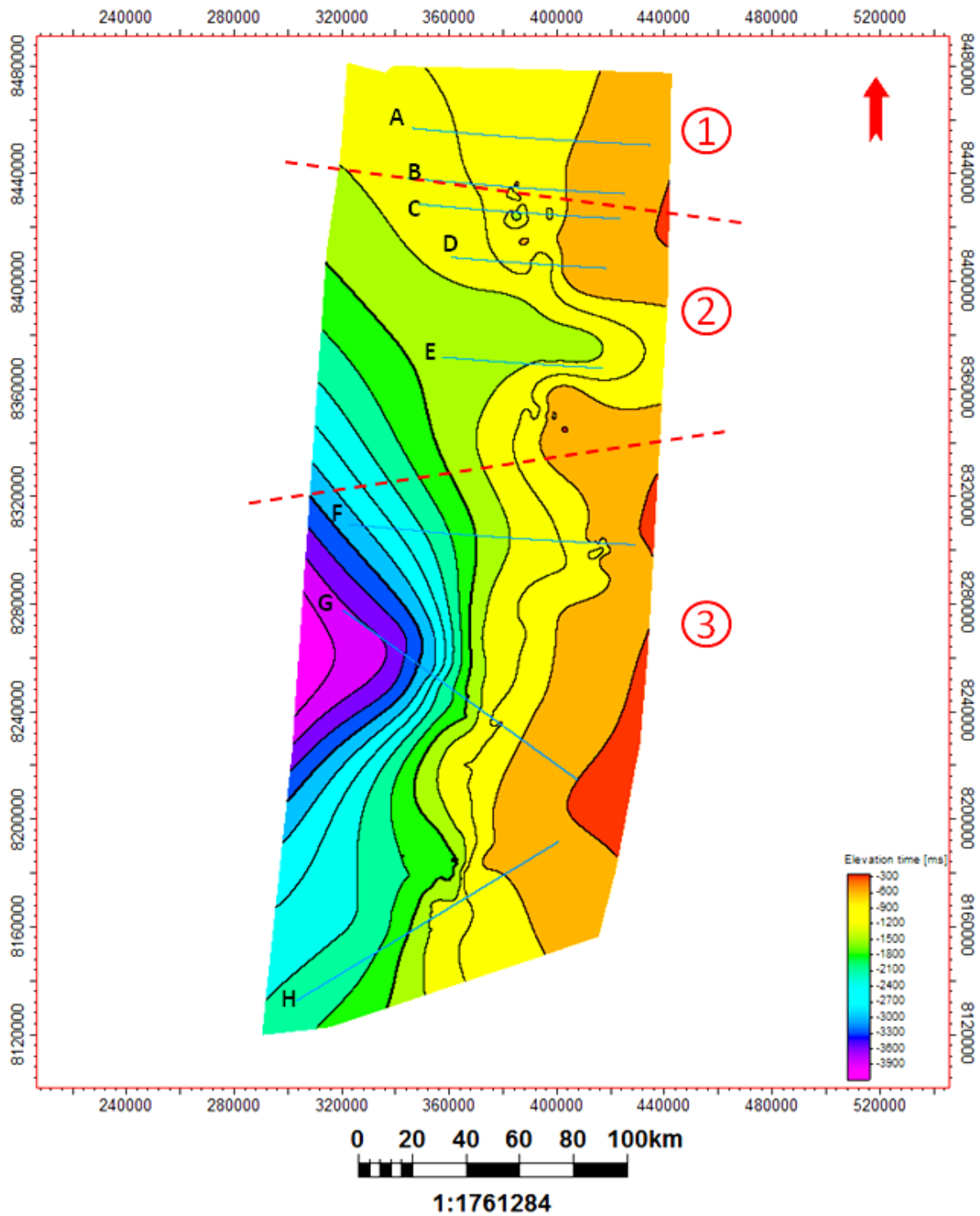


Figure 3.20: Time-structure map at the intra Miocene level with different segments shown. Location of the key seismic lines is also indicated.

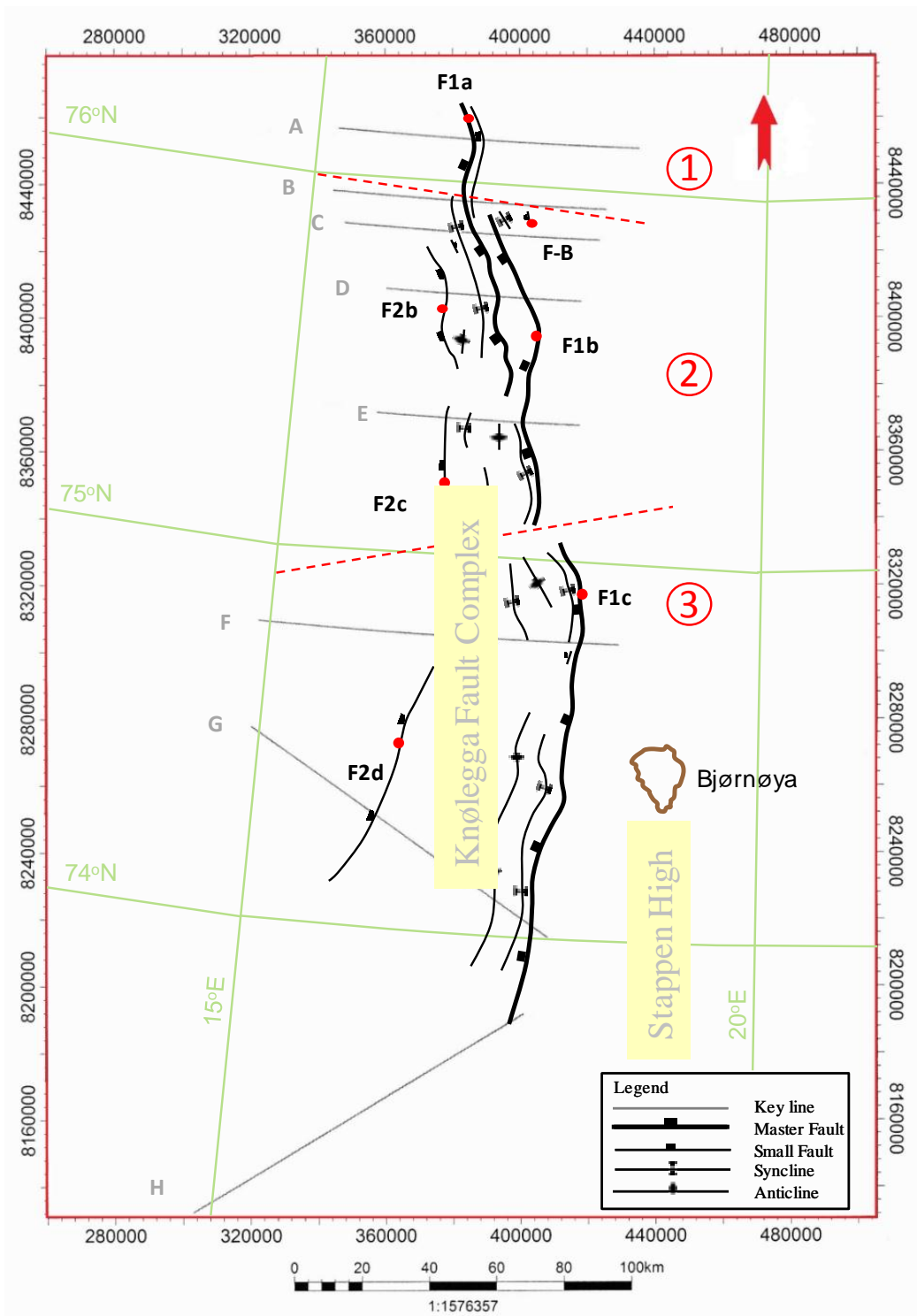


Figure 3.21: Fault map at the intra Miocene level with different segments of the master faults. Location of the key seismic lines is also indicated.

3.6 Time-Thickness Maps

The time-thickness maps between two consecutive reflections are also constructed to perceive thickness differences of sediment package within the Knølegga Fault Complex. These maps assist to build understanding of the depositional patterns and thickness variations of the study area within certain time interval. Three thickness maps are constructed between the four seismic reflections i.e., near base Eocene, intra Eocene, intra Oligocene and intra Miocene.

3.6.1 Intra Eocene-Near Base Eocene

The time-thickness map between these two seismic reflections specifies that the sediment thickens toward NW and SW of the area under investigation (*Fig. 3.22*). The thickness of sediments increases NW of the key line D and SW of the key line G (*Fig. 3.22*). The area covered between the key lines E and F shows increase in thickness of sediments, while the area defined between the key lines F and G shows reduced thickness (*Fig. 3.22*). The seismic line H also shows that the interval between intra Eocene and near base Eocene increases to the SW (*Fig. 3.16*). The lateral dissimilarity along key lines C, D, E, F and G is because of the difference in thickness of the synclines and anticline (*Fig. 3.22*).

3.6.2 Intra Oligocene-Intra Eocene

The time-thickness map of this interval illustrates maximum thickness of sediments in the west of the area between the key lines D and F (*Fig. 3.23*). This thickening in the west is also demonstrated by the key seismic line F (*Fig. 3.14*). Another important observation along the key lines B, D, F and G is the close contouring. This contouring reveals the lateral difference in thickness as a consequence of the synclines and anticline (*Fig. 3.23*). The thickness of this interval increases in the core of syncline and is reduced along the axis of anticline, as can also be seen in key seismic sections (*Figs. 3.10-3.14*).

3.6.3 Intra Miocene-Intra Oligocene

The thickening at the intra Miocene-intra Oligocene interval increases generally from the north to the south of the study area. The intra Miocene is not interpreted at the key line A, therefore, the thickness map of this interval shows decreased thickness to the north (*Fig. 3.24*). At the key line B, close contouring shows increase in thickness in the syncline (*Figs. 3.10, 3.24*). The minimum thickness is observed along the key line F, where the intra Miocene is interpreted only within the syncline Syn-A (*Figs. 3.14, 3.24*). The maximum thickness is observed in the south between the key lines G and H (*Fig. 3.24*).

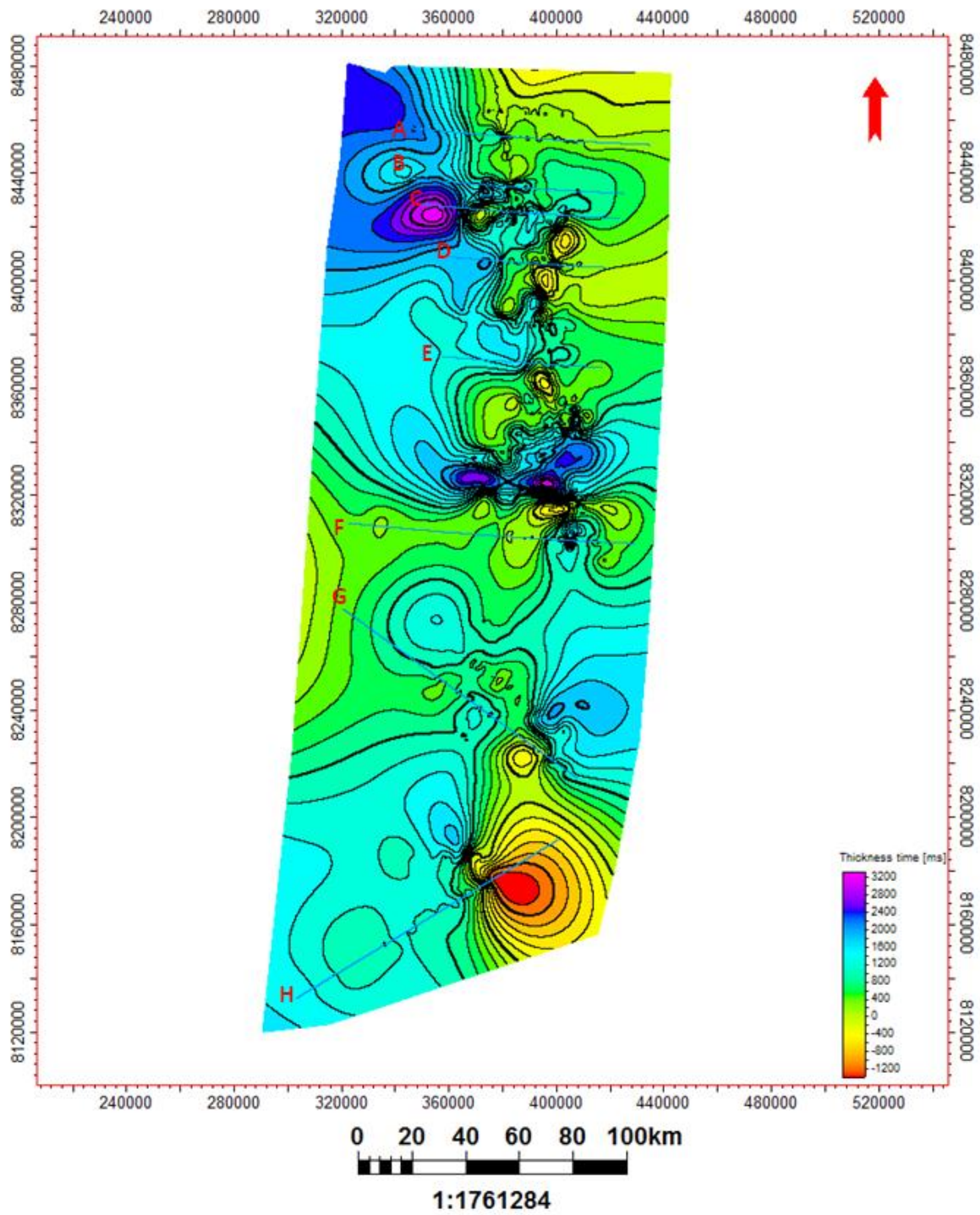


Figure 3.22: Time-thickness map between the interpreted intra Eocene and near base Eocene. The black lines particularly between the key lines B to F are because of close contouring of the software, performed to get maximum details of the thickness variations.

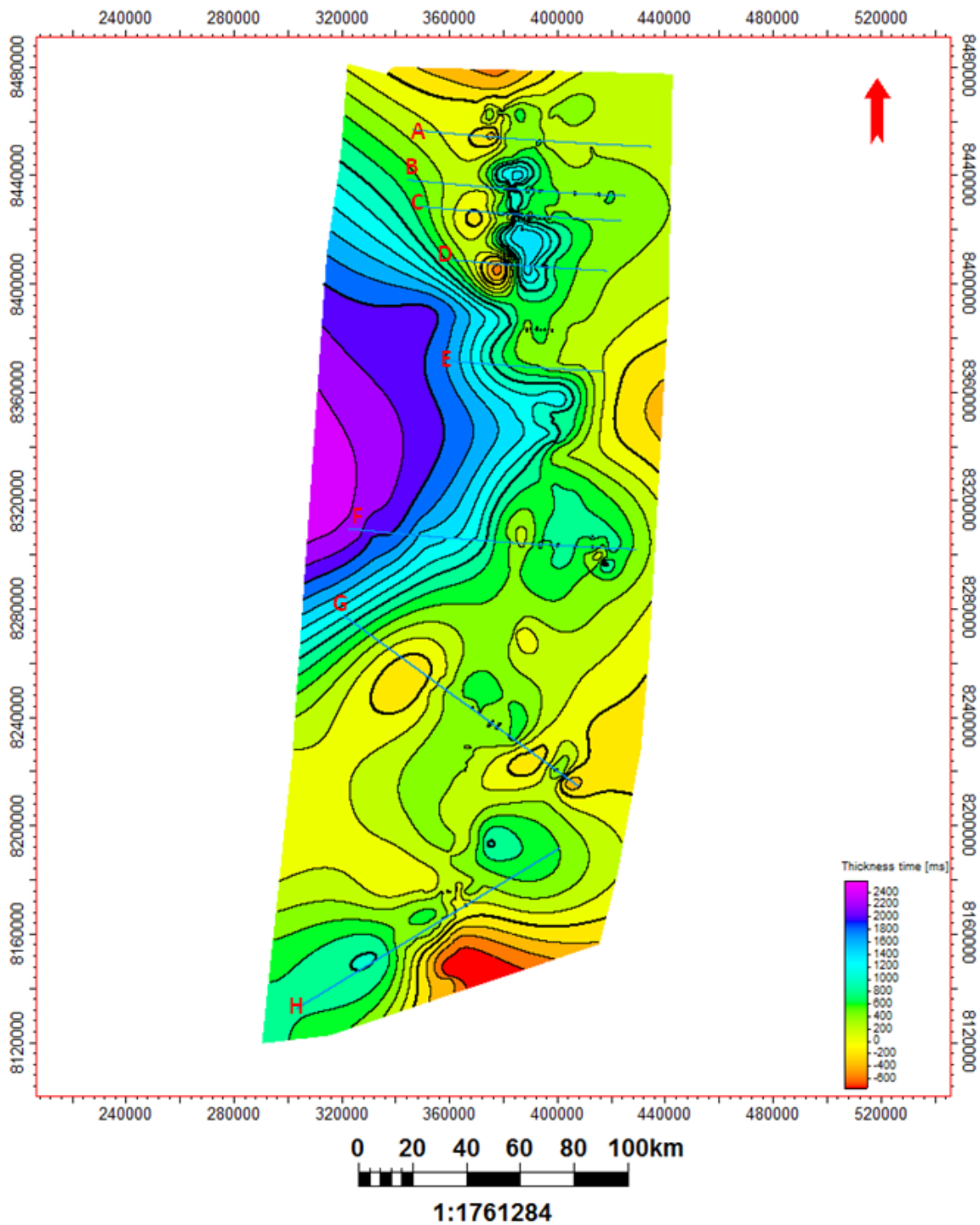


Figure 3.23: Time-thickness map between the interpreted intra Oligocene and intra Eocene. Location of the key seismic lines is also indicated.

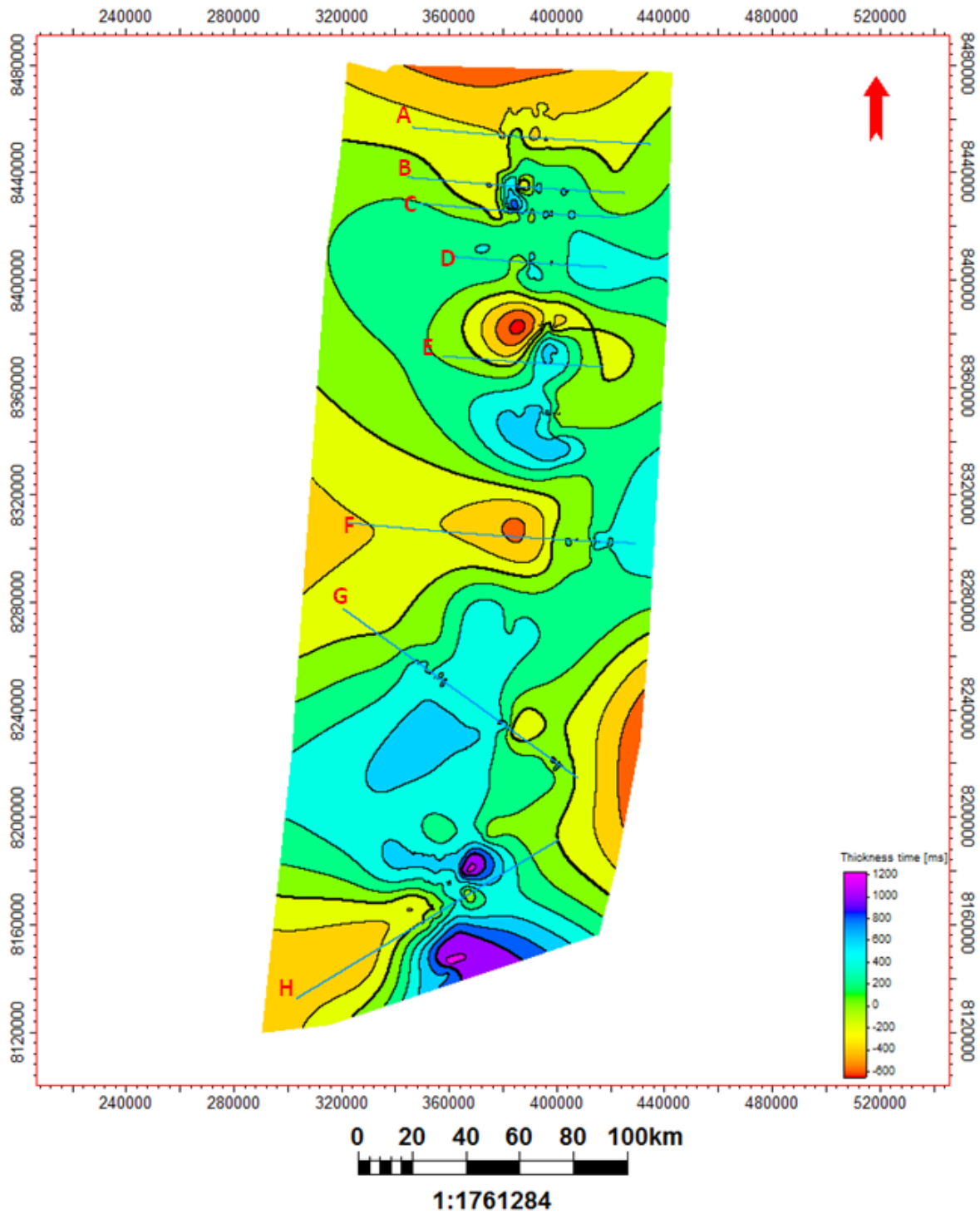


Figure 3.24: Time-thickness map between the interpreted Intra Miocene and Intra Oligocene. Location of the key seismic lines is also indicated.

Chapter 4 Discussion

This chapter mainly deals with discussion of the structural characteristics and evolution of the Knølegga Fault Complex, based on description of the seismic interpretation results already presented in the previous chapter by taking into account the work done on the same area by the previous authors. The integrated study of interpretation of key seismic lines, structure maps along with time-thickness maps helps in understanding the depositional as well as the deformational set-up which are dealt in this chapter.

The main focus of the discussion is:

1. Fault classification
2. Fault geometry
3. Fault dating (Timing of faults)
4. Structural architecture in the study area
5. Temporal evolution of the Knølegga Fault Complex

The term Knølegga Fault refers to part of the Hornsund Fault Zone as used by previous authors (Gabrielsen et al., 1990; Faleide et al., 2008; Faleide et al., 2010). This new knowledge demands a closer look and perhaps a revision of the nomenclature for the area. This revision would, however, be beyond the scope of the present study.

The first four sub-chapters (*sections 4.1-4.4*) discussed provide a basis for the last sub-chapter (*section 4.5*), geological evolution of the study area.

4.1 Fault Classification

The Knølegga Fault Complex consists of NW-SE and NE-SW trending extensional faults which constitute a linked fault system. According to Davison (1994), a linked fault system consists of largely contemporaneous branching faults and their linkage over a length-scale is much greater

than individual fault segments. Such a linked fault system truly branch out rather than cross-cut each other (Davison, 1994). ‘*Hard linkage*’ is accomplished by direct link-up of faults, while in ‘*soft linkage*’ faults are linked by highly-strained ductile zones, without through-going faults developing (Walsh and Watterson, 1991a; Davison, 1994). Thus, the master fault segments F-B, F1-b and F1-c are ‘*softly linked*’ as these are linked by highly-strained ductile zones rather than directly linking as in ‘*hard linkage*’.

The larger faults may be linked on the scale of the map, whereas the smaller faults are isolated on this scale. In extensional fault systems, different patterns of fault linkage show gradation from anastomosing with variations in angle and orientations to a reticulate style (Fig. 4.1) (Davison, 1994). Based on fault patterns in map view suggested by Davison (1994), synthetic and antithetic faults to the main boundary faults mapped within the study area are termed unlinked (Fig. 4.1a).

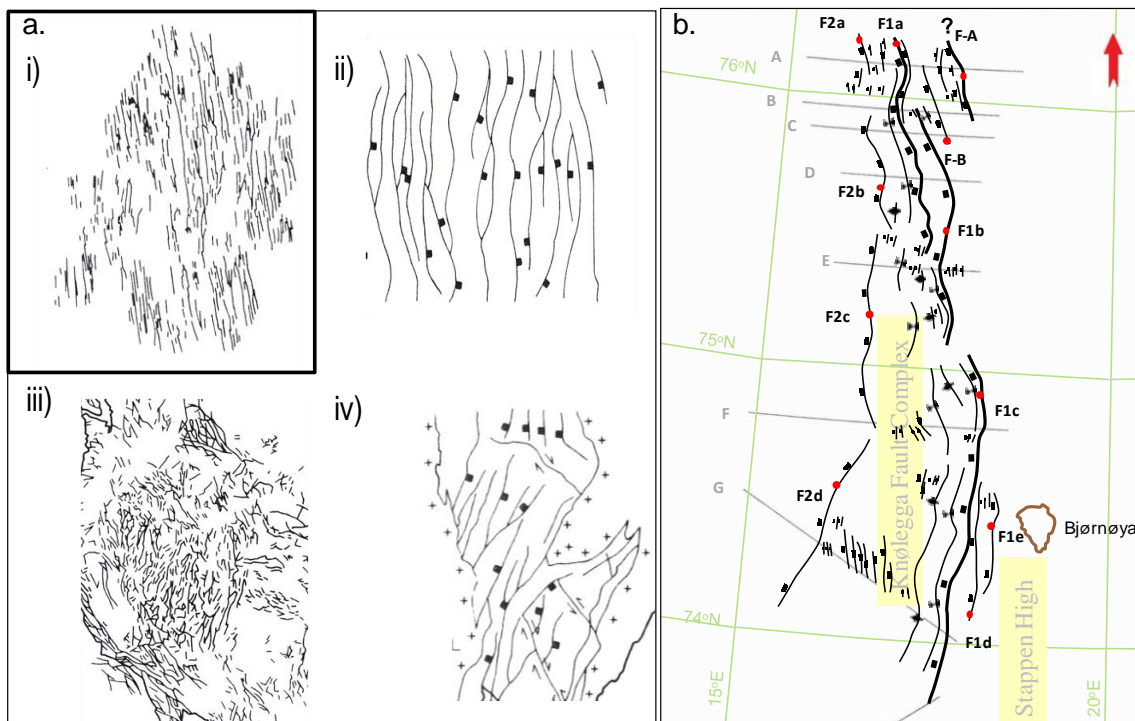


Figure 4.1: Comparison of fault system of the Knølegga Fault Complex **a)** Patterns of extensional fault systems in map view (with no scale) (i) Unlinked fault system due to parallelism (ii) sandbox model showing completely linked extensional faults (iii) highly variable fault orientations and mainly unlinked faults (iv) Reticulate fault pattern with highly oblique transfer faults linking-up with main extensional faults (modified from Milani and Davison, 1988; in Davison, 1994), **b)** Map view of the interpreted synthetic and antithetic faults within the Knølegga Fault Complex at the near base Eocene level showing unlinked fault system (a-i).

Morley et al., (1990) classified master faults in rifts where throw of the fault is transferred from one master fault to another. Figure 4.2 illustrates the classification of master faults on account of their mutual interactions (Morley et al., 1990). The two main classes are defined based on the relative dip directions of the master faults. These classes are ‘Synthetic’ and ‘Conjugate’ (Morley et al., 1990). These two classes further describe four map positions of the faults with reference to each other. Approaching and overlapping transfer zones are two of these map positions. When two fault tips fail to propagate past each other, the transfer zone is called ‘approaching’. In case when fault tips have propagated past each other, the transfer zone will be ‘overlapping’ (Morley et al., 1990). Following Morley et al., 1990 the master fault F-B and F1-b are termed ‘overlapping-synthetic’ fault segments, while F1-b and F1-c are termed ‘approaching-synthetic’ fault segments (*Fig. 4.2*).


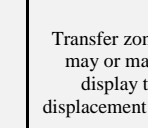
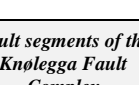

<i>Classification</i>	<i>Synthetic</i>		<i>Fault segments of the Knølegga Fault Complex</i>
Overlapping		Transfer zones that display true displacement transfer	
Approaching		Transfer zones that may or may not display true displacement transfer	

Figure 4.2: Classification of transfer zones between the unlinked and linked faults (after Morley et al., 1990; modified from Davison, 1994). The basic types of transfer are conjugate and synthetic depending upon the fault dip directions. This classification allows terming the master fault segments of the Knølegga Fault Complex F-B and F1-b as ‘overlapping-synthetic’ fault segments, while F1-b and F1-c as ‘approaching-synthetic’ fault segments.

According to Childs et al. (1995) the overlapping normal faults in 2D can be described as “the sub-parallel fault traces arranged en-echelon where both the overlapping length of the fault traces and the distance separating the traces are small relative to the full lengths of the constituent fault traces”. If the dip of the overlapping faults is in the same direction then these are termed as overlapping-synthetic (*Fig. 4.3*) (Childs et al., 1995). The volume of rock between the overlapping fault structures is called the ‘overlap zone’ (Childs et al., 1995).

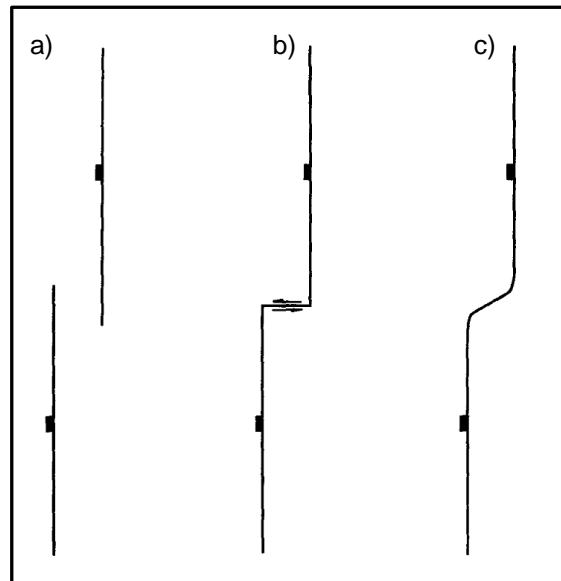


Figure 4.3: The schematic diagram delineating possible structures at an offset in a fault trace illustrated by Childs et al., 1995. **a)** An overlap zone or overlapping faults, **b)** a transfer fault and **c)** a fault bend. According to Childs et al., 1995 as shown in a), the master faults F-B and F1-b are overlapping faults.

Therefore, keeping in view the above explanation, faults F1-a and F1-b could be termed as the ‘synthetic-overlapping’ in the *segment 2* (*Fig. 4.2*). The overlapping is of two types i.e., a) relay zones and b) non-relay zones. In the relay zones displacement is transferred between the overlapping faults while, in the non-relay zones the displacement is not transferred (Childs et al., 1995). Hence F-B and F1-b are observed to be the relay zones as the displacement is transferred (*Fig. 3.5*).

The southwestern Barents Sea shows regionally a non-uniform striking behavior. The characteristics of fault systems in the southwestern Barents Sea have variation in different fault systems. These parameters involve geometry, appearance, age and tectonic setting (Gabrielsen, 1984). Fault systems have been classified by Gabrielsen (1984) into three fundamental classes (*Table 4.1*). The classification is defined on the basis of regional and tectonic significance, degree of involvement of basement and reactivation. Of these, the prime parameter to differentiate each class is the degree of basement involvement (Gabrielsen, 1984).

First Class	Basement Involved	Regional significance	Reactivated	Separate areas of different tectonic outline
Second Class	Basement Involved	Semi-regional	Reactivated/ not reactivated	Separate areas of different tectonic outline
Third Class	Basement Detached	Local significance	Not reactivated	Does not separate areas of different tectonic outline

Table 4.1: Classification of southwest Barents Sea fault systems into first, second and third classes proposed by Gabrielsen (1984).

Gabrielsen (1984) classify the Hornsund Fault Zone as '*First-Class*' fault system following the criteria defined in *Table 4.1*. The Knølegga Fault is characterized as a part of the Hornsund Fault Complex (Sundvor and Eldholm 1976; Myhre et al., 1982; Gabrielsen et al., 1984; Gabrielsen et al., 1990). In this study, the Knølegga Fault Complex has three main fault segments which are F-B, F1-a and F1-c, therefore the term 'master faults' refer to these three fault segments (*Fig. 3.5*). The stratigraphic control did not allow interpreting the basement involvement of the master faults. The parameters to put the master faults in '*First-Class*' are:

- The Knølegga Fault is part of the Hornsund Fault Zone
- It has regional significance
- The basement seems to be involved as the master faults cut the sediments at levels deeper than the Cenozoic succession
- It separates the areas of different tectonic outline (the less deformed footwall in the east and the deformed Knølegga Fault Complex in the west)

Based on the above reasons and following the classification of faults by Gabrielsen (1984), the master faults are considered close to the category of '*First-Class*' faults.

4.2 Fault Geometry

The Knølegga Fault Complex mainly encompasses normal faults which are generally striking NW-SE in the northern part of the area and NE-SW in the southern part of the area representing change in the trend of the faults along strike (*Figs. 3.5 and 4.4*). The master faults are divided into three segments, termed *segment 1*, *2* and *3* (refer to *section 3.4* for details). These three fault segments are F-B, F1-b and F1-c from the north to the south of the area under consideration (*Figs. 3.5 and 4.4*). As the part of the master faults F-B and F1-b is parallel, therefore these are termed as overlapping faults. The displacement along all the three master fault segments F-B, F1-b and F1-c is down-to-the-west (*Fig. 3.5*). All three master fault segments also define the eastern boundary of the structural feature Syn-A (*Fig. 3.5*).

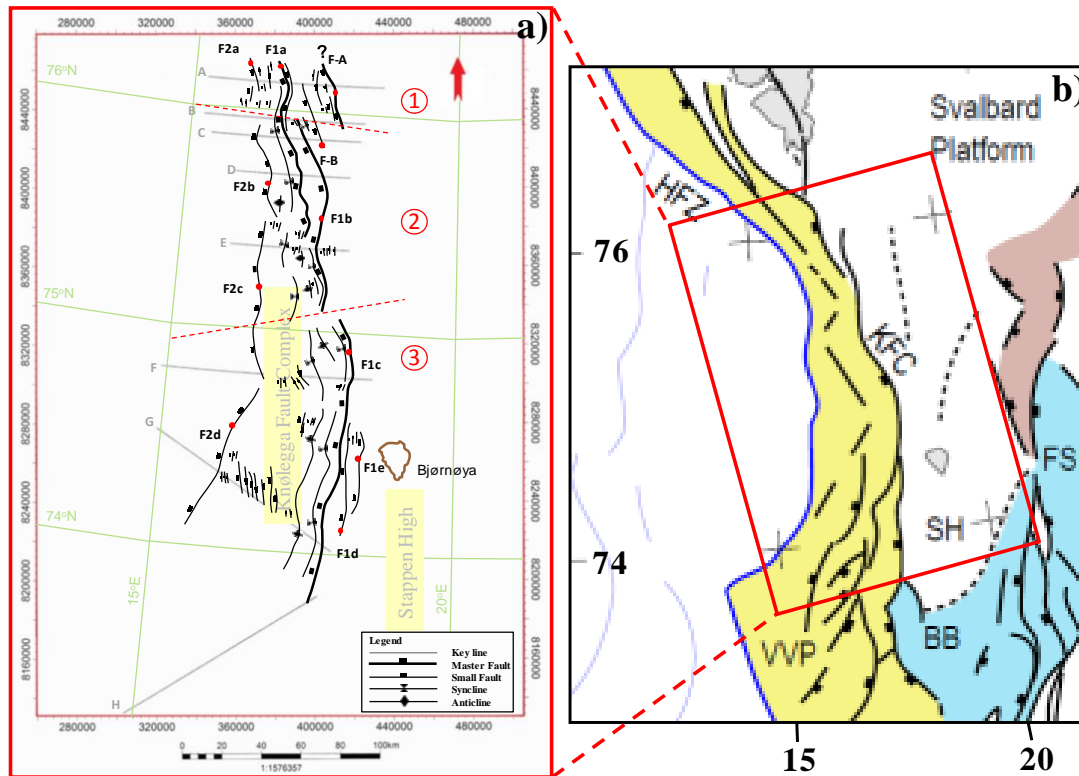


Figure 4.4: The comparison of **a)** fault map interpreted at the near base Eocene level shows similarity with **b)** the already published structural map of the Knølegga Fault Complex (in red rectangle) (modified from Faleide et al., 2010). The master fault F1-b and F1-c (**a)** shows nearly same trend but with minor differences as shown by Faleide et al. (2010).

The true dip of the master faults and fault plane geometries are not precisely determined as the seismic data is not depth converted. Analyzing the faults in the cross-section reveals that most of the faults are planar (twt). The master faults (F1-, F2-) are the extensional faults along which the most prominent normal vertical displacement occurred. F-B merges at shallower level of about 2 sec (twt) while, F1-b and F1-c becomes generally deeper more than c. 4 sec (twt) to the south of the fault system (Figs. 3.12-3.15). The dip of the master faults varies from 50-80° (twt) (Figs. 3.9-3.15).

4.2.1 Displacement along the master fault

The vertical deformation includes uplift and subsidence while the horizontal deformation encompasses lengthening and shortening (Angelier, 1994). The maximum displacement is along the central master fault segment F1-b at location of key seismic line E which is more than c. 3 sec (tw) (*Fig. 3.13*). The displacement generally decreases towards the north and south of key line E (*Figs. 3.9-3.15*). A vertical displacement of more than c. 2 sec (tw) is observed along the master fault segment F-B at location of key seismic line C (*Fig. 4.5*). The Cenozoic reflections interpreted in the hangingwall are the near base Eocene, the intra Eocene, the intra Oligocene and the intra Miocene, while the reflections within the footwall are the top Permian and the intra Triassic (refer to *Section 3.4* for details). The reference level near base Eocene in the hangingwall and top Permian in the footwall is an evidence of the large vertical throw of more than c. 3sec across the master fault as described by Gabrielsen et al., 1990 (*Figs. 4.5 and 4.6*).

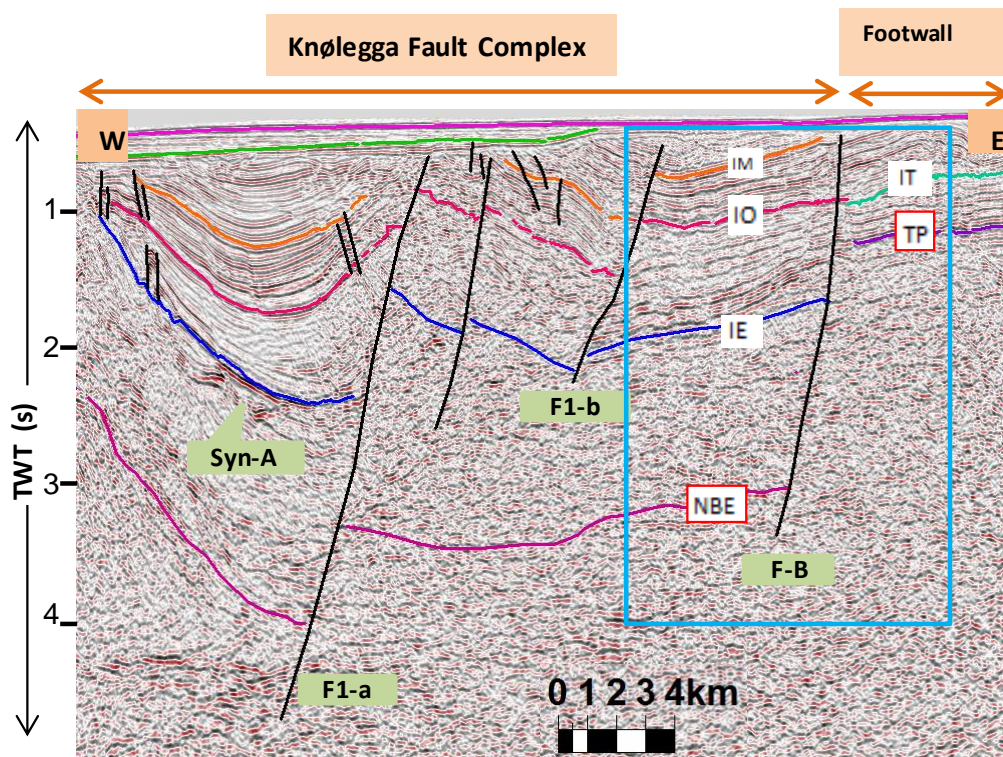


Figure 4.5: The vertical throw of more than c. 3 sec (tw) shown in the interpreted seismic section within the area under consideration. UN: upper Neogene, IP: intra Pliocene, IM: intra Miocene, IO: intra Oligocene, IE: intra Eocene, NBE: near base Eocene, IT: intra Triassic, TP: top Permian.

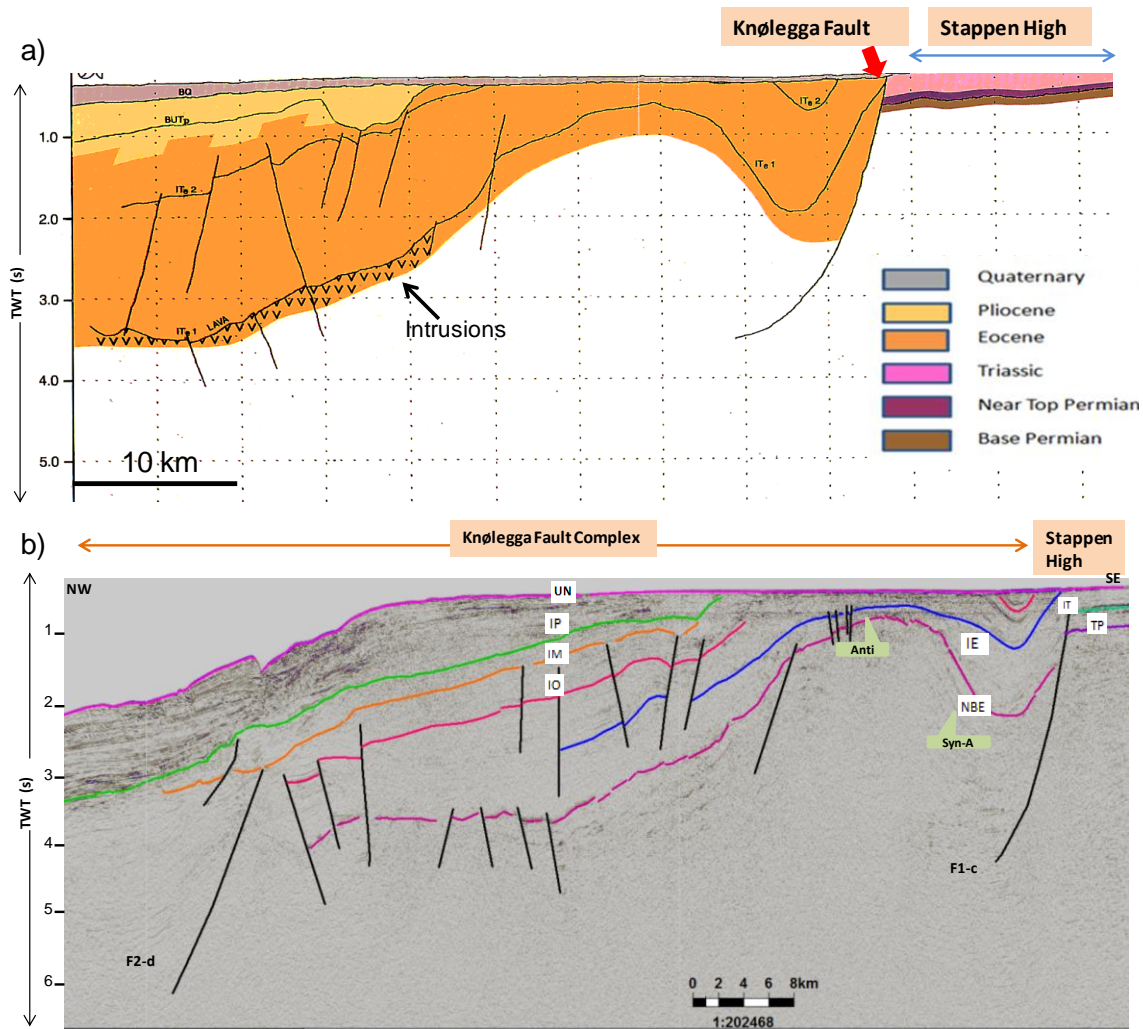


Figure 4.6: Seismic interpretation of key NW-SE oriented line G, demonstrating vertical throw of more than c. 2 sec (twt) along the master fault F1-c, as also illustrated by Gabrielsen et al., 1990. **a)** Proposed by Gabrielsen et al. (1990), legend for different color codes is also shown to right of Fig.a. **b)** Same seismic key line (G) interpreted in this study, the vertical displacement of more than c. 2 sec (twt) can be observed. This key line adds-on the interpretation of Gabrielsen et al. (1990) that sole of the Knølegga Fault is located at the Jurassic or a deeper level. See section 4.3 for text. UN: upper Neogene, IP: intra Pliocene, IM: intra Miocene, IO: intra Oligocene, IE: intra Eocene, NBE: near base Eocene, IT: intra Triassic, TP: top Permian.

4.3 Fault Dating

A study of the chronology of faulting can be performed using several techniques (Angelier, 1994). Two techniques suggested by Angelier (1994) are:

- The age of fault movements can be bracketed, or in some cases it could be determined with precision, by considering the ages of rock formations either affected or unaffected by the faults, also termed as the stratigraphic dating.
- The reconstruction of relative chronology can be done analyzing thickness variations of correlable stratigraphic sequences in the footwall and hangingwall of the fault.

The fault dating techniques adopted during this study includes stratigraphic as well as thickness analysis. In stratigraphic dating technique, fault movement post-dates deposition of the lower sedimentary rocks, whereas upper limit of fault age is assigned by the upper layers that are influenced by faulting (Angelier, 1994). The study area has experienced major fault activity in the early Eocene, as the thick Cenozoic sediments subsided along the master faults. The stratigraphic control within the hangingwall and footwall prevented dating of faults precisely as no common seismic reflection have been interpreted both within the hangingwall and the footwall.

The representative key lines C and D are analyzed for the stratigraphic dating of the master faults in the study area (*Figs. 4.7, 4.8*). The master fault F1-b at location of the key seismic line E cut sediments at levels deeper than the near base Eocene (*Fig. 4.7*). Minor faults have deformed the intra Oligocene representing the tectonic activity in the Oligocene time. Gabrielsen et al. (1990) documented that the sole of the Knølegga Fault is located at the Jurassic or a deeper level. The results from the present analysis is in agreement with that of Gabrielsen et al. (1990), as the Knølegga Fault do not die out within the Cenozoic sediments rather cutting the sediments at levels deeper than the Cenozoic succession (*Figs. 3.13-3.15*).

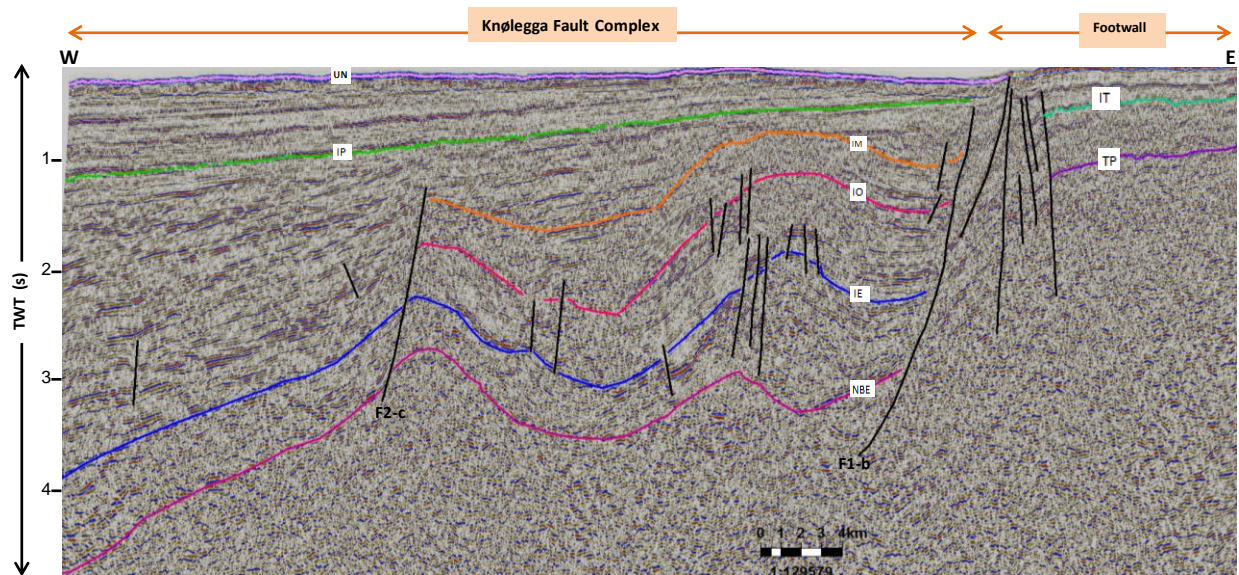


Figure 4.7: Key seismic line E bracketing the age of faults, the Pliocene sediments are undeformed representing the upper limit of faults. UN: upper Neogene, IP: intra Pliocene, IM: intra Miocene, IO: intra Oligocene, IE: intra Eocene, NBE: near base Eocene, IT: intra Triassic, TP: top Permian.

The other feature observed in line C that could be used for fault dating within the hangingwall is presence of a growth fault (*Fig. 4.8*). The yellow highlighted layer between the intra Eocene and intra Oligocene marks a clear difference in thickness across F1-a, represented by black arrowhead lines (*Fig. 4.8*). This feature is termed ‘syn-depositional fault’ as the age of sediments is the same as that of faulting, and the wedge formed is syn-sedimentary wedge. The growth fault observed within the intra Eocene and intra Oligocene reflections reveals that the study area has experienced tectonic activity in the Oligocene time (*Fig. 4.8a*). The model of syn-sedimentary wedge by Prosser (1993) demonstrates the deposition of sediments during the tectonic activity (*Fig. 4.8b*).

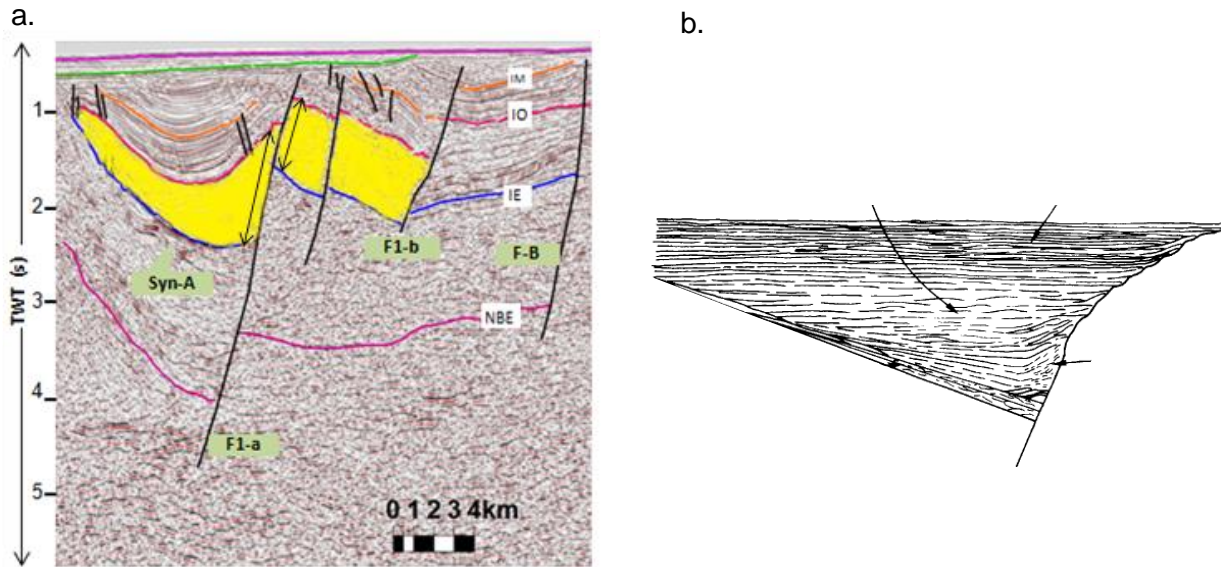


Figure 4.8: a) The growth fault observed at the location of key line C. The black line with arrows in yellow highlighted sediment layer parallel to F1-a, illustrates the increase in the thickness of strata which shows a notable difference of sediment thickness across the fault. b) An idealized line drawing section illustrating growth fault or syn-sedimentary wedge (modified from Prosser, 1993). This figure illustrates about the active faulting alongwith the deposition of the sediments as is observed at the location of key line C (a). IM: intra Miocene, IO: intra Oligocene, IE: intra Eocene, NBE: near base Eocene.

4.4 Structural Architecture of the study area (hangingwall block and footwall)

The significant structures to be addressed in the study area include:

- Extensional structures
- Contractual structures

In the study area all the faults (master faults, minor faults) interpreted are normal faults which provide evidence that the study area has been influenced by the extensional stress system during its geological history. The down faulting along f14, f15 and f16 is observed (Fig. 4.9) which is 'staircase normal faults geometry' (Fig. 4.10). In contrast with the staircase geometry, domino faults have similar vertical offset (Fig. 4.11). The horst observed is bounded by f17 in the East and f18 in the west (Fig. 4.9). This feature is interpreted at key line F only, while on the other key seismic lines the horst or graben structures are less abundant in the study area. The basin is observed at location of the key seismic line F, which could be a local basin as it has not been

interpreted on the other consecutive key seismic lines (Figs.3.9-3.15 and 4.14). Minor faulting has been observed particularly in the sediments older than the intra Eocene (Fig. 3.12), demonstrating a minor extension in the intra Oligocene (Figs. 3.9-3.15). The footwall is moderately influenced by faulting but this faulting is extensive in the north of key line C (Figs. 3.9-3.11). The splays of master fault have been observed in the footwall between the key lines F and G (Figs. 3.5, 3.14 and 3.15). Minor synthetic and antithetic faults have been interpreted at locations of the key seismic lines A, B and E in the footwall (Figs. 3.9, 3.10 and 3.13).

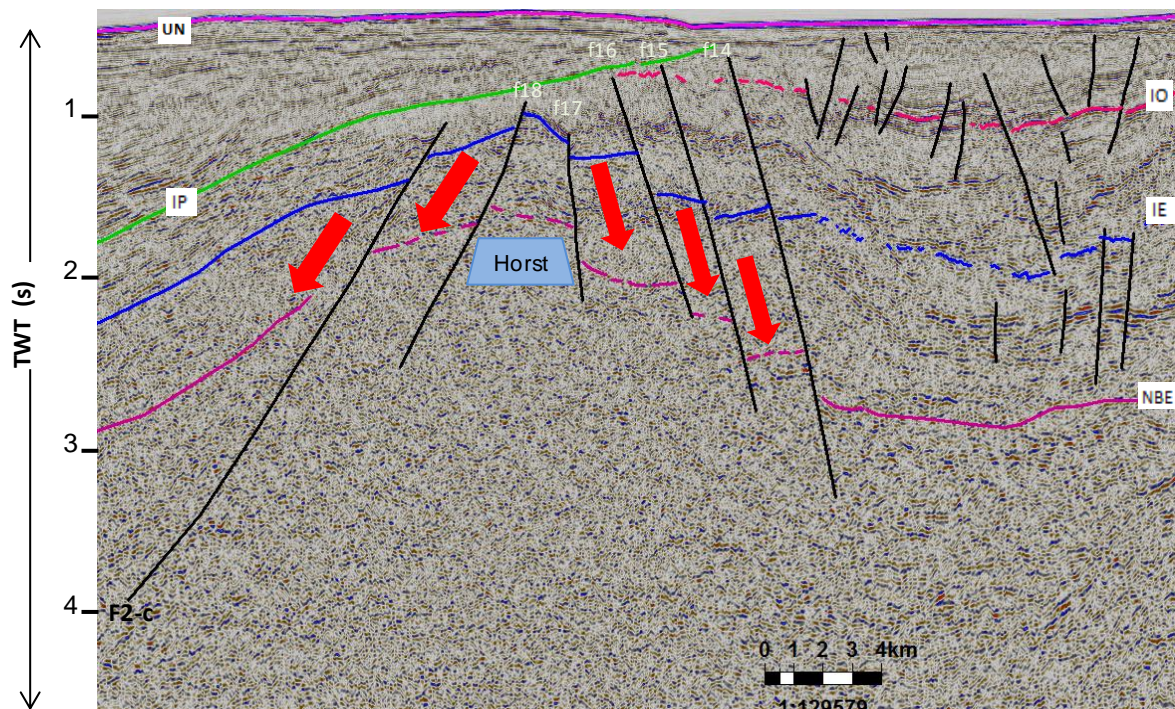


Figure 4.9: The staircase Normal Fault Geometry observed at location of the key seismic section F in the study area. The comparison of staircase geometry is shown by the figures 4.10 and 4.11 see figure 4.10 for the similarity of structures found. UN: upper Neogene, IP: intra Pliocene, IM: intra Miocene, IO: intra Oligocene, IE: intra Eocene, NBE: near base Eocene.

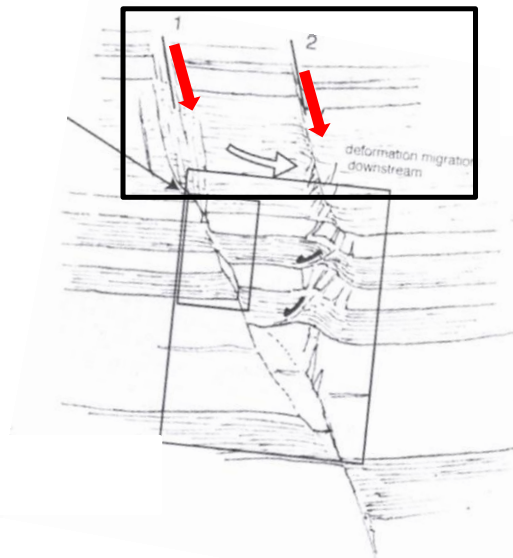


Figure 4.10: The fault geometry having resemblance with the structures illustrated in figure 4.9 (modified from Lansigu and Bouroulec, 2004).

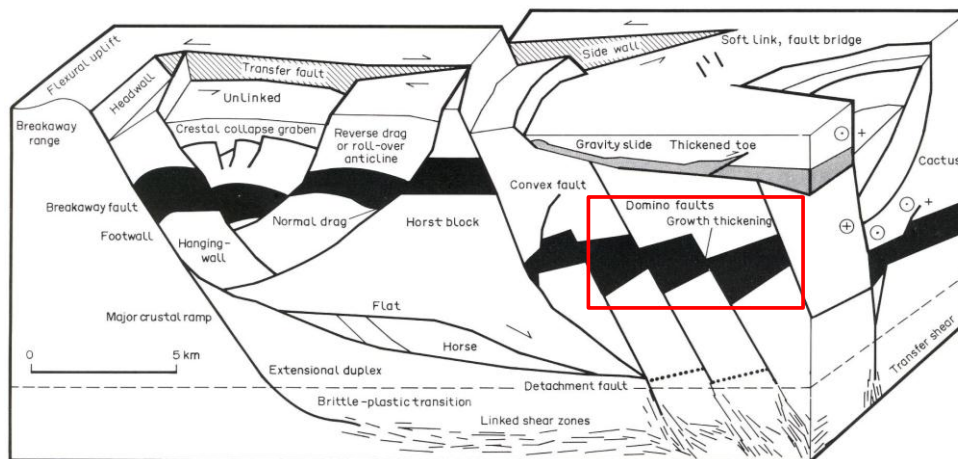


Figure 4.11: The nomenclature of extensional fault system as illustrated by Davison (1994). The domino faults are shown in red rectangle, which have simultaneous rotation of fault planes and bedding (modified from Davison, 1994).

The compressional stresses which are younger than the extension resulted in contractional structures within the study area both in the hangingwall and the footwall. The folding found within the hangingwall represents the ductile deformation of the strata, as more folding is observed than faulting. The hangingwall is more influenced by the contraction as prominent

synclines (Syn-A, Syn-B) and anticline are formed, while the footwall has also been affected by these contractional stresses as minor folding is observed in the footwall area. Simple geometries of folds in the footwall are also observed during the interpretation of the seismic data. The amplitude of folds observed in footwall is low (*Fig. 4.12*), hence the interlimb angle lies within $120-180^\circ$ putting these folds in the category of ‘gentle folds’. The layers of sediments from the intra Eocene to the intra Oligocene within Syn-A, despite the difference in thickness or mechanical properties of the individual layer, are buckled with nearly same wavelength if observed at each key line separately. This type of buckling is called ‘harmonic folding’ (Price and Cosgrove, 1990). The depth of Syn-A (twt) is maximum at key line C i.e. c. 4 sec (twt) while it decreases to c. 2 sec (twt) to the north and to the south of the key line C (*Figs. 3.9-3.11*). The amplitude and wavelength of the multi-layer folds particularly Syn-A increases from the key line A to D and then decreases from the key lines D to G. Therefore the maximum amplitude and wavelength of Syn-A is observed at the key line D, while a decrease in these properties of fold is observed both to the north and to the south of the key line D (*Figs. 3.9-3.15*). The interlimb angle is maximum at the location of key line E and could be termed as ‘gentle’, while it decreases to the north and to the south of this key line and could be put in ‘open folds’ category (*Table. 4.2*), which means Syn-A is wider at key line E location than at the other locations within the area under observation (*Fig. 3.11*).

<i>Interlimb angle</i>	<i>Description of folds</i>
180-120°	Gentle
120-70°	Open
70-30°	Close
30-0°	Tight
0°	Isoclinal
Negative angles	Mushroom or Elastica

Table 4.2: Types of folds in relevance with interlimb angle (after Price and Cosgrove, 1990).

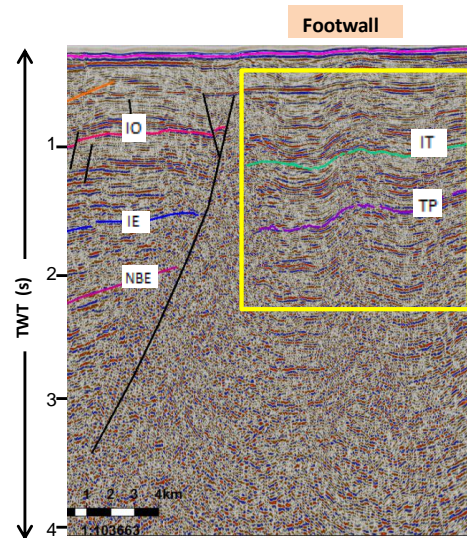


Figure 4.12: The footwall area showing deformation caused by the contractional stresses. No prominent fault is interpreted in the footwall in this key line, but along with hangingwall, footwall is also affected by the contractional stresses resulting in folded structures (yellow rectangle indicate the folded structures in the footwall). IO: intra Oligocene, IE: intra Eocene, NBE: near base Eocene, IT: intra Triassic, TP: top Permian.

4.5 Temporal Evolution of the study Area

This sub-chapter deals with the geological evolution of the study area and addresses the development of the extensional and contractional features observed. The Knølegga Fault is part of the Hornsund Fault Zone which marks the continent-ocean boundary in the NW Barents Sea (Gabrielsen et al., 1990). Therefore the study area lies along the Norwegian margin which is formed in response to early Cenozoic break-up followed by opening of the Norwegian Greenland Sea (Faleide et al., 2008). The Senja Fracture Zone and the Knølegga Fault Complex are the two important structural elements in the western Barents Sea along the margin. The Senja Fracture Zone represents the boundary between oceanic and continental crust while the Knølegga Fault Complex is a complicated rifted segment west of the Stappen High (Richardson et al., 1991).

Regionally, the margin is divided into three structural segments by Faleide et al. (1991). These structural segments are:

- A sheared margin along the Senja Fracture Zone in the south ($70\text{--}72^{\circ}30' \text{N}$)
- A central rifted volcanic margin ($72^{\circ}30' \text{--}75^{\circ} \text{N}$) and
- An initially sheared and later rifted margin associated with the Hornsund Fault Zone in the north ($75\text{--}80^{\circ} \text{N}$).

Gabrielsen et al. (1990) found that the Knølegga Fault Complex is situated between $73^{\circ}30' \text{N}$ to $75^{\circ}50' \text{N}$, hence, following structural segments division of Faleide et al. (1991), the complex lies within the central rifted margin. This point forward, area to the south of 73° and area to the north of 76° are beyond the focus of this study and belong to the sheared margins.

The structures developed in the Cenozoic time are result of the two-stage opening of the Norwegian-Greenland Sea and the formation of the predominantly sheared western Barents Sea continental margin (Faleide et al., 2008; Faleide et al., 2010). Reconstruction of plate tectonics from present to the time of break-up is illustrated by Faleide et al. (2010) (Fig. 4.13).

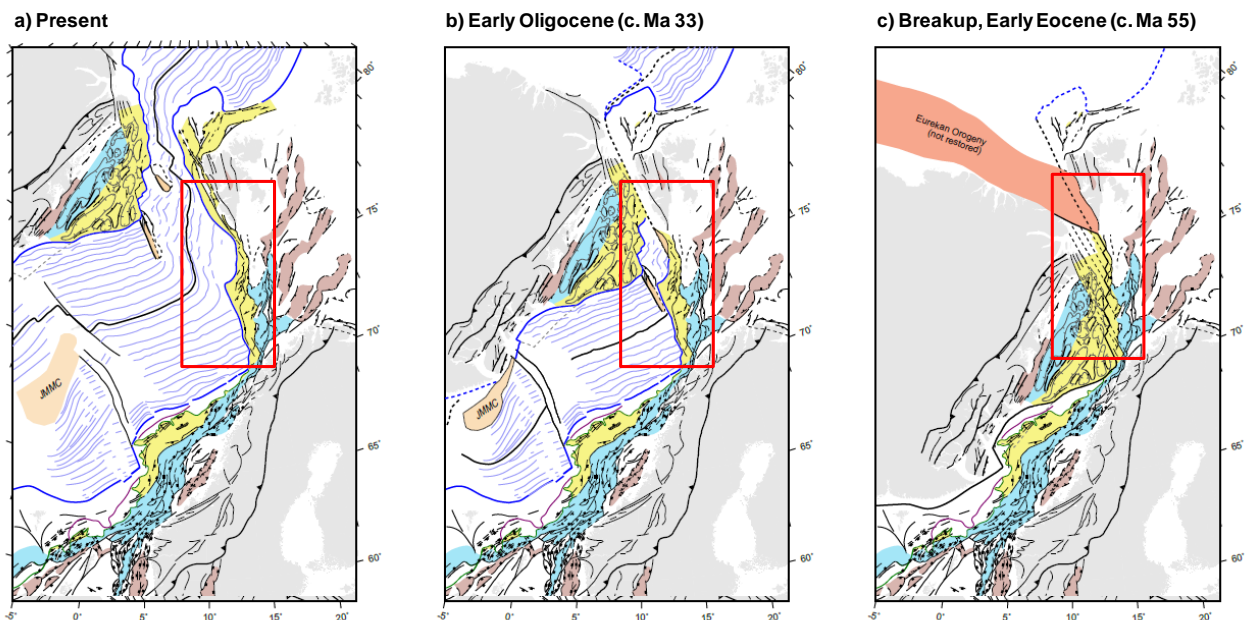


Figure 4.13: Reconstruction of plate tectonics of the Norwegian Continental Shelf and the adjacent areas affecting the NE Atlantic region. The red rectangle represents the location of the study area along the margin in three stages. a) Present, b) Reconstruction to the early Oligocene and, c) Reconstruction to the time of break-up i.e. early Eocene. JMMC: Jan Mayen microcontinent (modified from Faleide et al., 2010).

Eidvin et al. (1998) reported that the older lineaments along which the opening was initiated are the 'Knølegga Fault and its associated sub parallel features', and termed these features as the 'eastern boundary fault'. Bergh and Grogan (2003) documented that the frequency of contractional structures diminish abruptly to the south of 75°50' N, and are replaced by a geometry more influenced by the rifting phases. The Stappen high in the east of the Knølegga Fault Complex has undergone a complex tectonic history (Gabrielsen et al., 1990; Grogan et al., 1999). The tectonic history of the Stappen High involves several phases of uplift and tilting, forming in consequence a severely condensed Late Paleozoic and Mesozoic succession (Gabrielsen et al., 1990; Grogan et al., 1999). The High was a positive element in the late Paleozoic while its parts experienced subsidence in the early Cretaceous; it was uplifted later during the Cenozoic (Gabrielsen et al., 1990). The present study is in agreement with Gabrielsen et al. (1990) because the Cenozoic sediments are eroded over the footwall in the Stappen High area.

Faleide et al. (1991) noticed that between 73 and 76°N, the area comprises a down faulted terrace between the elevated Svalbard Platform and the deep ocean basin, which are bounded on both sides by major fault zones. These faults are mostly extensional, but the strike slip component cannot be ignored. This study confirms the observations of Faleide et al. (1991) that the area of the Knølegga Fault Complex has mainly extensional faulting as no prominent evidence of strike slip movement (e.g. positive or negative flower structures either full or half) has been observed within the study area.

Eocene:

The major rifting phase in the study area occurred in the Eocene as is clear from the interpretation work done on the key seismic lines (*Figs. 3.9-3.15*). The structure maps (fault map, time-structure map) generated at near base Eocene and intra Eocene levels notifies the tectonic activity during the Eocene time (*Figs. 3.5, 3.6, 3.16 and 3.17*). This observation of main rifting phase of the study area in the Eocene is also reported by Faleide et al. (1991). The master faults F-B, F1-b and F1-c experienced vertical offset that varies from more than 2 sec to 3 sec (tw) (*Figs. 4.5 and*

4.6) which includes both subsidence of the hangingwall and uplift of the footwall. This vertical throw could be associated with opening of the Norwegian-Greenland Sea. The Vestbakken Volcanic Province in the south of the study area has high amplitude seismic reflections, which can be interpreted as the lava intrusions covering older sediments. The Vestbakken Volcanic province has experienced two major igneous events, one at the initial time of breakup in the earliest Eocene followed by an earliest Oligocene event related to the plate tectonic reorganization. The intrusions are therefore younger than the lavas (Faleide et al, 1988; Gabrielsen et al., 1990). Such intrusions in the study area could be the near base Eocene reflection, as it has high amplitude in the south of the study area, such as interpreted at the location of key line G (Fig. 3.15) which has higher amplitude.

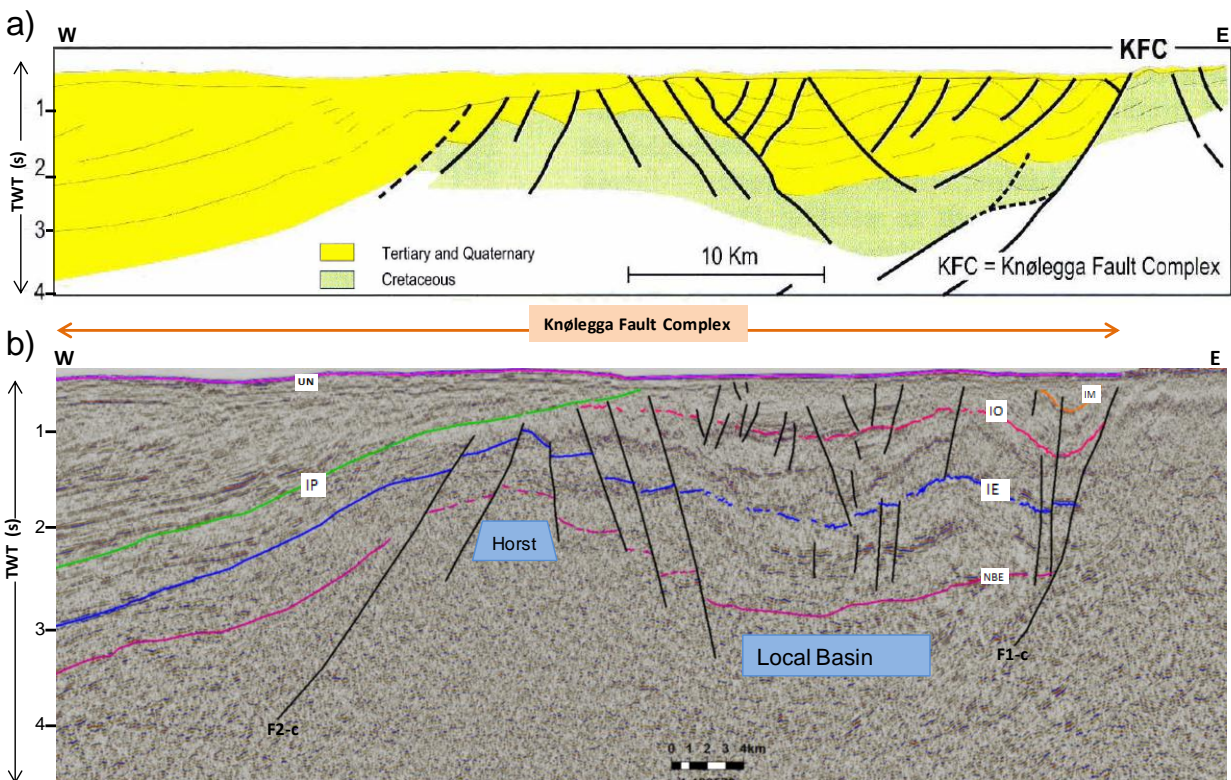


Figure 4.14: The comparison of key seismic line F. a) The key line F as illustrated by Grogan et al. (1999), legend of color codes is shown, and, b) same key line interpreted which shows that all the important features interpreted in this study area are also observed by Grogan et al. (1999). Notable normal faulting structures are horst and a local basin. The basin is termed as local as it was not observed in the other consecutive key seismic lines (refer to Figs. 3.9-3.15) UN: upper Neogene, IP: intra Pliocene, IM: intra Miocene, IO: intra Oligocene, IE: intra Eocene, NBE: near base Eocene.

Oligocene:

The opening direction was altered in the earliest Oligocene resulting in further extension and opening of the northern Greenland Sea (*Fig. 4.13*) (Faleide et al., 1996). The structure maps (fault map, time-structure map) constructed at the intra Oligocene level demonstrates that this reflection is deformed and is affected by the tectonism in the Oligocene (*Figs. 3.18 and 3.19*). The minor synthetic and antithetic faults (*Figs. 3.10-3.15*) and growth fault within the intra Eocene and intra Oligocene (*Fig.4.8*), represents that the faulting was active in the Oligocene time (*Figs. 3.19 and 3.20*). The Vestbakken volcanic province is also influenced by renewed extensional faulting and volcanism, related in the earliest Oligocene change in relative plate motion which overprinted the break-up structures (Faleide et al., 1993b). The intra Miocene reflection has not been interpreted in the north showing that the Miocene sediments are eroded in the north (*Fig. 3.9*). The depositional area becomes wider and deeper to the southern part of the study area (*Figs. 3.12-3.15*). These observations together demonstrate that the study area contemporaneously experienced uplifting in the north and subsidence in the south.

The study area has been deformed by extensional as well as contractional stresses. The deformation by faulting and folding convinced that study area lies in a setting where both extension and contraction has occurred. The normal faulting in an area represents that the area has experienced extension, while the contractional structures (synclines, anticline) are formed in consequence of contractional stresses. The contractional structures are observed in both the hangingwall and footwall, though contraction within the footwall is minor. The contractional structures are striking parallel to the main boundary faults (*Fig. 4.16*). In *segment 3* strike of contractional structure (syncline) is dominantly NE-SW to NS, parallel to the master fault F1-c (*Fig. 4.16*). This analysis is in agreement with that of Vågnes and Gabrielsen (1998), who described the Cenozoic contractional structures of the northwestern European margins trending N-S and NE-SW dominantly.

The contraction in the study area seems to be the result of far-field stresses. The contractional structures resulted in consequence of compression, it is important to consider that the compression notifies the stress system while contraction specifies the physical process of

shortening (Gabrielsen, 2010). The responsible stresses for the evolution of contractional structures in the study area could be one documented by Våagnes and Gabrielsen (1998). They reported that the far-field plate tectonic stresses, originating mainly from the Alpine Orogeny, seem to have been the most important cause of the NW European shelf contractional deformation. The younger sediments deformed by contractional stresses in the study area are the Oligocene, while no folding is observed within the Pliocene-Pleistocene sediments. This point forward, the contraction might have influenced the study area within the Oligocene and before the Pliocene time. A stage of compression in the Oligocene proposed that ridge push direction was changed from NW-SE to WNW-ESE at the Eocene-Oligocene boundary, caused by the adjustments of the poles of rotation in the North Atlantic (Boldreel and Andersen, 1993, in: Våagnes and Gabrielsen, 1998). Våagnes and Gabrielsen (1998) documented that the most Cenozoic contractional structures on the northwestern European shelf are generally found in the regions that witnessed both extensional tectonics during the late Jurassic, Cretaceous and in many situations the early Cenozoic, which also makes a sense in accordance to the structures developed in the study area.

Plio-Pleistocene:

The intra Pliocene reflection interpreted during this study represents an unconformity and base of the clastic wedge in the west of all the key seismic lines (*Figs. 3.9-3.11*). The depth of intra Pliocene increases from the north to the south of the study area. The seismic reflections over the intra Pliocene represent the glacially derived sediments that rest unconformably on the intra Oligocene and intra Miocene reflections (Faleide et al., 1996), as described in section 3.4 (*Figs. 3.9-3.11*). The interpreted reflection intra Pliocene could be compared to 'R7', which is one of the seven reflections illustrated by Faleide et al. (1996) (*Fig. 4.15*).

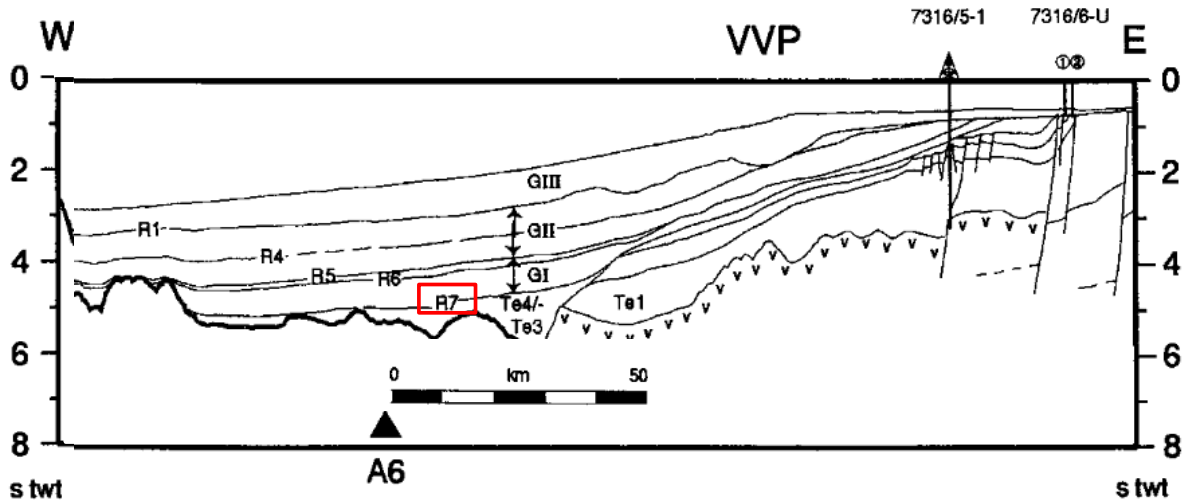


Figure 4.15: A regional seismic line across the Bjørnøya, which is to the west of the Knølegga Fault Complex. 'R7' reflector marks the boundary between the faulted and unfaulted sediments and shows similarity to the intra Pliocene reflection interpreted during the study (modified from Faleide et al., 1996). VVP: Vestbakken Volcanic Province

The present work supports that intra Pliocene reflection interpreted in this study represents the boundary between the faulted lower part of the Cenozoic sediments and the unfaulted upper younger sediments (Figs. 3.9-3.15). The oceanic crust formed along the entire Barents Sea margin witnessed subsidence and accumulation of a thick sedimentary wedge in Late Cenozoic. The wedge was fed by erosional sediments from the Barents Shelf and Svalbard (Faleide et al., 1996). This wedge of younger eroded sediments is observed in *sub-area 3* in all the key seismic lines. The late Mesozoic and Cenozoic sediments are eroded over the footwall which is the result of uplifting as reported by Faleide et al. (1993). The uplifting could have eroded the Cenozoic and older sediments absent over the footwall of the study area and then deposited in the west of the study area as is interpreted in *sub-area 3* (Figs. 3.12-3.15). The compressional stresses are older than the Pliocene-Pleistocene sediments because of the absence of contractional structures in the Pliocene-Pleistocene sediments.

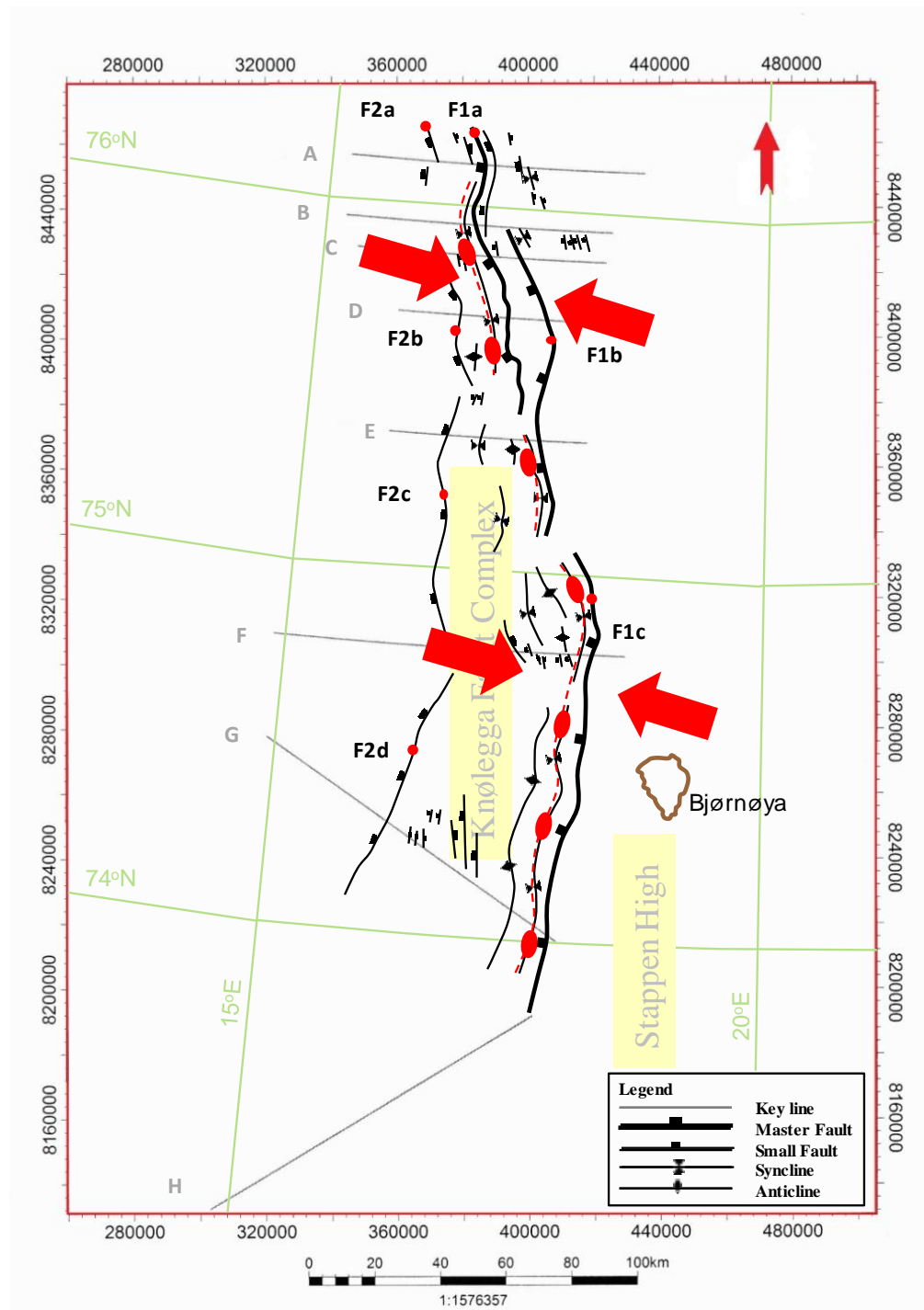


Figure 4.16: Contractional structures which seem to be the result of compressional stresses in consequence of compression in the Oligocene which caused change in the ridge push direction from NW-SE to WNW-ESE (Våagnes and Gabrielsen, 1998). The contractional structures are result of the head-on contraction as fold axis is striking parallel to the main boundary faults. The contractional stress directions WNW-ESE are shown in the fault map at the intra Oligocene level.

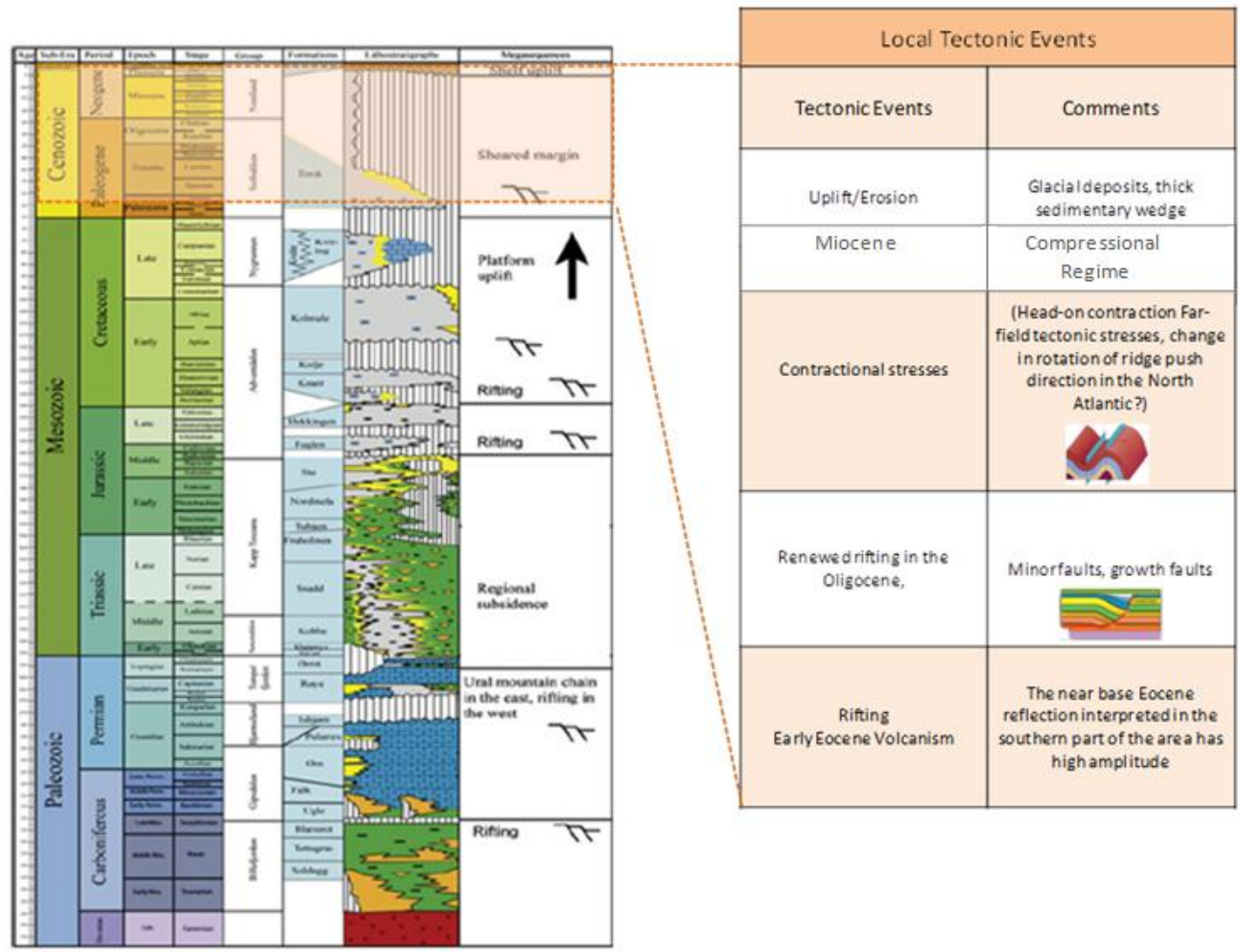


Figure 4.17: Comparison of regional tectonic evolution in SW Barents Sea (modified from Glørstad-Clark et al., 2011) to the local tectonic events of the study area during the Cenozoic sub-era.

Chapter 5 Summary of the Study

5.1 Conclusions

The main boundary faults of the Knølegga Fault Complex in the NW Barents Sea are three master fault segments F-B, F1-b and F1-c, which together form a softly-linked fault system. F-B and F1-b are ‘overlapping-synthetic’ fault segments, while F1-b and F1-c are ‘approaching-synthetic’ fault segments. The displacement along the three master fault segments is down-to-the west. The displacement is transferred between the different fault segments, therefore the master faults F-B, F1-a and F1-c represent the relay zones. F1-b and F1-c cut the sediments at levels deeper than the Cenozoic which at some locations is more than c. 3 sec (tw). Therefore, basement involvement of the master faults cannot be ignored. Although all three master faults exhibit regional significance and the possibility of the basement involvement qualifies them to be placed in the category of ‘*First-Class*’ faults following Gabrielsen (1984). The present analysis shows that sole of the master fault is located at the Jurassic or a deeper level which is in agreement with the previous authors. The maximum displacement is observed along the central master fault F1-b, which is more than c. 3 sec (tw) whereas, the displacement generally decreases towards the north and south. The timing of fault is determined by stratigraphic dating and growth fault, which shows that the faults have been active during the Oligocene. The Knølegga Fault Complex have a complicated structural architecture as it shows both extensional (normal faults) and contractional (synclines, anticline) structures in the hangingwall and footwall.

The major rifting event in the study area is related to the break-up of the Norwegian-Greenland Sea during the early Eocene. The Knølegga Fault Complex also experienced tectonic activity during the Oligocene as indicated by the growth faults and minor faults within the intra-Oligocene sediments. The contractional structures present in the study area could be the result of compression in the Oligocene?-Miocene in the direction from NW-SE to WNW-ESE. The compressional stresses have deformed both the hanging wall and footwall as minor folds have also been observed in the footwall. These contractional structures are not observed within the younger Pliocene-Pleistocene glacial sediments.

Hence, the compressional stresses have influenced only the older Cenozoic sediments than the Pliocene-Pleistocene sediments of the study area.

5.2 Recommendations for the future work

There are several aspects in the study area that can be addressed in future to enhance the understanding of the Knølegga Fault Complex. These are:

- The new knowledge of the Knølegga Fault Complex demands a closer look and perhaps a revision of the nomenclature for the area. This revision is, however, beyond the scope of the present study.
- A good stratigraphic control of sediments older than the Cenozoic (probably Triassic or Jurassic) in the hanging wall and over the footwall can help to determine the amount of vertical displacement or throw along the master faults more precisely.
- The depth conversion of the seismic sections using the interval velocities information from the well 7316/5-1 will enable to analyze the study area in depth domain.
- Analysis of 3D-seismic volume can provide better understanding of the study area and a more detailed structural analysis of the Knølegga Fault Complex can then be performed on such kind of data.

References

- ANGELIER, J., 1994. Fault slip analysis and paleostress reconstruction. In: Hancock, P.L., (Ed.) *Continental Deformation*, Pergamon Press, Oxford, p. 53-100.
- BERGH, S. G. & GROGAN, P., 2003. Tertiary structure of the Sorkapp-Hornsund region, south Spitsbergen, and implications for the offshore southern extension of the fold-thrust belt. *Norsk geologisk tidsskrift*, v. 83, p. 43.
- BOLDREEL, I.O. & ANDERSEN, M.S., 1993. Late Paleocene to Miocene compression in the Faroe–rockall area. In: Parker, J.R. (Ed.), *Petroleum Geology of Northwest Europe*. *Geological Society of London*, p. 1925–1034.
- CHILDS, C., WATTERSON, J. & WALSH, J. J., 1995. Fault overlap zones within developing normal fault systems. *Journal of the Geological Society*, v. 152, p. 535-549.
- CZUBA, W., GRAD, M., MJELDE, R., GUTERCH, A., LIBAK, A., KRÜGER, F., MURAI, Y., SCHWEITZER, J. & THE, I. P. Y. P. G., 2011. Continent–ocean-transition across a trans-tensional margin segment: off Bear Island, Barents Sea. *Geophysical Journal International*, v. 184, p. 541-554.
- DAVISON, I., 1994. Linked fault systems; extensional, strike-slip and contractional. In: Hancock, P.L., (Ed.) *Continental Deformation*, Pergamon Press, Oxford, p. 121-142.
- EIDVIN, T., GOLL, R.M., GROGAN, P., SMELROR, M., ULLEBERG, K., 1998b. The Pleistocene to Middle Eocene stratigraphy and geological evolution of the western Barents Sea continental margin at well site 7316/5-1(Bjørnøya West Area). *Norsk Geologisk Tidsskrift*, v. 78, p. 99-123.

- FALEIDE, J.I., GUDLAUGSSON, S.T. AND JACQUART, G., 1984. Evolution of the western Barents Sea. *Marine and Petroleum Geology*, v.1, p. 123–150.
- FALEIDE, J.I., MYHRE, A.M., AND ELDHOLM, O., 1988. Early Tertiary volcanism at the western Barents Sea margin, in Morton, A. and Parson, L.M., eds., Early Tertiary volcanism and the opening of the NE Atlantic: *Geological Society Special Publications*, v. 39, pp. 135–146.
- FALEIDE, J. I., GUDLAUGSSON, S. T., ELDHOLM, O., MYHRE, A. M. & JACKSON, H. R., 1991. Deep seismic transects across the sheared western Barents Sea-Svalbard continental margin. *Tectonophysics*, v. 189, p. 73-89.
- FALEIDE, J.I., VÅGNES, E & GUDLAUGSSON, S.T., 1993a. Late Mesozoic-Cenozoic evolution of the southwestern Barents Sea. In: Parker, J.R. (Ed.), Petroleum Geology of Northwest Europe, Proceedings of the 4th Conference. *The Geological Society of London, London*, p. 933-950.
- FALEIDE, J.I., VÅGNES, E & GUDLAUGSSON, S.T., 1993b. Late Mesozoic Cenozoic evolution of the south-western Barents Sea in a regional rift-shear tectonic setting. *Marine and Petroleum Geology*, v. 10, p. 186-214.
- FALEIDE, J. I., SOLHEIM, A., FIEDLER, A., HJELSTUEN, B. O., ANDERSEN, E. S. & VANNESTE, K., 1996. Late Cenozoic evolution of the western Barents Sea-Svalbard continental margin. *Global and Planetary Change*, v. 12, p. 53-74.
- FALEIDE, J.I., TSIKALAS, F., BREIVIK, A.J., MJELDE, R., RITZMANN, O., ENGEN, Ø., WILSON, J. AND ELDHOLM, O., 2008. Structure and evolution of the continental margin off Norway and the Barents Sea. v. 31, p. 82–91.
- FALEIDE, J.I., BJØRLYKKE, K., GABRIELSEN, R.H., 2010. Geology of the Norwegian Continental Shelf. In ‘Petroleum Geoscience: From Sedimentary Environments to Rock Physics, 2010, Published by *Springer*, p. 489-497.

- GABRIELSEN, R. H., 1984. Long-lived fault zones and their influence on the tectonic development of the southwestern Barents Sea. *Journal of the Geological Society*, v. 141, p. 651-662.
- GABRIELSEN, R.H., FÆRSETH, R.B., JENSEN, L.N., KALHEIM, J.E. AND RIIS, F., 1990. Structural elements of the Norwegian continental shelf, Part II: The Norwegian Sea Region. *Norwegian Petroleum Directorate, Bulletin 6*, p. 1-33.
- GABRIELSEN, R.H., 2010. The structure and hydrocarbon traps of sedimentary basins. In 'Petroleum Geoscience: From Sedimentary Environments to Rock Physics, 2010, Published by *Springer*, p. 299-327.
- GLØRSTAD-CLARK, E., FALEIDE, J. I., LUNDSCHIEN, B. A. & NYSTUEN, J. P., 2010. Triassic seismic sequence stratigraphy and paleogeography of the western Barents Sea area. *Marine and Petroleum Geology*, v. 27, p. 1448-1475.
- GLØRSTAD-CLARK, E., BIRKELAND, E. P., NYSTUEN, J. P., FALEIDE, J. I. & MIDTKANDAL, I., 2011. Triassic platform-margin deltas in the western Barents Sea. *Marine and Petroleum Geology*, v. 28, p. 1294-1314.
- GROGAN, P., ØSTVEDT-GHAZI, A.-M., LARSSSEN, G. B., FOTLAND, B., NYBERG, K., DAHLGREN, S. & EIDVIN, T., 1999. Structural elements and petroleum geology of the Norwegian sector of the northern Barents Sea. *Geological Society, London, Petroleum Geology Conference, series*, v. 5, p. 247-259.
- GUDLAUGSSON, S. T., FALEIDE, J. I., JOHANSEN, S. E. & BREIVIK, A. J., 1998. Late Paleozoic structural development of the South-western Barents Sea. *Marine and Petroleum Geology*, v. 15, p. 73-102.
- HJELSTUEN, B. O., ELVERHØI, A. & FALEIDE, J. I., 1996. Cenozoic erosion and sediment yield in the drainage area of the Storfjorden Fan. *Global and Planetary Change*, v. 12, p. 95-117.

- MILANI, E.J., & DAVISON, I., 1988, Basement Control and transfer tectonics in the Reconcavo-Tucano Jatoba Basin, NE Brazil: *Tectonophysics*, v. 154, p. 41-70.
- MORK, M. B. E. 1999. Compositional variations and provenance of Triassic sandstones from the Barents Shelf. *Journal of Sedimentary Research*, v. 69, p. 690-710.
- MORLEY, C. K., NELSON, R. A., PATTION, T. L., & MUNN, S. G., 1990 Transfer zones in the East African Rift System and their relevance to hydrocarbon exploration in rifts: *AAPG Bulletin*, v. 74, p. 1234-1253.
- MYHRE, A.M., ELDHOLM, O. & SUNDVOR, E., 1982. The margin between Senja and Spitsbergen fracture zones: implications from plate tectonics. *Tectonophysics*, v. 89, p. 33-50.
- MYHRE, A. M. & ELDHOLM, O., 1988. The western Svalbard margin (74°–80°N). *Marine and Petroleum Geology*, v. 5, p. 134-156.
- PRICE N. J. & COSGROVE J.W., 1990. Analysis of Geological Structures. *Cambridge University Press*, p. 241-330.
- PROSSER, SARAH, 1993, Rift-related linked depositional systems and their seismic expression, Tectonics and Seismic Sequence Stratigraphy, *Geological Society Special Publication*, v. 71, p. 35-66.
- RICHARDSEN, G., HENRIKSEN, E. & VORREN, T. O., 1991. Evolution of the Cenozoic sedimentary wedge during rifting and seafloor spreading west of the Stappen High, western Barents Sea. *Marine Geology*, v.101, p. 11-30.
- SUNDVOR. E. & ELDHOLM, O., 1976. Marine geophysical survey on the continental margin from Bear Island to Hornsund. Spitsbergen. *Univ. Bergen Seismol. Obs. Sci. Rep.*, v. 3, p. 28.

- TALWANI, M. & ELDHOLM, O., 1977. Evolution of the Norwegian-Greenland Sea. *Geological Society of America Bulletin*, v. 88, p. 969-999.
- VÅGNES, E., GABRIELSEN, R. H. & HAREMO, P. 1998. Late Cretaceous–Cenozoic intraplate contractional deformation at the Norwegian continental shelf: timing, magnitude and regional implications. *Tectonophysics*, v. 300, p. 29-46.
- WALSH, J. J., & WATTERSON, J., 1991a, Geometric and kinematic coherence and scale effects in normal fault systems. In: A. M., Yielding, G., and Freeman, B., (Eds.), *The geometry of normal faults: Geological Society of London Special Publication*, v. 56, p. 193-206.
- WORSLEY, D., 2008. The post-Caledonian development of Svalbard and the western Barents Sea. *Polar Research*, v. 27 (3), p. 298-317.
- <http://factpages.npd.no/factpages/Default.aspx?culture=en>. Last accessed 31st May, 2012.
- <http://www.slb.com/services/software/geo/petrel.aspx>. Last accessed 31st May, 2012.